INFORMATION TO USERS

This manuscript has been reproduced from the microfilm master. UMI films the text directly from the original or copy submitted. Thus, some thesis and dissertation copies are in typewriter face, while others may be from any type of computer printer.

The quality of this reproduction is dependent upon the quality of the copy submitted. Broken or indistinct print, colored or poor quality illustrations and photographs, print bleedthrough, substandard margins, and improper alignment can adversely affect reproduction.

In the unlikely event that the author did not send UMI a complete manuscript and there are missing pages, these will be noted. Also, if unauthorized copyright material had to be removed, a note will indicate the deletion.

Oversize materials (e.g., maps, drawings, charts) are reproduced by sectioning the original, beginning at the upper left-hand corner and continuing from left to right in equal sections with small overlaps.

ProQuest Information and Learning
300 North Zeeb Road, Ann Arbor, MI 48106-1346 USA
800-521-0600

University of Alberta

Complexity Analysis in Hybrid Systems

by

Guofeng Zhang 

A thesis submitted to the Faculty of Graduate Studies and Research in partial fulfillment of the requirements for the degree of **Doctor of Philosophy**.

in

Applied Mathematics

Department of Mathematical and Statistical Sciences

Edmonton, Alberta
Fall 2005

University of Alberta

Library Release Form

Name of Author: Guofeng Zhang

Title of Thesis: Complexity Analysis in Hybrid Systems

Degree: Doctor of Philosophy

Year this Degree Granted: 2005

Date: August 24, 2005

They have strange limits and one must learn to observe them. It is that surface simplicity of theirs which makes a trap for the stranger. One's first impression is that they are entirely soft. Then one comes suddenly upon something very hard, and you know that you have reached the limit and must adapt yourself to the fact.
— Sir Arthur Conan Doyle, *His Last Bow*

University of Alberta

Faculty of Graduate Studies and Research

The undersigned certify that they have read, and recommend to the Faculty of Graduate Studies and Research for acceptance, a thesis entitled **Complexity Analysis in Hybrid Systems** submitted by Guofeng Zhang in partial fulfillment of the requirements for the degree of **Doctor of Philosophy** in Applied Mathematics.

—

—

—

—

—

—

ng.)

—

_)

Date: August 12, 2005

To my mom and dad
for their moral and financial support
over the many, many years.

Abstract

The aim of this thesis is to investigate the complexity in a class of hybrid systems: networked control systems (NCSs), where sampling, quantization, time delay, packet dropout, network protocol and controller design are the main design issues. The study begins with limiting behavior of digital implementations of analog control systems. It is shown that as the sampling period tends to zero, internal stability and performance of an analog system can be recovered in the digital implementation via the bilinear transformation. Following this is a new network data transmission strategy that is proposed to reduce network traffic thus avoiding large time delays and high percentage of packet dropout. The effectiveness of this transmission strategy is illustrated by simulations. Then the qualitative behavior of the nonsmooth dynamical systems arising from the aforementioned transmission strategy is investigated. Though appears innocent, surprisingly, this type of nonsmooth systems possesses bewildering dynamics. Local stability of fixed points, existence of periodic orbits, strange attractors and topological entropies are investigated in considerable detail first for scalar cases. Then it is proved that this type of systems is not structurally stable. Following this is the analysis of the difficulties involved in studying these systems. Next the two-dimensional cases are studied with emphasis on their geometric structures. After that, a two-dimensional continuous-time system, the counterpart of the above-mentioned discrete one is discussed, where special attention is paid to the demonstration of its rather complex dynamics. Because this study originates in the analysis of networked control systems, some control problems are discussed after the foregoing analysis. Finally several open problems are listed as our future

research directions.

Keywords. Digital control, networked control systems, nonsmooth dynamical systems, bifurcation, chaos, numerical precision.

Acknowledgements

The research explored by this thesis is thoroughly enjoyable. This enjoyment is largely a result of the interaction that I have had with my supervisors, colleagues and friends. I feel very privileged to have worked with my supervisors: Professor Tongwen Chen and Professor Yanping Lin. To each of them I owe a great debt of gratitude for their patience, inspiration, encouragement and friendship. I give special thanks to Professor Tongwen Chen. His technical knowledge and valuable comments were extremely inspiring during the time I was writing my first paper with him. By all means this has and will continue to be a tremendous influence on my academic career. The majority of this research is on the analysis of the qualitative behavior of nonsmooth dynamical systems, which was new to us. Because it is a difficult topic, I had been frustrated greatly during the first phase of this research. Professor Tongwen Chen told me that this was a very good topic: simple formulation with an intricate and elaborate inherent structure. His encouragement kept me moving forward. Of course his insightful comments helped me with the formulation of the problems greatly. I would also like to thank Professor Michael Y. Li, from whose lectures I learned qualitative analysis of dynamical systems. I have discussed with him my research intensively, his expertise in dynamical systems, his suggestions and comments were tremendously helpful in my research. I have to thank Dr. Maria D'Amico, the discussions with whom gave me many opportunities to get more insights into the problems I was investigating. Her cooperation helped clarifying the presentation of this work enormously. I would also like to thank Prof. Guanrong Chen, whom I visited at the City University of Hong Kong last year. I spend many enjoyable days with my lab members in the ECE Department, fellow students in the Mathematics Department and colleagues in the Centre for Chaos Control and Synchronization (CCCS) at the City University of Hong Kong. In particular, many thanks to Prof. Feng Ding, Prof. Horacio Marquez, Prof. Yajun Pan, Prof. Yang Shi, Dr. Liqian Zhang, Dr. Shujun Li, Dr. Cailin Xu, Dr. Wenxiang Liu, Mr. Hongbin Li, Mr. Danlei Chu, Mr. Xinghua Deng and Mr. Hongbin Guo. Without this rich environment I doubt that many of my ideas would have come to fruition. Thanks also are given to my family who have been extremely understanding and supportive of my studies. Finally I gratefully acknowledge the financial support from NSERC, made available by Professor Tongwen Chen in the form of research assistantship, teaching assistantship of the University of Alberta, and a University of Alberta Dissertation Fellowship.

Contents

List of Tables

List of Figures

Chapter 1

Introduction

After a brief discussion of the problems involved in the analysis and design of networked control systems, this chapter reviews existing literature, then provides a vague exposition of a new network data transmission strategy, and finally gives the outline of the thesis.

1.1 Background

In a traditional control system, system components such as processes, controllers, sensors and actuators are connected directly by dedicated wiring; signals are assumed to be communicated accurately and without time delays. Control systems based on such "direct" connection have achieved great success. However, as modern control systems are becoming more and more complex in terms of their scales and functionalities, the huge number of components of a system will lead to enormous wiring if the aforementioned *point-to-point* connection is used. Obviously it is also hard to maintain. Therefore, the complexity of control systems demands new efficient connection structures.

The fast-developing secure, high speed computer networks [72, 102] make control over networks possible. In this framework, system components are regarded as nodes, and connected via common computer networks, i.e., they use communication media to send and receive signals.

Networked control systems can be classified roughly into two broad categories: local and internet-based networked control systems. Clearly, local networked control systems are built with all system components connected via local communication media. On the contrary, internet-based control systems are truly distributed geographically; system components are tied together by both local networks and the Internet.

Compared with the traditional point-to-point connection, the main advantages of connecting various system components via communication networks are wire reduction, low cost and easy maintenance, among others. Thanks to these merits, networked control systems have been built successfully in various fields such as automobiles [42, 68], aircrafts [75, 94], robotic controls [59, 91]. In the field of distributed control, networks may provide distributed subsystems with more information so that performance can be improved [37].

However, the insertion of communication networks into a control system will incur several problems unexpected in a conventional control system.

There are four of these issues we'd like to draw your attention to:

1. Signal quantization — control signals have to be quantized and encoded into

packets of finite bits before being transmitted through communication media. This procedure will introduce quantization errors and lead to certain time delays.

2. Time delays

   Time delays involved in a networked control system include at least:

   - Sampling of a continuous-time process.
   - Quantization and coding time — the time required to quantize and then encode signals to be transmitted.
   - Waiting time — packets have to wait in queues (there are sensor queues, controller queues and actuator queues to accommodate process outputs, controller outputs and process inputs respectively) before getting access to communication media.
   - Propagation time — time taken for packets to travel over communication channels.

   Time delays may be deterministic or random, constant or time varying. For local networked control systems, it may be possible to analyze the nature of time delays, then design controllers to achieve control performance by taking them into account. The Internet can provide control systems with certain quality of service(QoS), which in general is in the form of bounded time delays or probabilities of time delays and packet dropouts. Time delays induced by the Internet are definitely time-varying and random. Therefore it is more reasonable to assume that time delays are unknown but bounded. However, some deficiencies occur when making this assumption.

   - Considering only the upper bound introduces conservatism to controller design.
   - Controllers designed to compensate bounded delays may not perform well for time-varying delays [78, 82].

   Time delays, especially time-varying ones, normally will degrade system performance; however, quite often, controllers designed taking time delays into

account can improve system performance. These make the analysis and design of delayed control systems very challenging as well as extremely interesting. For a recent survey on time-delay dynamical systems, interested readers may refer to [82].

3. Packet dropouts — packets may get lost due to collision, noise saturation or large time delays.

4. Multiple transmission — signals have to be coded into two or more packets for transmission if their size is too big.

These detrimental effects often coexist and will damage system performance or even lead to instability. Therefore, to design a networked control system is really challenging. Coding methods, network protocols and controllers have to be carefully chosen or designed if a networked control system of high performance is to be built.

1.2 Literature review

In this section some lines of research on networked control systems will be briefly reviewed. Let us first look at a typical networked control system in shown Figure 1.1. System G is a process usually described by a set of differential equations

$$\begin{aligned} \dot{x}(t) &= f(x,u,t), \\ y(t) &= g(x,u,t), \end{aligned} \tag{1.1}$$

where $x \in \mathbb{R}^n$, $u \in \mathbb{R}^m$, $y \in \mathbb{R}^p$ are system state, input and output respectively. f and g are both continuous functions (or even continuously differentiable, specified when modelling) of x, u, and t.

Sensors sample y periodically. For example, suppose the sampling period of the sensor S1 is T_1, then the output of S1 is $y_{d1}(k) = y_1(kT_1)$, $k \in \mathbb{Z}^+$, the set of all nonnegative integers. Now we look at actuators shown in Figure 1.1. Each actuator contains a holder which transforms a discrete signal ϕ into a continuous one. For instance, assume the holding time of the actuator A1 is h_1, then $u_1(t) = \phi_1(k)$, $t \in [kh_1, (k+1)h_1)$, $k \in \mathbb{Z}^+$. In general $\phi_1(k)$ is not identical with $u_{d1}(k)$ in Figure 1.1 because u_{d1} may undergo other operations in the block 'A1'.

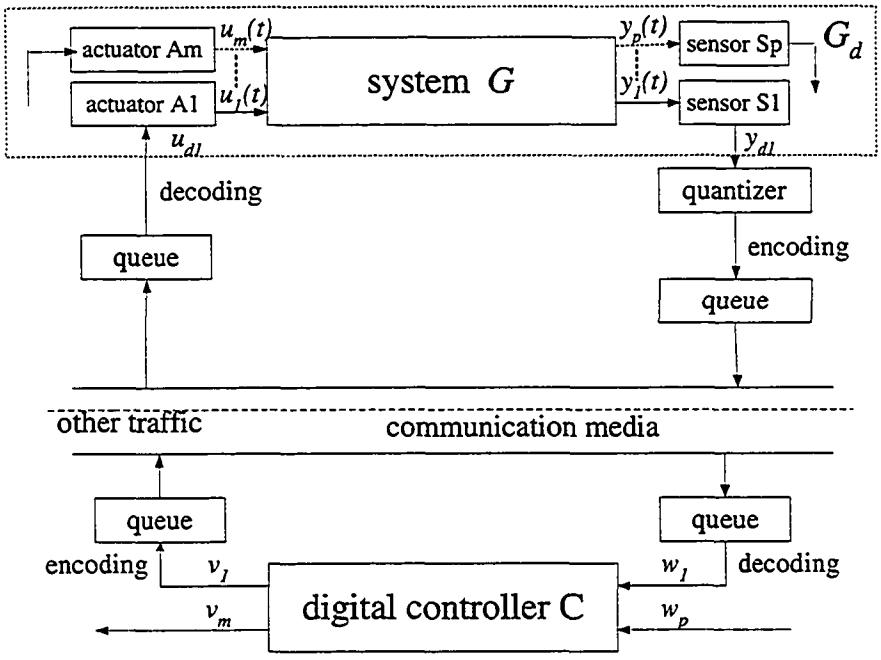

Figure 1.1: A typical networked control system

A discrete system denoted G_d is obtained if we cascade actuators, the system G and sensors together. For G_d, a digital controller C can be designed to fulfill certain system performance such as tracking. Interested readers can refer to [11, 22] for some detailed discussions. One fundamental problem involved here is:

Problem 1.1 *Ignoring the network connection (queues, communication media and other traffic), what is the limiting behavior of the digital system composed of G_d and C as h and T tend to zero? Suppose C is obtained from an analog controller K via some discretization method, Will internal stability and performance of the analog system composed of G and K be recovered in the digital control system composed of G_d and C?*

The step-invariant (the ZOH equivalent) and bilinear transformations are two most commonly used discretization techniques. Suppose their corresponding digital controllers are K_d and K_{bt} respectively, two versions of C in Figure 1.1. In the literature, there are pieces of work studying limiting properties of K_d. Assume

$h = T$. As h tends to zero, internal stability and performance of the analog system are recovered in the digital control system using K_d [11]. However, Åström *et al.* [2] points out that if the relative degree of the transfer function of K is greater than 3, then $K_d(z)$ is non-minimum-phase as h goes to zero; Properties of limiting zeros are also studied in [9, 35, 108]. On the other hand, concrete examples reveal that even as the sampling period approaches zero, the best sampled-data closed-loop performance may not necessarily converge to the best analog closed-loop performance [69]. A similar problem is investigated in [70].

In light of a result of [2], if K is minimum-phase, K_d can be non-minimum-phase as h goes to zero; whereas K_{bt} is always minimum-phase. However, will internal stability and performance of the analog system be recovered in the digital control system using K_{bt}? An affirmative answer will be given in Chapter 2, thus partially answering Problem 1.1. However we should warn you that the sampling period of a digital system can not be made arbitrarily small. One reason is that sampling rates are not always re-designable; another is that fast sampling may even degrade system performance. For example, the simultaneous effect of sampling and quantization is studied in [3], where it is shown via simulation that performance will degrade *unboundedly* as the sampling period tends to zero if some time-invariant quantizer is inserted into a system controlled by an unstable controller. Therefore it is fair to say that the problem — performance of quantized sampled-data systems — is very complicated and challenging. Much research is required here. We next address the problem of quantization in some detail.

Before the sampled system output y_d enters a queue to be broadcast, it is usually quantized and encoded. A quantizer $q = (q_1, ..., q_n)'$ with quantization size $\Delta = (\Delta_1, ..., \Delta_n)'$, $\Delta_i > 0$, $i = 1, ..., n$, is a map from $\mathbb{R}^n$ to a finite or countable subset $L = \{l_j\}_{j \in \mathbb{Z}}$ of $\mathbb{R}^n$. One possible quantizer can be constructed in the following way: Given a scalar $\Delta_1 > 0$, partition continuously $\mathbb{R}$ into finite or countably many subsections $\Omega_1 := \{\Omega_{1j}\}_{j \in \mathbb{Z}}$ satisfying 1) $\bigcup_{j \in \mathbb{Z}} \Omega_{1j} = \mathbb{R}$; 2) $\Omega_{1j} \bigcap \Omega_{1i} = \phi$, $\forall i \neq j$; 3) $0 \in \Omega_{10}$ and $0 \notin \Omega_{1i}$ for $\forall i \neq 0$. One choice of partition methods is $\Omega_{1j} = [(j - 1/2)\Delta_1, (j + 1/2)\Delta_1)$, $j \in \mathbb{Z}$. Choose a finite or countable subset

$l_1 = \{l_{1j}\}_{j\in\mathbb{Z}}$ of $\mathbb{R}$. Then q_1 is the map:

$$\begin{aligned} q_1 \quad &: \quad \mathbb{R} \to \{l_{1j}\}_{j\in\mathbb{Z}}, \\ &\qquad x \longmapsto l_{1j}, \quad \forall x \in \Omega_{1j}. \end{aligned} \tag{1.2}$$

Analogously, one can similarly define Ω_2, ..., Ω_n, l_2, ..., l_n, and then q_2, ..., q_n. Let $q = (q_1, ..., q_n)'$, then q is a quantizer. If Δ is fixed, q is called *time-invariant*, otherwise *time-varying*. For the simplicity of description, we call the partitioned subsets of $\mathbb{R}^n$ *quantization subsets*.

If the quantizer q is inserted into the closed-loop system composed of G_d and C, then a quantized "nonlinear" sampled-data system is obtained. Thus an interesting problem is: What is the effect of q on this system?

This problem is actually now a continuing interest in the literature. For example, suppose G is a linear and time-invariant (LTI) unstable system, and $h = T$. If a (dynamic) controller C is used with a time-invariant quantizer, the closed-loop system can never be asymptotically stable; moreover, chaos may occur in this closed-loop system [16]. This complexity is further addressed in [23] for the SISO case and in [24] for a system with multi-dimensional state and one-dimensional input. In [24], the complexity of a controller is characterized by three numbers: L being the number of the states of the controller while N and M being the numbers of quantization subsets of the controller output and state respectively. Then the tradeoff among L, M, N and T, the mean time required to shrink the state of the plant from a starting point to a target set, is studied. In [38], an upper bound for T ($h = T$ is assumed) is calculated geometrically using state feedback for an unstable LTI system G with a proposed time-invariant quantizer under which the trajectories of the closed-loop system do not converge to the origin; instead, they enter and stay in a region of attraction around it. In order to achieve asymptotic stability, time-varying quantizers must be adopted. In [6], for an unstable LTI system G, choosing a quantizer q with variable sensitivity Δ, an LTI controller is designed to yield global asymptotic stability. This problem is also studied in [20] for exponential stability using logarithmic quantizers. In [63], exponential stabilization of a finite-dimensional LTI system with a quantizer in the closed loop is studied based on probability theory.

To be transmitted over communication media, quantized signals should be encoded to form packets which are the true objects transmitted over the networks. Different networks have different packet formats in terms of packet length, data length, head size, etc. At this stage, there is a possible problem: if a signal is very big, it has to be first decomposed and then encoded into several packets (*multiple packeting*). Then if one of them is lost during transmission or discarded due to queue overflow, how will this affect the control performance? Fortunately, normal control signals are relatively small, multiple packeting is thus not a big problem.

A packet waits in a queue before being allowed to be transmitted. This procedure is managed by a media access control (MAC) algorithm which, together with the encoding algorithm, is a critical component of network protocols. A network protocol is a suit of algorithms managing how network packets are formulated, transmitted successfully, in addition to other functionalities such as network security. There are many commercially successful network protocols such as TCP/IP, Ethernet, ControlNet, DeviceNet, and so on. However, most of them were created originally for data networks rather than for control networks. One of the significant differences between data and control networks is: Packets of data networks are relatively big, their transmission is infrequent and there is no critical timing requirement; whereas packets of control networks are relatively small, however they demand frequent transmission and critical timing guarantee. Therefore how to adopt data network protocols to control networks or design protocols directly for control networks is an important problem faced by control engineers. Another requirement on network protocols is that protocols should also be adaptable in terms of update of softwares and insertion of new nodes and insertion of a local NCS to the Internet.

At this point, one can claim that a networked control system is a delayed sampled-data system with quantization, signal loss, sampling, and network protocols as its major design concerns. All these make the analysis of networked control systems difficult, and the controller design based on the analysis fairly complicated. This can be best summarized by the following sentences in [58] reported in the April issue of IEEE Control Systems Magazine, 2003:

> *Current control systems are almost universally based on synchronous, clocked systems, so they require communication networks that guarantee*

delivery of sensor, actuator, and other signals with a known, fixed delay. Although current control systems are robust to variations that are included in the design process (such as a variation in some aerodynamic coefficient, motor constant, or moment of inertia), they are not at all tolerant of (unmodeled) communication delays or dropped or lost sensor or actuator packets. Current control system technology is based on a simple communication architecture: all signals travel over synchronous dedicated links, with known (or worst-case bounded) delays and no packet loss. Small dedicated communication networks can be configured to meet these demanding specifications for control systems, but a very interesting question is whether we can develop a theory and practice for control systems that operate in a distributed, asynchronous, packet-based environment.

Many network protocols and various control strategies have been proposed. Loosely speaking, these considerations fall into three general categories.

The first category merely regards a networked control system as a control system with bounded time delays and studies the problem of determining how big the upper bounds can be.

Work of Walsh, Bushnell, Ye, *et al.*

In a series of papers [103, 104, 105, 106, 110], a new network protocol, TOD (try-once-discard), is proposed and analyzed. Its basic configuration is: regarding the subsystems (including G, C and other traffic in Figure 1.1) connected by a common communication medium as a whole system, we get a multi-input multi-output (MIMO) system. Omit the quantization effect and assume the network from the controller to the actuator is transparent. Also suppose the sampling period and holding time are equal, equidistant, and small enough so that the control system can be viewed as a continuous one. Then denote the plant dynamic by

$$\begin{aligned} \dot{x}_p(t) &= f_p(t, x_p(t), u_p(t)), \\ y(t) &= g_p(t, x_p(t), u_p(t)), \end{aligned} \tag{1.3}$$

and the controller by

$$\begin{aligned} \dot{x}_c(t) &= f_c(t, x_c(t), \hat{y}(t)), \\ u_p(t) &= g_c(t, x_c(t)), \end{aligned} \tag{1.4}$$

where $\hat{y}(t)$ is the input to the controller, a (possibly delayed) version of $y(t)$; f_p, g_p, f_c, g_c are continuously differentiable. Let $e(t) = y(t) - \hat{y}(t)$, $x = (x_p', x_c')'$. Then combining equations (1.3) and (1.4) together, one can obtain

$$\begin{aligned} \dot{x}(t) &= f(t, x(t), e(t)), \\ \dot{e}(t) &= g(t, x(t), e(t)). \end{aligned} \tag{1.5}$$

Note that the vector $e(t)$ is the error between the plant output $y(t)$ and the input to the controller $\hat{y}(t)$. Suppose the dimension of $y(t)$ is r, $y(t) = (y_1(t), ..., y_r(t))'$. If at time t_0, $y_i(t_0) = \hat{y}_i(t_0)$, i.e., $e_i(t_0) = 0$, then y_i is transmitted successfully. Suppose that there is one and only one $y_i(t)$ which can be transmitted over the network at each sampling instant, then $y_i(t)$ for which $|e_i(t)| = \|e(t)\|_\infty$ is transmitted, i.e., the element with the largest error gets access to the network. This is the so-called *try-once-discard (TOD)* protocol they proposed. The question studied there is: Suppose the original system with network transparent is exponentially stable, how small the sampling period T should be to guarantee exponential stability of this networked control system? A sufficient condition is obtained based on perturbation theory [39] and the Gronwall's inequality.

This idea is further generalized in [66] to derive a set of Lyapunov UGES (Uniformly Globally Exponentially Stable) protocols in the L^p framework.

In [111], assuming bounded time delays and packet dropouts, a robust H_∞ control problem is studied for networked control systems.

Obviously regarding a NCS simply as a system of bounded time delays is rather conservative, so there comes the second category.

The second category models network time delays and packet dropouts as random processes such as Markov chains. In this way, some specific features of these random processes are utilized to design controllers guaranteeing desired system performance.

Work by Krtolica, *et al.*

In their work [42, 68], assuming $h = T$, the discrete system G_d in Figure 1.1 is described by a set of difference equations:

$$\begin{aligned} x(k+1) &= Ax(k) + Bu(k), \\ y(k) &= Cx(k). \end{aligned} \tag{1.6}$$

The controller C is

$$\begin{aligned} p(k+1) &= Fp(k) + Ew(k), \\ v(k) &= Hp(k) + Ew(k). \end{aligned} \tag{1.7}$$

Here matrices A, B, C, E, F and H are all constant with compatible dimensions. Omit quantizers, queues, and communication media, and suppose

$$u(k) = \sum_{i=0}^{D_1} \alpha_i(k)\, v(k-i), \; w(k) = \sum_{i=0}^{D_2} \beta_i(k)\, y(k-i), \tag{1.8}$$

where $\sum_{i=0}^{D_1} \alpha_i(k) = 1$, $\sum_{i=0}^{D_2} \beta_i(k) = 1$ with $\alpha_i(k)$ and $\beta_i(k) \in \{0,1\}$. D_1 and D_2 are two given positive integers which act as upper bounds of sensor-to-controller and controller-to-actuator time delays respectively. In this way one can derive a closed-loop system as a time-varying one via state augmentation, necessary and sufficient conditions of stability are obtained based on time-varying Lyapunov equations. Alternatively, Regarding $\alpha(k)$ and $\beta(k)$ as Markovian chains with given probability transition matrices, the networked control system is therefore framed to be a discrete-time jumped linear system, and necessary and sufficient conditions of mean-square exponential stability are thus derived via the stochastic Lyapunov method.

A similar approach is adopted in [118] where sensor-to-controller and controller-to-actuator time delays are assumed to behave according to Markov chains respectively. The plant G may be unstable, which is very hard to control if there are unknown delays from a controller to an actuator. By augmenting the system to obtain a delay-free system and then with resort to LMI techniques, a sufficient condition is derived which guarantees the closed-loop system is stochastically stable. Based on this, a time-varying controller is constructed. It is worth mentioning that

time-varying controllers are always necessary when there are delays from a controller to an actuator.

Remark 1.1 One drawback of this method is that time delays are assumed to be integer multiples of the sampling period T. Unfortunately, this is unrealistic. Also no analysis was conducted when sampling and quantization effects are involved.

In [96], the network transmission process is modeled as a Bernoulli process with a parameter $0 < \lambda < 1$, and its effect on a discrete-time Kalman filtering problem is studied. It is shown there exists such a λ_c that the expectation of the estimation error covariance of the system state is always finite if the probability of the arrival of an observation is $\lambda > \lambda_c$. Explicit upper and lower bounds on λ_c are also derived.

Work done in Lund Institute of Technology

There are two major pieces of work done in papers [12, 60, 61, 62, 109]: One is theoretic analysis and controller design of a real-time system in the stochastic framework, and the other is two simulation toolboxes which can be employed to analyze the timing problem in networked control systems. First we briefly outline that theoretic one.

Suppose the system G is:

$$\dot{x}(t) = Ax(t) + Bu(t) + Fv(t), \tag{1.9}$$

where $v(t)$ is an external input and assumed to be white noise with unit incremental variance. Assume $h = T$, then one can get a discrete model G_d at time interval $[kh, (k+1)h)$ for some $k \in \mathbb{Z}^+$:

$$\begin{aligned} x(k+1) &= \Phi x(k) + \Gamma_0(\tau_k^{sc}, \tau_k^{ca})u(k) + \Gamma_1(\tau_k^{sc}, \tau_k^{ca})u(k-1) + v(k) \\ y(k) &= Cx(k) + w(k) \end{aligned} \tag{1.10}$$

where τ_k^{sc}, τ_k^{ca} denote the sensor-to-controller and controller-to-actuator time delays at time instant kh respectively. Furthermore, suppose τ_k^{sc}, τ_k^{ca} are 1) random; 2) independent; 3) having known probability distributions; 4) $\tau_k^{sc} + \tau_k^{ca} < h$. Assume also $v(k)$ and $w(k)$ are uncorrelated white noise with zero mean and covariance

matrices R_1 and R_2 and

$$\Phi = e^{Ah},\ \Gamma_0\left(\tau_k^{sc}, \tau_k^{ca}\right) = \int_0^{h-\tau_k^{sc}-\tau_k^{ca}} e^{At}dtB,\ \Gamma_1\left(\tau_k^{sc}, \tau_k^{ca}\right) = \int_{h-\tau_k^{sc}-\tau_k^{ca}}^{h} e^{At}dtB,$$

then the problem raised there is reduced to designing a controller C minimizing the standard LQG function

$$\lim_{N\to\infty} J_N = x^{'}(N)\,Q_N x(N) + \mathcal{E}\left\{\sum_{k=0}^{N-1}\begin{bmatrix} x(k) \\ u(k) \end{bmatrix}^{'} Q \begin{bmatrix} x(k) \\ u(k) \end{bmatrix}\right\}, \tag{1.11}$$

where Q_N and Q are both symmetric and positive-definite matrices. $\mathcal{E}$ is the expectation operator.

Then an optimal state feedback controller as well as an output feedback (suboptimal) controller is designed using the same techniques as those for the standard LQG problem.

In [36], the condition 4) $\tau_k^{sc} + \tau_k^{ca} < h$ is relaxed.

Remark 1.2 The above work is done within the stochastic framework where the probability distributions of τ_k^{sc} and τ_k^{ca} are crucial. Therefore, it is important to know these distributions. For a well-configured local networked control system, they may possibly be discerned successfully by experiments; however it is really hard to get them for internet-based control systems. Furthermore, it is not justified to assume that τ_k^{sc} and τ_k^{ca} are independent.

Two Matlab toolboxes, Jitterbug and TrueTime, are introduced in [12]. The basic principle is that networked control systems can be seen as delayed sampled-data systems with quantization effect. These two toolboxes can be used as experimental platforms for research on real-time control systems. They can easily and quickly assert how sensitive a control system is to delay, jitter, lost samples, etc. However, no quantization analysis is involved in these two toolboxes.

These two categories deal with network effect passively, namely, solely concentrating on the effect of network traffic on the control systems concerned, instead of the interwinding effect between control systems and communication networks. This later consideration leads to the third category which pays special attention to the tradeoff between data rate and control performance. One key problem is: How many bits are required to ensure system performance?

Work by Wong and Brockett

In papers [107], the effect of quantization error, quantization and propagation time on the stability of networked control systems is studied. Suppose G is a continuous-time system, its output y is sent to a continuous-time controller K through a quantizer and a communication channel; computed control signal is then sent to the actuator through that communication channel. Assume the bandwidth of the channel is R bits per second, then it takes $\delta = 1/R$ second to send a byte. Denote by c_i and d_i the coded quantized system output and control signal at ith time instant, respectively. Suppose the encoder l is of variable length which is a function of c_i and d_i. Denote time taken for signals to travel from the quantizer to the controller by s_i, and from the controller to the actuator by r_i, where i stands for the ith time instant, then one obtains

$$\begin{aligned} s_i &= r_i + l(c_i)\,\delta, \quad r_0 = 0, \\ r_{i+1} &= s_i + l(d_i)\,\delta, \quad i \geq 1. \end{aligned} \tag{1.12}$$

Based on these relations, a necessary condition for the closed-loop system to be containable is derived:

Theorem 1.1 *If the system is containable, then the following inequalities hold*

$$\begin{aligned} \sum_0^\infty \frac{1}{p^{m_i}} &\leq 1, \\ \sum_0^\infty \frac{1}{p^{n_i}} &\leq 1, \\ \sum_0^\infty \frac{1}{\tau^{m_i+n_i}} &\leq 1, \end{aligned} \tag{1.13}$$

where $m_i = l(c_i)$, $n_i = l(d_i)$, $\tau = e^{\delta tr(A)}$. *p is the dimension of the encoder, and A is the "A" matrix of G.*

Work by Ray's group

In [75], concentrated on distributed digital avionics, several control protocols are compared in terms of sampling periods and time-varying transport delays due to data latency of messages at different terminals of the control loop. In [32, 87], due

to time-varying and possibly stochastic delays, a finite-dimensional, time-varying, discrete-time model is proposed to approximate the networked control systems and its effectiveness is analyzed using simulation. For related work, interested readers may refer to [33, 50, 51, 52, 53, 54, 76, 77, 78, 81, 83].

Work by Tatikonda, *et al.*

The networked control system studied by Tatikonda, *et al.* in [97, 98, 100] is a closed loop starting from an unstable discrete-time system G, through an encoder E, a communication channel CN, a decoder D and an controller C, then returning back to G (Figure 1.2). In [97], the following stochastic linear quadratic Gaussian

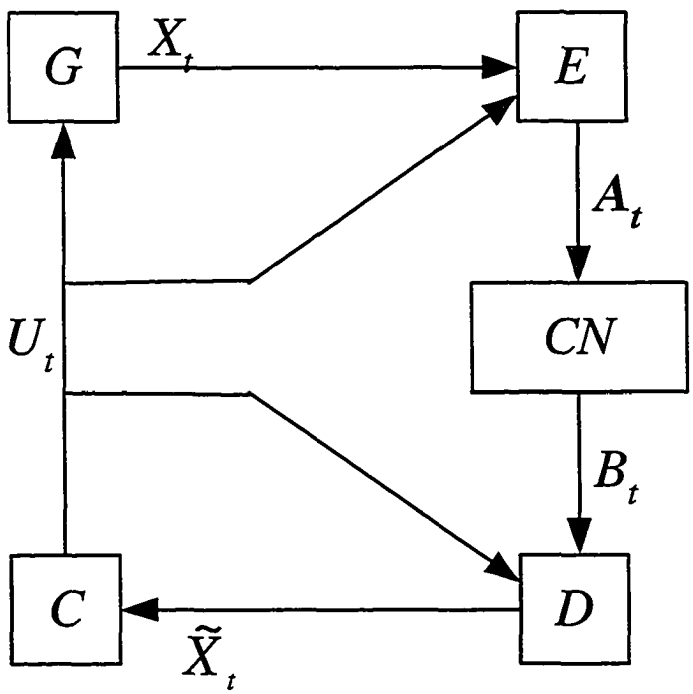

Figure 1.2: System plot in reference [97]

problem is studied. Suppose the system G is given by

$$X_{t+1} = Fx_t + GU_t + W_t, \tag{1.14}$$

where $\{W_t\}$ is an independent and identically distributed sequence of Gaussian random variables with zero mean and covariance σ_W. Suppose the initial state X_0

is also Gaussian. Here the performance objective is to minimize:

$$\lim_{T\to\infty} \limsup_{T\to\infty} \frac{1}{T}\mathcal{E}\left\{\sum_{t=0}^{T-1} X_t' Q X_t + U_t' S U_t\right\} \tag{1.15}$$

where Q and U are positive definite.

As is well-known, if there is no network constraint, the optimal cost in Eq. (1.15) is given by $tr(P)\sigma_W$ where $tr(P)$ is the trace of the matrix P. Obviously the insertion of a finite bandwidth communication network will distort the state X_t, so the question studied in the paper is: How will the network CN affect the performance in Eq. (1.15) and how to design the encoder E and the decoder D to ensure good performance? To address this problem, the concept of no dual effect is introduced, which states essentially that the estimate of the state error, $X - \tilde{X}$, is independent of the system input U. Then some necessary conditions are given to guarantee this so-called no dual effect. Under this assumption, the optimal cost defined in Eq. (1.15) is decomposed into two parts: $tr(P)\sigma_W$ and $tr((F'PF - P + Q))\Lambda$ where Λ is the steady state estimation error covariance of $X - \tilde{X}$. In view of this decomposition, the problem is converted to the design of encoders and decoders which in the sequel have been addressed based on information theory.

The deterministic case is studied in [100], where the system is given by

$$X_{t+1} = AX_t + BU_t. \tag{1.16}$$

Suppose (C, G) is observable, which means the initial state X_0 can be uniquely determined. How will the communication network affect this observability? To address this problem, the concept of asymptotic observability is proposed. Let $e_t = X_t - \tilde{X}_t$, then asymptotic observability states that the error e_t cannot grow unbounded for bounded X_0 and the error decreases to zero uniformly if $X_0 \to 0$. Suppose the data rate of the network channel CN is R, then a necessary condition to asymptotic observability is

$$R > \sum_{\lambda(A)} \max\{0, \log|\lambda(A)|\}. \tag{1.17}$$

Following this study, the effect of the communication channel CN on asymptotic observability of the system is discussed. Correspondingly the concept of asymptotic

stabilizability is proposed and a necessary condition to guarantee it is given by the same formula, namely Eq. (1.17). Finally the design of encoder E and decoder D guaranteeing asymptotic observability and stabilizability is investigated.

Work by Goodwin, *et al.*

Consider the networked control system in shown Figure 1.3. The problem investi-

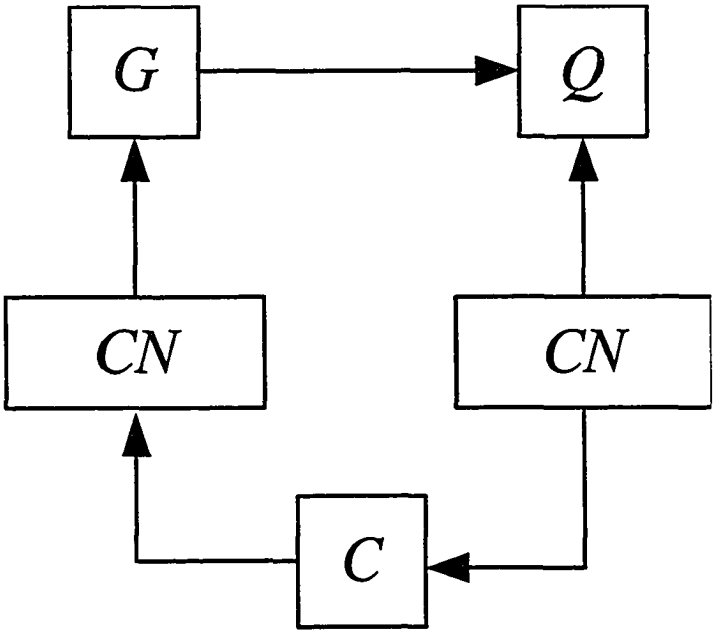

Figure 1.3: System plot in reference [27]

gated in [27] is: Given the system G and the communication channel CN, design quantizer Q and controller C to minimize network traffic. On the up-link side (from G to C), quantizer Q is designed to reduce network traffic, however this will affect state estimation which is always important in control. On the down-link side (from C to G), delay due to network can not be detected by the controller C. To resolve these two problems, instead of a fixed controller, a set of controllers is employed based on online moving horizon techniques.

Other Work

There is a pretty much amount of work reported in the literature. In [48, 49], some detailed descriptions of design consideration and performance evaluation are

reported. In [117], a systematic networked control method designed specifically to handle the constraints of the networked realization of a linear time invariant control system is studied. The general structure of the proposed controller requires switching between the open loop and closed loop subsystems of the controller which is specified by the behavior of the communication network. In [73], a maximum allowable delay bound is derived for a class of networked control systems under which the control systems are stable.

Our proposal

In this thesis, a new network data transmission strategy is proposed to reduce network traffic. By adding constant deadbands to both the controller and the plant in Figure 3.2 in Chapter 3, signals will be communicated only when necessary. So by adjusting the deadbands, a tradeoff between satisfactory control performance and reduction of network transmission can be achieved.

More importantly, the data transmission strategy we proposed is more suitable to fit a control network into an integrated communication networks composed of control and data networks, so as to fulfill the need for a new breed geared toward total networking [79]. This problem is of course very appealing as depicted by Raji in [79]; and at the same time is fundamentally important, so is listed in [58] as a future direction in control in an information-rich world (see Page 9). Essentially speaking, under the network transmission strategy proposed in this thesis, in an integrated network composed of data and control networks, it is required that networks provide sufficient communication bandwidth upon request of control systems. As a payoff, control systems will save network resources by deliberately dropping packets without degrading system performance severely. This is a crucial tradeoff. On the one hand, control signals are normally time critical, hence the priority should be given to them whenever requested; on the other hand, due to one characteristic of control networks, namely, small packet size but frequent packets, it is somewhat troublesome because it demands frequent transmission. Our scheme aims at relieving this burden for the whole communication network. This is exactly the motivation of this research.

There are three main topics in this thesis. The first one is the analysis of efficacy of the above-mentioned network data transmission strategy. The control system in

this framework is a type of nonsmooth dynamical systems. Clearly the analysis of this class of systems will shed some light on the nature of this data transmission strategy, hence our second topic is the qualitative analysis of nonsmooth dynamical systems in this context. This research originates in the networked control systems, hence naturally, our third, the last, topic is the controller design under this network data transmission strategy. In the next section, a chapter-by-chapter review will disclose more details .

1.3 Outline of the thesis

Chapter 2 addresses some issues involved in digital implementations of analog control systems. From an analog system K, digital systems K_d and K_{bt} are often obtained via the step-invariant (the ZOH equivalent) and bilinear transformations, respectively. For the case when K is stable, SISO or MIMO, it is shown that K_{bt} converges to K_d in l_p induced norms as the sampling period tends to zero for all $1 \leq p \leq \infty$. Furthermore, K_{bt} converges to K_d in the graph metric as the sampling period tends to zero no matter whether K is stable or not. Thus, internal stability and performance recovery properties for K_d in the literature can be translated to those for K_{bt}.

In chapter 3, a new network data transmission strategy is proposed in order to reduce network traffic, thus avoiding large time delays and high percentage of data loss. The stability of the resulting nonsmooth dynamical systems is analyzed briefly. Some simulations are conducted to illustrate the effectiveness of this network data transmission strategy in terms of system performance and network traffic reduction rate.

From Chapter 4 through Chapter 7, complex dynamics of the discrete-time nonsmooth dynamical systems discussed in Chapter 3 are studied in detail. These nonsmooth dynamical systems are switching systems each composed of two linear systems governed by a switching law. In Chapter 4, following some motivational examples, qualitative analysis of a two-dimensional switching system is conducted with emphasis on local stability of fixed points, existence and stability of periodic orbits, bifurcations and first return maps.

Chapter 5 addresses difficulties involved in the analysis of the strong nonlinearity

inherent in these nonsmooth dynamical systems. Here we point out why traditional methods fail and propose some new numerical methods primarily based on softwares such as Mathematica and Matlab.

Chapter 6 investigates structural stability of a switching system. By introducing a parameter λ to derive a line of systems, with one end point being a linear stable system and the other being the original nonsmooth dynamical system, we seek phase transition as λ moves from 1 to 0. We are interested in the invariance or continuous functions of λ as it goes from 1 to 0.

A higher-order discrete-time nonsmooth dynamical system, induced by the same switching machinery as those in the aforementioned two-dimensional systems, is studied in Chapter 7. Some examples are first used to illustrate geometrically the rich dynamics of this system, then fixed points and switching surfaces are discussed. Finally an example is given to show the rich dynamics of the class of higher dimensional nonsmooth dynamical systems.

A continuous-time nonsmooth dynamical system, the counterpart of that studied in Chapter 7, is discussed in Chapter 8. Intriguing behavior of this system such as sensitive dependence on initial conditions and coexisting attractors is demonstrated by simulations using Matlab/Simulink. Then the machinery leading to this strong nonlinearity is investigated from the viewpoint of numerical solutions of the trajectories of the system.

We return back to the issue of control in Chapter 9 which can be divided into three parts: Part one is about chaotic control; part two contains some simulations of system performance under the new controller design; part three converts the design problem into an optimization one, which can be studied via LMIs.

Finally some open problems are listed in Chapter 10 to close this thesis.

1.4 Collections of definitions

For the convenience of readers, some important definitions are collected and given in this section. For details please refer to [11], [85] and the references therein.

1.4.1 Step-invariant transformation

Given a real function $y(t)$, where $t \in \mathbb{R}$, an ideal sampler S with input y and output ψ is defined as

$$\psi(k) = S(y(t)) := y(hk), \tag{1.18}$$

where $k \in \mathbb{Z}$. Also, a zero-order holder (ZOH) H transforms a discrete-time signal v to a continuous-time one $u(t)$ in the following way:

$$u(t) = H(v(k)) := v(k), \quad kh \leq t < (k+1)h. \tag{1.19}$$

Then a *step-invariant transformation* G_d mapping a discrete-time signal v to a discrete-time φ is defined as:

$$\varphi = G_d v := SGHv, \tag{1.20}$$

where G is a continuous-time system.

1.4.2 Bilinear transformation

Given $s \in \mathbb{R}$ and $\lambda \in \mathbb{Z}$, where $\mathbb{R}$ and $\mathbb{Z}$ denote the sets of real numbers and integers respectively. Define the following *bilinear transformation*:

$$s = \frac{2}{h}\frac{1-\lambda}{1+\lambda}, \tag{1.21}$$

where the real number $h \geq 0$ is a sampling period. Then, under this transformation, a continuous-time transfer function $G(s)$ can be mapped to a discrete-time one, $G_{bt}(\lambda)$, which has the form:

$$G_{bt}(\lambda) = G\left(\frac{2}{h}\frac{1-\lambda}{1+\lambda}\right). \tag{1.22}$$

1.4.3 Non-wandering set

Let X be a metric space, and $f : X \to X$ a map. An element x of X is a wandering point if there is a neighborhood U of x and an integer N such that, for all $n \geq N$, $f^n(U) \cap U = \emptyset$, where $\emptyset$ denotes the empty set. If x is not wandering, we call it a non-wandering point. Equivalently, x is a non-wandering point if for every neighborhood U of x there is $n \geq 1$ such that $f^n(U) \cap U$ is nonempty. The set of all non-wandering points is called the *non-wandering set* of f, and is denoted by $\Omega(f)$.

If X is compact, then $\Omega(f)$ is compact, nonempty, and forward invariant; if, additionally, f is an homeomorphism, then $\Omega(f)$ is invariant.

1.4.4 ω-limit set

Let $\Phi(t,x)$ be the flow of the differential equation $x' = f(x)$, where $f \in C^k(M, \mathbb{R}^n)$, with $k \geq 1$ and M an open subset of $\mathbb{R}^n$. For any given $x \in M$, the *ω-limit set* of x, denoted $\omega(x)$, is the set of points $y \in M$ such that there exists a sequence $t_n \to \infty$ with $\Phi(t_n, x) = y$. Similarly, the α-limit set of x, denoted $\alpha(x)$, is the set of points $y \in M$ such that there exists a sequence $t_n \to -\infty$ with $\Phi(t_n, x) = y$.

1.4.5 Poincaré-Bendixson theorem

Let M be an open subset of $\mathbb{R}^2$, and $f \in C^1(M, \mathbb{R}^2)$. Consider the planar differential equation $x' = f(x)$. For a fixed $x \in M$, suppose that the ω-limit set $\omega(x) \neq \emptyset$ is compact, connected, and contains only finitely many equilibria. Then one of the following holds:

1. $\omega(x)$ is a fixed orbit (a periodic point with period zero, i.e., an equilibrium).
2. $\omega(x)$ is a regular periodic orbit.
3. $\omega(x)$ consists of (finitely many) equilibria $\{x_j\}$ and non-closed orbits $\gamma(y)$ such that $\omega(y) \in \{x_j\}$ and $\alpha(y) \in \{x_j\}$ (where $\alpha(y)$ is the alpha limit set of y).

The same result holds when replacing ω-limit sets by α-limit sets.

1.4.6 Topological entropy

Let (X, d) be a compact metric space and $f\colon X \to X$ a continuous map. For each $n \geq 0$, we define a new metric d_n by $d_n(x,y) = \max\{d(f^i(x), f^i(y)) : 0 \leq i < n\}$. Two points are ϵ-close with respect to this metric if their first n iterates are ϵ-close. For $\epsilon > 0$ and $n \geq 0$ we say that $F \subset X$ is an (n, ϵ)-separated set if for each pair x, y of points of E we have $d_n(x,y) > \epsilon$. Denote by $N(n, \epsilon)$ the maximum cardinality of an (n, ϵ)-separated set (which is finite, because X is compact). Roughly, $N(n, \epsilon)$ represents the number of "distinguishable" orbit segments of length n, assuming we cannot distinguish points that are less than ϵ apart. The *topological entropy* of f is defined by $h_{top}(f) = \lim_{\epsilon \to 0} \left(\limsup_{n \to \infty} \frac{1}{n} \log N(n, \epsilon) \right)$. It is easy to see that this limit always exists, but it could be infinite. A rough interpretation of this number is that it measures the average exponential growth of the number of distinguishable

orbit segments. Hence, roughly speaking again, we could say that the higher the topological entropy is, the more essentially different orbits we have.

Topological entropy was first introduced in 1965 by Adler, Konheim and McAndrew. In this thesis we use its generalized form given in [40] for piece-wise linear dynamics.

1.4.7 Homeomorphism

A *homeomorphism* f of topological spaces is a continuous, bijective map such that f^{-1} is also continuous. We also say that two spaces are homeomorphic if such a map exists.

If two topological spaces are homeomorphic, they are topologically equivalent – using the techniques of topology, there is no way of distinguishing one space from the other.

1.4.8 Structural stability

Given a metric space (X, d) and an homeomorphism $f\colon X \to X$, we say that f is structurally stable if there is a neighborhood V of f in Homeo(X) (the space of all homeomorphisms mapping X to itself endowed with the compact-open topology) such that every element of V is topologically conjugate to f.

1.4.9 Sensitive dependence on initial conditions

A map f on a metric space X is said to have *sensitive dependence on initial conditions* if there is an $r > 0$ (independent of the point) such that for each point $x \in X$ and each $\epsilon > 0$ there is a point $y \in X$ satisfying $d(x, y) < \epsilon$ and a $k \geq 0$ such that $d\left(f^k(x), f^k(y)\right) \geq r$.

1.4.10 Expensive

A map f on a metric space X is said to be *expensive* if there is an $r > 0$ (independent of the points) such that for each pair of points $x, y \in X$ there is a $k \geq 0$ such that $d\left(f^k(x), f^k(y)\right) \geq r$.

1.4.11 Topologically transitive

A map $f : X \to X$ is *topologically transitive* on an invariant set $Y \subset X$ if there exists a point $y \in Y$ such that $\cup_{n=0}^{\infty} f^n(y)$ is dense in Y.

1.4.12 Chaos (Definition I)

Let (X, d) be a metric space, $f: X \to X$ a map, and Λ a set of X with at least two points. Λ is called a *scrambled set* of f if $\forall x, y \in \Lambda$, $x \neq y$,

- $\limsup_{n\to\infty} |f^n(x) - f^n(y)| > 0$;
- $\liminf_{n\to\infty} |f^n(x) - f^n(y)| = 0$.

f is said to be *chaotic* in the sense of Li-Yorke if there exists an uncountable scrambled set Λ.

1.4.13 Chaos (Definition II)

A map on a metric space X is said to be *chaotic* on an invariant set $Y \subset X$ if

- f is topologically transitive on Y;
- f has sensitive dependence on initial conditions on Y;
- Periodic points are dense in Y.

If f is continuous on Y, it is proved that the third item in the above definition is redundant, hence there comes the following definition.

1.4.14 Chaos (Definition III)

A map f on a metric space X is said to be *chaotic* on an invariant set $Y \subset X$ if

- f is topologically transitive on Y;
- f has sensitive dependence on initial conditions on Y.

Chapter 2

Convergence in digital control systems

In this chapter, some issues involved in digital implementations of analog control systems are discussed. From an analog system K, digital systems K_d and K_{bt} are often obtained via the step-invariant (the ZOH equivalent) and bilinear transformations, respectively. For the case when K is stable, SISO (Sec. 2.1.2) or MIMO (Sec. 2.1.4), it is shown that K_{bt} converges to K_d in ℓ_p induced norms as the sampling period tends to zero for every $1 \leq p \leq \infty$. Furthermore, K_{bt} converges to K_d in the graph metric as the sampling period tends to zero no matter whether K is stable or not (Sec. 2.1.3). Thus, internal stability and performance recovery properties for K_d in the literature can be translated to those for K_{bt} (Sec. 2.2).

2.1 Asymptotic behavior of $K_d - K_{bt}$

Given an analog system $K(s)$, the step-invariant (the ZOH equivalent) and bilinear transformations are denoted by discrete-time systems $K_d(z)$ and $K_{bt}(z)$, respectively. In terms of state-space data, take a minimal realization for $K(s)$, namely, (A, B, C, D), and assume $A \in \mathbb{R}^{m\times m}$, $B \in \mathbb{R}^{m\times p}$, $C \in \mathbb{R}^{q\times m}$, $D \in \mathbb{R}^{q\times p}$; $K_d(z)$ has a corresponding state-space model (A_d, B_d, C, D) with

$$A_d = \mathrm{e}^{Ah}, \quad B_d = \int_0^h \mathrm{e}^{A\tau} d\tau B, \tag{2.1}$$

where h is the sampling period; and $K_{bt}(z)$ has a state-space model $(A_{bt}, B_{bt}, C_{bt}, D_{bt})$ with

$$\begin{aligned} A_{bt} &= \left(I - \frac{h}{2}A\right)^{-1}\left(I + \frac{h}{2}A\right), \quad B_{bt} = \frac{h}{2}\left(I - \frac{h}{2}A\right)^{-1} B, \\ C_{bt} &= C\left(I + A_{bt}\right) = 2C\left(I - \frac{h}{2}A\right)^{-1}, \quad D_{bt} = D + \frac{h}{2}C\left(I - \frac{h}{2}A\right)^{-1} B. \end{aligned} \tag{2.2}$$

Note that K_d and K_{bt} are the most commonly used discretizations [41]. In this section we will prove the following: the ℓ_p norm of $K_d(h) - K_{bt}(h)$ converges to zero as h tends to zero for all $1 \le p \le \infty$ when K is stable; and $K_d(h) - K_{bt}(h)$ converges to zero in the graph metric even if K is unstable.

2.1.1 Convergence in ℓ_p induced norms

In this subsection, assuming that K is stable and SISO (single-input-single-output), we investigate the convergence properties between K_d and K_{bt} in terms of ℓ_p induced norms when the sampling period h goes to zero.

Letting $\{a_n\}_{n=0}^{\infty}$ and $\{b_n\}_{n=0}^{\infty}$ denote respectively the impulse responses of K_d and K_{bt}, we have

$$a_n = \begin{cases} D, & n = 0, \\ C\mathrm{e}^{A(n-1)h}\int_0^h \mathrm{e}^{A\tau} d\tau B, & n \ge 1, \end{cases}$$

$$b_n = \begin{cases} D + \frac{h}{2}C(I - \frac{h}{2}A)^{-1}B, & n = 0, \\ hC\left(I - \frac{h}{2}A\right)^{-(n+1)}\left(I + \frac{h}{2}A\right)^{n-1} B, & n \ge 1. \end{cases}$$

Define $c_n = a_n - b_n$. It follows easily that $|c_0| \to 0$ as $h \to 0$. When $n \ge 1$,

$$c_n = C\left(\mathrm{e}^{A(n-1)h}\int_0^h \mathrm{e}^{A\tau} d\tau - h\left(I - \frac{h}{2}A\right)^{-(n+1)}\left(I + \frac{h}{2}A\right)^{n-1}\right) B = Cd_nB,$$

where

$$d_n := \mathrm{e}^{A(n-1)h}\int_0^h \mathrm{e}^{A\tau}d\tau - h\left(I-\frac{h}{2}A\right)^{-(n+1)}\left(I+\frac{h}{2}A\right)^{n-1}. \qquad (2.3)$$

Therefore $|c_n| \le \|C\|\cdot\|d_n\|\cdot\|B\|$, where the norm $\|\cdot\|$ on a matrix $M\in\mathbb{R}^{m\times r}$ is defined as $\sum_i\sum_j|m_{ij}|$, which is a matrix norm. Thus looking at the 1-norm of $K_d - K_{bt}$, we have

$$\|K_d - K_{bt}\|_1 := \sum_{n=0}^{\infty}|c_n| \to 0, \text{ as } h\to 0 \text{ if } \sum_{n=1}^{\infty}\|d_n\| \to 0, \text{ as } h\to 0. \qquad (2.4)$$

The following lemma is crucial in the succeeding development.

Lemma 2.1 *Assume that K is SISO and stable and the matrix A is diagonalizable with all real eigenvalues. Then* $\lim_{h\to 0^+}\|K_d - K_{bt}\|_1 = 0$.

Proof. Under the assumptions above, without loss of generality, we suppose that A is in the form $A = \mathrm{diag}\,(a_i)_{i=1,\ldots,m}$ with $a_i < 0$. Then we have

$$\begin{aligned}
\mathrm{e}^{A(n-1)h}\int_0^h \mathrm{e}^{A\tau}d\tau &= \mathrm{diag}\left(\frac{\mathrm{e}^{a_ih}-1}{a_i}\mathrm{e}^{a_i(n-1)h}\right)_{i=1,\ldots,m},\\
\left(I-\frac{h}{2}A\right)^{-(n+1)}\left(I+\frac{h}{2}A\right)^{n-1} &= \mathrm{diag}\left(\frac{\left(1+\frac{h}{2}a_i\right)^{n-1}}{\left(1-\frac{h}{2}a_i\right)^{n+1}}\right)_{i=1,\ldots,m}.
\end{aligned}$$

According to Eq. (2.3),

$$(d_n)_i = \frac{\mathrm{e}^{a_ih}-1}{a_i}\mathrm{e}^{a_i(n-1)h} - \frac{\left(1+\frac{h}{2}a_i\right)^{n-1}}{\left(1-\frac{h}{2}a_i\right)^{n+1}}h = \frac{\mathrm{e}^{a_i(n-1)h}}{\left(1-\frac{h}{2}a_i\right)^{n+1}}(e_n)_i,\ i=1,\ldots,m,$$

where $(d_n)_i$ denotes the i-th diagonal element of the matrix d_n, and

$$(e_n)_i := \frac{\mathrm{e}^{a_ih}-1}{a_i}\left(1-\frac{h}{2}a_i\right)^{n+1} - h\mathrm{e}^{-a_i(n-1)h}\left(1+\frac{h}{2}a_i\right)^{n-1}.$$

Thus, for all n, $(d_n)_i \ge 0$ is equivalent to $(e_n)_i \ge 0$.

Next we will use induction to prove that $(e_n)_i \ge 0, \forall n \ge 1$, if $h < 1/|a_i|$. For $n=1$,

$$\begin{aligned}
(e_1)_i &= \frac{\mathrm{e}^{a_ih}-1}{a_i}\left(1-\frac{h}{2}a_i\right)^2 - h = \frac{1}{a_i}\left(1-ha_i+\frac{h^2}{4}a_i^2\right)\sum_{n=1}^{\infty}\frac{a_i^nh^n}{n!} - h\\
&= \sum_{n=1}^{\infty}\frac{(-n)\,a_i^nh^{n+1}}{(n+1)!} + \frac{1}{4}\sum_{n=1}^{\infty}\frac{a_i^{n+1}h^{n+2}}{n!}\\
&= -\frac{a_i}{2}h^2 - \frac{a_i^2}{4\cdot 3}h^3 + \sum_{n=3}^{\infty}\frac{n-2}{4\cdot(n+2)}\frac{a_i^{n+1}}{n!}h^{n+2}.
\end{aligned}$$

Since under the condition $h < 1/|a_i|$,

$$\frac{\frac{(2k+1)-2}{4\cdot((2k+1)+2)}\frac{1}{(2k+1)!}|a_i|^{(2k+1)+1}h^{(2k+1)+2}}{\frac{(2k+2)-2}{4\cdot((2k+2)+2)}\frac{1}{(2k+2)!}|a_i|^{(2k+2)+1}h^{(2k+2)+2}} = \frac{2k-1}{2k}\frac{2k+4}{2k+3}(2k+2)\frac{1}{|a_i|h} > 1,\ \forall k \geq 1,$$

we have

$$\sum_{n=3}^{\infty}\frac{n-2}{4\cdot(n+2)}\frac{a_i^{n+1}}{n!}h^{n+2} \geq 0.$$

Furthermore,

$$-\frac{a_i}{2}h^2 - \frac{a_i^2}{4\cdot 3}h^3 = -\frac{a_i h}{4\cdot 3}(6+a_i h) \geq 0, \text{ if } h < \frac{6}{|a_i|}.$$

Thus

$$(e_1)_i \geq 0 \text{ for } h < 1/|a_i|.$$

Suppose $(e_k)_i \geq 0$ for $h < 1/|a_i|$.

$$\begin{aligned}(e_{k+1})_i &= \frac{e^{a_i h}-1}{a_i}\left(1-\frac{h}{2}a_i\right)^{k+1}\left(1-\frac{h}{2}a_i\right) \\ &\quad -he^{-(k-1)ha_i}\left(1+\frac{h}{2}a_i\right)^{k-1}e^{-ha_i}\left(1+\frac{h}{2}a_i\right).\end{aligned}$$

By the above assumption,

$$\frac{e^{a_i h}-1}{a_i}\left(1-\frac{h}{2}a_i\right)^{k+1} \geq he^{-(k-1)ha_i}\left(1+\frac{h}{2}a_i\right)^{k-1} \geq 0, \text{ for } h < \frac{1}{|a_i|};$$

therefore

$$(e_{k+1})_i \geq 0 \Leftrightarrow \left(1-\frac{h}{2}a_i\right) \geq e^{-ha_i}\left(1+\frac{h}{2}a_i\right).$$

Define

$$f(h) := 1-\frac{h}{2}a_i - e^{-ha_i}\left(1+\frac{h}{2}a_i\right). \tag{2.5}$$

Then $f(0) = 0$, and $f(h) \geq 0$ for $h \geq 0$, thus $(e_{k+1})_i \geq 0$ for $h < 1/|a_i|$. By induction, $(e_n)_i \geq 0$, $\forall n \geq 1$, if $h < \frac{1}{|a_i|}$; so is $(d_n)_i$. Therefore,

$$\begin{aligned}\sum_{n=1}^{\infty}\|d_n\| &= \sum_{n=1}^{\infty}\sum_{i=1}^{m}(d_n)_i = \sum_{i=1}^{m}\left(\frac{e^{a_i h}-1}{a_i}\cdot\frac{1}{1-e^{a_i h}} - \frac{h}{\left(1-\frac{h}{2}a_i\right)^2}\frac{1}{1-\frac{1+\frac{h}{2}a_i}{1-\frac{h}{2}a_i}}\right) \\ &= \sum_{i=1}^{m}\left(-\frac{1}{a_i}+\frac{1}{a_i}\frac{1}{1-\frac{h}{2}a_i}\right) \to 0 \text{ as } h \to 0.\end{aligned}$$

By Eq. (2.4), the lemma is proven. ■

According to the discrete-time version of Theorem 9.1.2 in [11], for all $1 \leq p \leq \infty$, $\|K_d - K_{bt}\|_{\ell_p} \leq \|K_d - K_{bt}\|_1$, the left hand side being the ℓ_p induced norm (the right hand side $\|K_d - K_{bt}\|_1$ is actually $\|K_d - K_{bt}\|_{\ell_\infty}$). Thus we conclude the following.

Theorem 2.1 *Under the same assumptions as in Lemma 2.1, we have*

$$\lim_{h \to 0^+} \|K_d - K_{bt}\|_{\ell_p} = 0$$

for all $1 \leq p \leq \infty$.

2.1.2 Convergence in the graph metric

In this subsection, we remove the assumption that K must be stable. Thus K_d and K_{bt} may be possibly unstable. For convergence of unstable systems, norm metrics are not suitable, we hence adopt the graph metric introduced by [101]. It is easy to find two unstable digital systems converging to each other under the graph metric, whereas induced norms are unbounded as the sampling period approaches zero. Therefore, the graph metric is more suitable in measuring the "closeness" between two unstable systems. We also comment that here K can be MIMO (multi-input-multi-output).

Some preliminaries are necessary for the development.

Lemma 2.2 *Assume that the pair* (A, B) *is stabilizable. Then there exists a common constant matrix* F *such that* $A + BF$ *and* $A + 2BF$ *are both stable.*

Proof. Since (A, B) is stabilizable, it is well known that there exists a positive definite matrix P such that $A'P + PA - PBB'P < 0$. Define $F = -\frac{1}{2}B'P$. It can be verified that $(A + BF)'P + P(A + BF) = A'P + PA - PBB'P < 0$, $(A + 2BF)'P + P(A + 2BF) = A'P + PA - 2PBB'P < 0$. By the Lyapunov theorem, $A + BF$ and $A + 2BF$ are both stable. ■

Lemma 2.3 *If* $A + BF$ *is stable (in continuous time), both* $A_d + B_dF$ *and* $A_{bt} + B_{bt}F$ *are stable (in discrete time) for sufficiently small* h.

We omit the proof of Lemma 2.3. Now we have set up for the main result.

Theorem 2.2 *In the graph metric,* $K_d - K_{bt}$ *converges to zero as the sampling period* h *goes to zero.*

Proof. By Lemma 2.2, there exists a matrix F such that $A+BF$ and $A+2BF$ are stable simultaneously. By Lemma 2.3, both $A_d + B_dF$ and $A_{bt} + 2B_{bt}F$ are stable for h sufficiently small. Define

$$\left[\begin{array}{c} M_d(z) \\ N_d(z) \end{array}\right] = \left[\begin{array}{c|c} A_d + B_dF & B_d \\ \hline F & I \\ C + DF & 0 \end{array}\right], \quad \left[\begin{array}{c} M_{bt}(z) \\ N_{bt}(z) \end{array}\right] = \left[\begin{array}{c|c} A_{bt} + 2B_{bt}F & B_{bt} \\ \hline 2F & I \\ C + 2DF & 0 \end{array}\right].$$

Then $K_d = N_d M_d^{-1}$ and $K_{bt} = N_{bt} M_{bt}^{-1}$ are right coprime factorizations [115]. Thus

$$M_d(z) - M_{bt}(z) = F\left[zI - (A_d + B_dF)\right]^{-1} B_d - 2F\left[zI - (A_{bt} + 2B_{bt}F)\right]^{-1} B_{bt}.$$

Substituting in the expressions for A_d and B_d in Eq. (2.1), and A_{bt} and B_{bt} in Eq. (2.2), and simplifying a bit, we have $M_d(z) - M_{bt}(z) = FT(z)B$ with

$$\begin{aligned} T(z) \;:=\; & \left[zI - I - \int_0^h \mathrm{e}^{At}dt\,(A+BF)\right]^{-1} \int_0^h \mathrm{e}^{At}dt \\ & -2\left[zI - \left(I - \frac{h}{2}A\right)^{-1}\left(I + \frac{h}{2}(A+2BF)\right)\right]^{-1} \frac{h}{2}\left(I - \frac{h}{2}A\right)^{-1}. \end{aligned} \tag{2.6}$$

Let $z = \mathrm{e}^{-j\theta}$, $\theta \in [-\pi, \pi)$. If $\theta = 0$, $z = 1$, then

$$\begin{aligned} T(1) \;=\; & \left[I - \left(I + \int_0^h \mathrm{e}^{At}dt\,(A+BF)\right)\right]^{-1} \int_0^h \mathrm{e}^{At}dt \\ & -2\left[I - \left(I - \frac{h}{2}A\right)^{-1}\left(I + \frac{h}{2}(A+2BF)\right)\right]^{-1} \frac{h}{2}\left(I - \frac{h}{2}A\right)^{-1} \\ =\; & -(A+BF)^{-1} - h\left[I - \frac{h}{2}A - \left(I + \frac{h}{2}(A+2BF)\right)\right]^{-1} \\ =\; & -(A+BF)^{-1} + (A+BF)^{-1} = 0. \end{aligned}$$

If $\theta \neq 0$, $z = \mathrm{e}^{-j\theta} \neq 1$. According to Eq. (2.6), $\lim_{h\to 0^+} T(z) = 0$. Thus we conclude that

$$\lim_{h\to 0^+} \|M_d(z) - M_{bt}(z)\|_\infty = \lim_{h\to 0^+} \sup_{-\pi\le\theta<\pi} \|M_d(\mathrm{e}^{-j\theta}) - M_{bt}(\mathrm{e}^{-j\theta})\| = 0.$$

Similarly, we can show that $\lim_{h\to 0^+} \|N_d(z) - N_{bt}(z)\|_\infty = 0$. It follows then that $K_d - K_{bt}$ converges to zero in the graph metric. ∎

If K is stable, both K_d and K_{bt} are stable. In this case the graph metric induces the same topology as that induced by the H_∞ norm. We have:

Corollary 2.1 *If K is stable,* $\lim_{h\to 0^+} \|K_d(z) - K_{bt}(z)\|_\infty = 0$.

According to Corollary 2.1, for the H_∞ norm (ℓ_2 induced norm), the assumptions in Theorem 2.1 can be relaxed. In fact, Corollary 2.1 holds for all norms induced by unitarily invariant matrix norms [74].

2.1.3 Convergence in ℓ_p induced norms revisited

In this subsection we will remove the assumptions in Theorem 2.1, thus obtaining a general result for the Convergence of $\|K_d - K_{bt}\|$ in ℓ_p induced norms as h goes to zero.

Let P and Q denote the controllability and observability Gramians of $K(s)$ respectively. Then

$$AP + PA' + BB' = 0,$$

and

$$A'Q + QA + C'C = 0.$$

Define

$$\tilde{P} := \frac{h}{4}P, \quad \tilde{Q} := \frac{4}{h}Q.$$

Then following the technique in [28],

$$\begin{aligned} A_{bt}\tilde{P}A_{bt}' - \tilde{P} + B_{bt}B_{bt}' &= \left(I - \frac{h}{2}A\right)^{-1}\left(I + \frac{h}{2}A\right)\tilde{P}\left(I + \frac{h}{2}A'\right)\left(I - \frac{h}{2}A'\right)^{-1} \\ &\quad -\tilde{P} + \frac{h^2}{4}\left(I - \frac{h}{2}A\right)^{-1}BB'\left(I - \frac{h}{2}A'\right)^{-1} \\ &= \frac{h^2}{4}\left(I - \frac{h}{2}A\right)^{-1}(AP + PA' + BB')\left(I - \frac{h}{2}A'\right)^{-1} \\ &= 0. \end{aligned}$$

Similarly, since

$$A_{bt} - I = h\left(I - \frac{h}{2}A\right)^{-1}A,$$

i.e.,

$$A_{bt} = I + h\left(I - \frac{h}{2}A\right)^{-1}A,$$

$$
\begin{aligned}
A_{bt}'\tilde{Q}A_{bt} - \tilde{Q} &= \left(I + h\left(I - \frac{h}{2}A'\right)^{-1}A'\right)\tilde{Q}\left(I + h\left(I - \frac{h}{2}A\right)^{-1}A\right) - \tilde{Q} \\
&= h\left(I - \frac{h}{2}A'\right)^{-1}A'\tilde{Q} + h\tilde{Q}\left(I - \frac{h}{2}A\right)^{-1}A \\
&\quad + h^2\left(I - \frac{h}{2}A'\right)^{-1}A'\tilde{Q}\left(I - \frac{h}{2}A\right)^{-1}A.
\end{aligned}
$$

Consequently,

$$
\begin{aligned}
&\left(I - \frac{h}{2}A'\right)\left(A_{bt}'\tilde{Q}A_{bt} - \tilde{Q} + C_{bt}'A_{bt}\right)\left(I - \frac{h}{2}A\right) \\
&= hA'\tilde{Q} + h\tilde{Q}A + 4C'C \\
&= 4\left(A'Q + QA + C'C\right) = 0.
\end{aligned}
$$

Therefore, $K(s)$ and $K_{bt}(z)$ have the same Hankel singular values, denoted by $\sigma_H = \{\sigma_1, \cdots, \sigma_N\}$, where $\sigma_1 \geq \cdots \geq \sigma_N \geq 0$.

Based on Corollary 2.1, we have

Theorem 2.3 *Assume K is stable, $\lim_{h\to 0^+} \|K_d - K_{bt}\|_{\ell_p} = 0$ for all $1 \leq p \leq \infty$.*

Proof. Observe that

$$
K_d(z) - K_{bt}(z) = \left[\begin{array}{cc|c} A_d & 0 & B_d \\ 0 & A_{bt} & B_{bt} \\ \hline C & -C_{bt} & -\frac{h}{2}C\left(I - \frac{h}{2}A\right)^{-1}B \end{array}\right].
$$

Let

$$
K_{cl}(z) := \left[\begin{array}{cc|c} A_d & 0 & B_d \\ 0 & A_{bt} & B_{bt} \\ \hline C & -C_{bt} & 0 \end{array}\right], \quad D_{cl} := \frac{h}{2}C\left(I - \frac{h}{2}A\right)^{-1}B.
$$

Then

$$
K_d(z) - K_{bt}(z) = K_{cl}(z) + D_{cl}.
$$

By Corollary 2.1,

$$
\lim_{h\to 0^+} \|K_{cl}(z)\|_\infty = 0.
$$

Suppose the Hankel singular values of $K_{cl}(z)$ are $\sigma_H^h = \{\sigma_1^h, \cdots, \sigma_N^h\}$ where $\sigma_1^h \geq \cdots \geq \sigma_N^h \geq 0$. According to the discrete-time counterpart of Theorem 7.8 in [115], we have

$$
\|K_{cl}(z)\|_1 \leq 2\sum_{k=1}^{N} \sigma_i^h.
$$

As a result,

$$\lim_{h\to 0^+} \|K_{cl}(z)\|_1 = 0.$$

Obviously $D_{cl} \to 0$ as $h \to 0$. Therefore

$$\lim_{h\to 0^+} \|K_d(z) - K_{bt}(z)\|_1 = 0.$$

Furthermore, according to the discrete-time version of Theorem 9.1.2 in [11],

$$\|K_d - K_{bt}\|_{\ell_p} \leq \|K_d - K_{bt}\|_1 \text{ , for all } 1 \leq p \leq \infty.$$

■

Remark 2.1 The above theorem is applicable to MIMO systems. Also the restriction of "A" being diagonalizable with all real eigenvalues is removed. Thus it is a generalization of Theorem 2.1. In this way, along with Theorem 9.4.1 in [11], if the step-invariant or bilinear transformation is applied to analog systems, internal stability as well as other performance specifications of the analog system can be recovered as the sampling period tends to zero. This is the topic of the next section.

2.2 Performance recovery

In this section, we discuss an application of Theorem 2.3. It is well-known that internal stability of an analog control system can be recovered if the controller is implemented via the step-invariant transformation. Similar results can be proved for other types of performance specifications. More concretely, consider the feedback system $\sum_1$ in Figure 2.1 where P and K are finite-dimensional, LTI and strictly causal, and W is finite-dimensional, LTI, strictly causal and stable, introduced as a pre-filter before the sampler for later digital implementation. This closed-loop system is said to be *internally stable* [11] if the mapping

$$\begin{bmatrix} I & P \\ -K & I \end{bmatrix}^{-1} : \begin{bmatrix} r \\ d \end{bmatrix} \longmapsto \begin{bmatrix} z \\ u \end{bmatrix}$$

is bounded $\mathcal{L}_2(\mathbb{R}_+) \to \mathcal{L}_2(\mathbb{R}_+)$.

Do a digital implementation as in Figure 2.2, denoted $\sum_2$, using K_d obtained by the step invariant transformation. We first have the following properties.

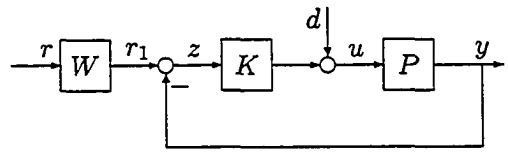

Figure 2.1: Analog system $\sum_1$

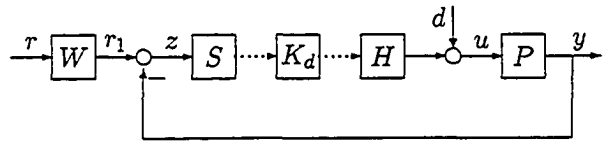

Figure 2.2: Digital system $\sum_2$ via the step-invariant transformation

Proposition 2.1 *Suppose* $\sum_1$ *is internally stable and satisfies* $\sup_{\|r\|_p \le 1} \|z\|_p < \epsilon$, *for some* $\epsilon > 0$. *Then*

(a) $\sum_2$ *is internally stable as* $h \to 0$;

(b) furthermore, if K *is strictly causal and stable, then* $\sup_{\|r\|_p \le 1} \|z\|_p < \epsilon$ *as* $h \to 0$.

The proof of (a) was given in [11], and (b) can be proved in a similar way. Here, we give another intuitive interpretation, though being not a rigorous proof. To this end, we need the following result.

Proposition 2.2 *[10] If* F *is finite-dimensional, LTI, strictly causal and stable, then* HSF *converges to* F *as* $h \to 0$ *in the* $\mathcal{L}_p(\mathbb{R}_+)$*-induced norm for every* $1 \le p \le \infty$.

According to this proposition, $HSW \to W$, $HSK \to K$ as $h \to 0$; therefore for any given $u \in \mathcal{L}_p(\mathbb{R}_+)$, let $z = (K - HK_dS)Wu$,

$$\begin{aligned}
\|z\| &= \|(K - HK_dS)Wu\| \le \|(K - HK_dS)W\| \cdot \|u\| \\
&= \|(K - SHKSH)W\| \cdot \|u\| \\
&\le \|KW - KHSW\| \cdot \|u\| + \|KHSW - SHKSHW\| \cdot \|u\| \\
&\le \|K\|\|(I - HS)W\| \cdot \|u\| + \|(I - HS)K\|\|HSW\| \cdot \|u\| \to 0 \text{ as } h \to 0.
\end{aligned}$$

Thus, as $h \to 0$, HK_dS in Figure 2.2 can be regarded as a very good approximation of K, therefore it is natural to assume that Proposition 2.1 holds. Next, we will show that $HK_{bt}S$ has the same desirable property.

If we replace K_d in Figure 2.2 by K_{bt}, we get another digital system $\sum_3$ as shown in Figure 2.3. We have the following result which is the counterpart of Proposition 2.1.

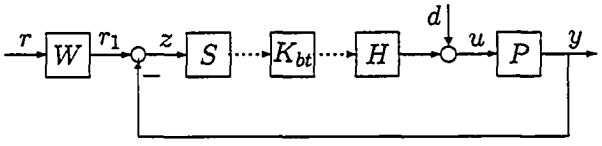

Figure 2.3: Digital system $\sum_3$ via the bilinear transformation

Theorem 2.4 *Suppose $\sum_1$ is internally stable and satisfies $\sup_{\|r\|_p \le 1} \|z\|_p < \epsilon$, for some $\epsilon > 0$. Then*

(a) $\sum_3$ is internally stable as $h \to 0$;

(b) furthermore, if K is strictly causal and stable, then $\sup_{\|r\|_p \le 1} \|z\|_p < \epsilon$ as $h \to 0$.

In order to prove this theorem, we first note the following: Suppose G is a stable, finite-dimensional, LTI, discrete-time system, then

$$\|G\|_p \le \|G\|_1, \quad \forall p \in \mathbb{N} \cup \infty, \tag{2.7}$$

where $\|G\|_p$ is the ℓ_p-induced norm of G.

Proof of Theorem 2.4. First we reconfigure the system $\sum_3$ in the way as shown in Figure 2.4. The system G_1 can be viewed as a perturbation to the system under

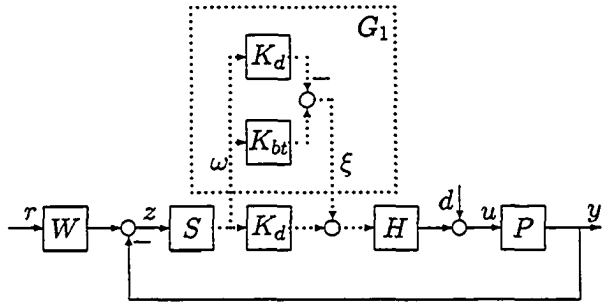

Figure 2.4: The equivalent system of $\sum_3$

it, which is exactly the system $\sum_2$ in Figure 2.2. Therefore, if the norm from ω to ξ

tends to zero as $h \to 0$, then according to the small gain theorem, we can ascertain that the system $\sum_3$ is internally stable. Hence the problem is reduced to showing property (b) for the system $\sum_3$. For this and in view of Eq. (2.7), it is sufficient to show $\lim_{h\to 0} \|G_1\|_1 = 0$, which is given by Theorem 2.3. ■

Remark 2.2 Digital controllers obtained via the bilinear transformation have similar closed-loop properties as those obtained via the step-invariant transformation. However, if the analog controller K is minimum-phase, so is K_{bt}; whereas K_d may be non-minimum-phase if h is sufficient small [2].

In the following, we will illustrate Theorem 2.4 with a simple example.

Example 2.1 Consider the analog system in Figure 2.1 and its digital implementation via the bilinear transformation in Figure 2.3 with $W = I$, $d = 0$, and

$$P(s) = \frac{20}{s(1+s/10)(1+s/50)}, \quad K(s) = \frac{s^2 + 10.42s + 20}{s^2 + 32.44s + 20}.$$

(*This example was used by [80] and [90] in the optimal digital redesign.*) Figure 2.5 is the closed-loop step tracking for different values of h. We see that the step response of y of the digital system in Figure 2.5 converges to that of the analog system as $h \to 0$.

2.3 Conclusions

In this chapter, some limiting properties of digital implementations of analog controllers via the bilinear and step-invariant transformations have been studied. It is shown proved that the ℓ_p-induced norm of $K_d(h) - K_{bt}(h)$ converges to zero as h tends to zero for all $1 \le p \le \infty$ when K is stable; and $K_d(h) - K_{bt}(h)$ converges to zero in the graph metric even if K is unstable. Hence all results involving the digital controllers obtained for the step-invariant transformation can be translated to those obtained via the bilinear transformation.

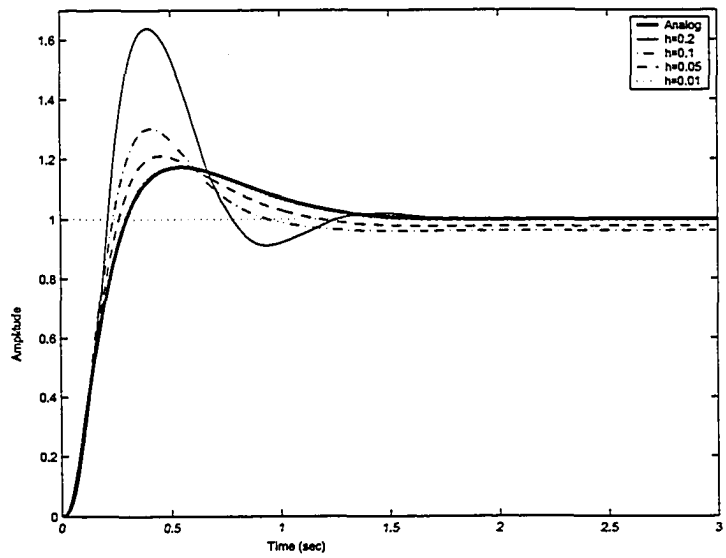

Figure 2.5: Step response simulation

Chapter 3

A new network data transmission strategy

With the rapid development of communication networks, more and more control systems are constructed in the framework of networks. Besides the advantages of connecting system components with communication channels, time delay and packet loss are two of the biggest problems induced by networks. Various network protocols and control methods have been proposed to deal with these problems. In this chapter, a new network data transmission strategy is proposed to reduce network traffic so as to avoid large time delays and high percentages of data loss. Stability of the resulting nonsmooth dynamical system is analyzed briefly. The effectiveness of this strategy is illustrated via simulations. Its dynamical behavior will be the main topic of the following several chapters.

3.1 A new networked control technique

Consider the feedback system shown in Figure 3.1, where G is a discrete-time system

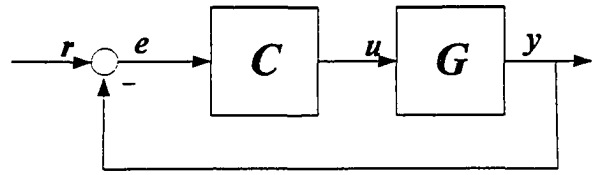

Figure 3.1: A standard feedback system

of the form:

$$\begin{aligned} x(k+1) &= Ax(k)+Bu(k), \\ y(k) &= Cx(k), \end{aligned} \tag{3.1}$$

with the state $x \in \mathbb{R}^n$, the input $u \in \mathbb{R}^m$, the output $y \in \mathbb{R}^p$; C is a stabilizing controller:

$$\begin{aligned} x_d(k+1) &= A_d x_d(k)+B_d e(k), \\ u(k) &= C_d x_d(k)+D_d e(k), \\ e(k) &= r(k)-y(k), \end{aligned} \tag{3.2}$$

with its state $x_d \in \mathbb{R}^{n_c}$ and the reference input $r \in \mathbb{R}^p$. Let $\xi = \begin{bmatrix} x \\ x_d \end{bmatrix}$. Then the closed-loop system from r to e can be modeled by

$$\begin{aligned} \xi(k+1) &= \begin{bmatrix} A-BD_dC & BC_d \\ -B_dC & A_d \end{bmatrix}\xi(k)+\begin{bmatrix} BD_d \\ B_d \end{bmatrix}r(k), \\ e(k) &= \begin{bmatrix} -C & 0 \end{bmatrix}\xi(k)+r(k). \end{aligned} \tag{3.3}$$

Now we add nonlinear constraints on both u and y. Specifically, consider the system shown in Figure 3.2. The nonlinear constraint H_1 is defined as: for a given $\delta_1 > 0$, let $v(-1) = 0$; for $k \geq 0$,

$$v(k) = H_1(u_c(k), v(k-1)) = \begin{cases} u_c(k), & \text{if } \|u_c(k)-v(k-1)\|_\infty > \delta_1, \\ v(k-1), & \text{otherwise.} \end{cases} \tag{3.4}$$

Similarly H_2 is defined as: for a given $\delta_2 > 0$, let $z(-1) = 0$; for $k \geq 0$,

$$z(k) = H_2(y_c(k), z(k-1)) = \begin{cases} y_c(k), & \text{if } \|y_c(k)-z(k-1)\|_\infty > \delta_2, \\ z(k-1), & \text{otherwise.} \end{cases} \tag{3.5}$$

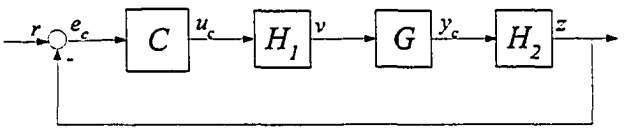

Figure 3.2: A constrained feedback system

It can be shown that, for the SISO case, i.e., $p = m = 1$, $\|H_1\|$, the induced norm of H_1, equals 2, so is $\|H_2\|$.

In a networked control system, there are normally computer networks along the routes from the controller C to the system G and from G to C. These networks (usually shared by other clients) will introduce time delays into the closed-loop system. It it quite appealing to compensate this adverse effect. If we regard H_1 as a component of C and H_2 of G, G (resp. C) contains the previous version of v (resp. z), then there will have no signal transmission from C to G and (or) from G to C if the inequalities in Eq. (3.4) and (or) Eq. (3.5) are not satisfied, suggesting that we are reducing network traffic. We expect this will benefit the overall system connected by the common networks. One example will be given in Sec. 3.3 to illustrate this point.

Similar work is done in [71] where *adjustable* deadbands are proposed to reduce network traffic. In that formulation, the closed-loop system with deadbands is modeled as a perturbed system; then its exponential stability follows that of the original system based on the perturbation theory [39]. The constraints proposed here are fixed (specified δ_1 and δ_2), we will see that stability of the system in Figure 3.2 is quite complicated (e.g., only local stability result can be obtained). However, the advantage of fixed deadbands is that they will reduce network traffic more effectively. Furthermore, the stability region can be scaled as large as desired. This is one advantage of our proposed scheme. Moreover, we find out that the system in Figure 3.2 has rather complex dynamics — it appears chaotic. As is known chaotic behavior will in general provide more system dynamics, namely, more information of the underlying system, therefore we hope we can achieve better control in the framework of Figure 3.2. We will address this problem more rigorously in Chapter 9.

For the "constrained" system in Figure 3.2, let p denote the state of the system G, and p_d denote that of C, then

$$\begin{aligned} p(k+1) &= Ap(k) + Bv(k), \\ y_c(k) &= Cp(k), \end{aligned}$$

and

$$\begin{aligned} p_d(k+1) &= A_d p_d(k) + B_d e_c(k), \\ u_c(k) &= C_d p_d(k) + D_d e_c(k), \\ e_c(k) &= r(k) - z(k). \end{aligned}$$

Let $\eta = \begin{bmatrix} p \\ p_d \end{bmatrix}$; then the closed-loop system from r to e is

$$\begin{aligned} \eta(k+1) &= \begin{bmatrix} A & 0 \\ 0 & A_d \end{bmatrix} \eta(k) + \begin{bmatrix} B & 0 \\ 0 & B_d \end{bmatrix} \begin{bmatrix} v(k) \\ -z(k) \end{bmatrix} + \begin{bmatrix} 0 \\ B_d \end{bmatrix} r(k), \qquad (3.6) \\ e_c(k) &= \begin{bmatrix} -C & 0 \end{bmatrix} \eta(k) + r(k), \end{aligned}$$

where v and z are given in Eqs. (3.4)-(3.5).

3.2 Stability analysis

In this section, Stability of system (3.6) is addressed. Firstly a sufficient condition ensuring local exponential stability is derived. Secondly a positive invariant set is constructed. Finally it is proven that the Lebesgue measure of the set of trajectories converging to a certain fixed point is zero if either the system G or the controller C is unstable.

Letting $r = 0$, system (3.6) becomes

$$\begin{aligned} \eta(k+1) &= \begin{bmatrix} A & 0 \\ 0 & A_d \end{bmatrix} \eta(k) + \begin{bmatrix} B & 0 \\ 0 & B_d \end{bmatrix} \begin{bmatrix} v(k) \\ -z(k) \end{bmatrix}, \qquad (3.7) \\ \begin{bmatrix} u_c(k) \\ y_c(k) \end{bmatrix} &= \begin{bmatrix} 0 & C_d \\ C & 0 \end{bmatrix} \eta(k) + \begin{bmatrix} 0 & D_d \\ 0 & 0 \end{bmatrix} \begin{bmatrix} v(k) \\ -z(k) \end{bmatrix}, \\ \begin{bmatrix} v(k) \\ -z(k) \end{bmatrix} &= \begin{bmatrix} H_1(u_c(k), v(k-1)) \\ -H_2(y_c(k), z(k-1)) \end{bmatrix}, \quad k \geq 0. \end{aligned}$$

We have the following result regarding local stability.

Lemma 3.1 *If both the system G and the controller C are stable, the origin is locally exponentially stable.*

Proof. Define

$$\tilde{A} = \begin{bmatrix} A & 0 \\ 0 & A_d \end{bmatrix}, \quad \tilde{C} = \begin{bmatrix} 0 & C_d \\ C & 0 \end{bmatrix}.$$

Since both G and C are stable, $\rho(\tilde{A}) < 1$ where $\rho(M)$ is the spectral radius of a square matrix M. Then for any given $\varepsilon > 0$ satisfying $\rho(\tilde{A}) + \varepsilon < 1$, there exists a matrix norm $\|\cdot\|_*$ such that $\left\|\tilde{A}\right\|_* \leq \rho(\tilde{A}) + \varepsilon$ [29]. Furthermore, this matrix norm satisfies $\|MN\|_* \leq \|M\|_* \|N\|_*$ for any two matrices M and N of dimension $n + n_c$. In this spirit, for a vector x of dimension $n + n_c$, one can define a vector norm $|x|_*$ such that $|Mx|_* \leq \|M\|_* |x|_*$. One way to define such a norm is the following. Let $\mathcal{O}$ denote the zero vector of dimension $n + n_c$, define

$$|x|_* := \left\| \left[x, \underbrace{\mathcal{O}, \cdots, \mathcal{O}}_{n+n_c-1} \right] \right\|_* .$$

Then

$$|Mx|_* = \|[Mx, \mathcal{O}, \cdots, \mathcal{O}]\|_* \leq \|M\|_* \|[x, \mathcal{O}, \cdots, \mathcal{O}]\|_* = \|M\|_* |x|_* .$$

For a vector ω of dimension $\nu < n + n_c$, denote by O the zero vector of dimension $n + n_c - \nu$. Define $|\omega|_* := \left| \begin{bmatrix} \omega' & O' \end{bmatrix}' \right|_*$, then $|\cdot|_*$ is a norm on the vector space $\mathbb{R}^{\nu \times 1}$. We treat a matrix of dimension less than $n + n_c$ in the similar way.

Let $\|\cdot\|_1$ be the induced matrix norm of the vector norm $\|\cdot\|_\infty$, then there exist positive constants c_1 and c_2 such that $c_1 \|M\|_* \leq \|M\|_1 \leq c_2 \|M\|_*$ for any matrix $M \in \mathbb{R}^{n+n_c}$. Let $\delta := \min\{\delta_1, \delta_2\}$, then $\|M\|_1 \leq \delta$ if $\|M\|_* \leq \delta/c_2$. Hence, in the sequel we concentrate on the matrix norm $\|\cdot\|_*$ and the upper bound δ/c_2. Now we are ready to derive local stability of system (3.7). We claim that the stability region contains a ball centered at the origin with radius

$$\iota := \min\left\{ \frac{\delta_1}{c_2 \left\| \begin{bmatrix} 0 & C_d \end{bmatrix} \right\|_*}, \frac{\delta_2}{c_2 \left\| \begin{bmatrix} C & 0 \end{bmatrix} \right\|_*} \right\}, \tag{3.8}$$

denoted $\mathfrak{B}(0, \iota)$.

Suppose $|\eta(0)|_* \leq \iota$, by Eq. (3.7),

$$|y_c(0)|_* \leq \left\| \begin{bmatrix} C & 0 \end{bmatrix} \right\|_* |\eta(0)|_* \leq \frac{\delta_2}{c_2},$$

then

$$\|y_c(0)\|_\infty \leq \delta_2,$$

hence

$$z(0) = H_2(y_c(0), z(k-1)) = z(-1) = 0.$$

Accordingly

$$|u_c(0)|_* \leq \left\| \begin{bmatrix} 0 & C_d \end{bmatrix} \right\|_* |\eta(0)|_* \leq \frac{\delta_1}{c_2},$$

indicating

$$\|u_c(0)\|_\infty \leq \delta_1,$$

and

$$v(0) = H_1(u_c(0), v(k-1)) = v(-1) = 0.$$

Therefore

$$\eta(1) = \tilde{A}\eta(0).$$

Similarly,

$$\begin{aligned} |y_c(1)|_* &\leq \left\| \begin{bmatrix} C & 0 \end{bmatrix} \right\|_* |\eta(1)|_* = \left\| \begin{bmatrix} C & 0 \end{bmatrix} \right\|_* \left\|\tilde{A}\right\|_* |\eta(0)|_* \\ &\leq \left\| \begin{bmatrix} C & 0 \end{bmatrix} \right\|_* \left(\rho\left(\tilde{A}\right) + \varepsilon\right) |\eta(0)|_* \leq \frac{\delta_2}{c_2}, \end{aligned}$$

$$\|y_c(1)\|_\infty \leq \delta_2,$$

$$H_2(y_c(1), z(0)) = z(0) = 0.$$

Moreover,

$$\begin{aligned} |u_c(1)|_* &\leq \left\| \begin{bmatrix} 0 & C_d \end{bmatrix} \right\|_* |\eta(1)|_* = \left\| \begin{bmatrix} 0 & C_d \end{bmatrix} \right\|_* \left\|\tilde{A}\right\|_* |\eta(0)|_* \\ &\leq \left\| \begin{bmatrix} 0 & C_d \end{bmatrix} \right\|_* \left(\rho\left(\tilde{A}\right) + \varepsilon\right) |\eta(0)|_* \leq \frac{\delta_1}{c_2}, \end{aligned}$$

indicating

$$\|u_c(1)\|_\infty \leq \delta_1,$$

and

$$v(1) = H_1(u_c(1), v(0)) = v(0) = 0.$$

Then

$$\eta(2) = \tilde{A}\eta(1) = \tilde{A}^2\eta(0)$$

implying there is no updating for the inputs to G and C. Following this process, we see

$$\eta(k) = \tilde{A}^k\eta(0)$$

converges to zero as k tends to ∞. ■

Remark 3.1 Though the origin is locally exponentially stable, it is hard to find the exact stability region except for a scalar system controlled by a static feedback. However, even in this scalar case, the system may have very complex dynamics. We postpone this interesting topic to the next chapter.

Remark 3.2 It is worth pointing out that in this chapter $v(-1)$ and $z(-1)$ are always assumed to be 0. The origin will not be the only fixed point if this condition is relaxed. This problem will be discussed in the following chapters.

Now we return to our analysis of higher dimensional systems in Figure 3.2. We will find a positively invariant set for this system. For simplicity, let $D_d = 0$. Define

$$\check{A} := \begin{bmatrix} A & BC_d \\ -B_dC & A_d \end{bmatrix}, \quad \check{B} := \begin{bmatrix} B & 0 \\ 0 & -B_d \end{bmatrix}, \quad \tilde{B} := \check{B}\tilde{C} = \begin{bmatrix} 0 & BC_d \\ -B_dC & 0 \end{bmatrix}.$$

Since the controller C is stabilizing, the closed-loop system in Figure 3.1 is asymptotically stable. As a result, there exists a Lyapunov function $v(\xi(k)) = \xi'(k)P\xi(k)$ with $P = \begin{bmatrix} P_1 & P_2 \\ P_2' & P_3 \end{bmatrix} > 0$ such that

$$\begin{aligned} \Delta v(\xi(k)) &= \xi'(k+1)P\xi(k+1) - \xi'(k)P\xi(k) \\ &= \xi'(k)\left(\check{A}'P\check{A} - P\right)\xi(k) \\ &= -\|\xi(k)\|_2^2 \quad \text{for all } \xi(k). \end{aligned}$$

Correspondingly, define $v_c(\eta(k)) = \eta'(k)P\eta(k)$; then

$$\begin{aligned} \Delta v_c(\eta(k)) &= \eta'(k+1)P\eta(k+1) - \eta'(k)P\eta(k) \\ &= \eta'(k)\left(\check{A}'P\check{A} - P\right)\eta(k) \\ &\quad +2\eta'(k)\check{A}'P\check{B}\left(\begin{bmatrix} H_1(u_c(k), v(k-1)) \\ H_2(y_c(k), z(k-1)) \end{bmatrix} - \begin{bmatrix} u_c(k) \\ y_c(k) \end{bmatrix}\right) \\ &\quad +\left(\begin{bmatrix} H_1(u_c(k), v(k-1)) \\ H_2(y_c(k), z(k-1)) \end{bmatrix} - \begin{bmatrix} u_c(k) \\ y_c(k) \end{bmatrix}\right)' \check{B}'\cdot \\ &\qquad P\check{B}\left(\begin{bmatrix} H_1(u_c(k), v(k-1)) \\ H_2(y_c(k), z(k-1)) \end{bmatrix} - \begin{bmatrix} u_c(k) \\ y_c(k) \end{bmatrix}\right) \\ &\leq -\|\eta(k)\|_2^2 + 2\|\eta(k)\|_2 \cdot \left\|\check{A}'P\check{B}\right\|_\infty \cdot \gamma \cdot \bar{\delta} + (\gamma\cdot\bar{\delta})^2 \cdot \left\|\check{B}'P\check{B}\right\|_\infty, \end{aligned}$$

where $\gamma = \sqrt{m+p}$ and $\bar{\delta} = \max\{\delta_1, \delta_2\}$. Hence $\Delta v_c(\eta(k)) < 0$ if

$$\|\eta(k)\|_2 > \gamma\cdot\bar{\delta}\left\|\check{A}'P\check{B}\right\|_\infty + \gamma\cdot\bar{\delta}\sqrt{\left\|\check{A}'P\check{B}\right\|_\infty^2 + \left\|\check{B}'P\check{B}\right\|_\infty}.$$

For convenience, define

$$\begin{aligned} r_1 &:= \gamma \cdot \bar{\delta} \left\| \check{A}' P \check{B} \right\|_\infty + \gamma \cdot \bar{\delta} \sqrt{\left\| \check{A}' P \check{B} \right\|_\infty^2 + \left\| \check{B}' P \check{B} \right\|_\infty}, \\ r_2 &:= \left\| \check{A} \right\|_\infty r_1 + \left\| \check{B} \right\|_\infty \bar{\delta}, \end{aligned}$$

then we have

Theorem 3.1 *The set Ω defined by*

$$\Omega := \left\{ \eta \left| \eta'(k) P \eta(k) \leq \max \left\{ \bar{\sigma}(P) r_1^2,\ \bar{\sigma}(P) r_2^2 \right\} \right. \right\}$$

is a positively invariant set, where $\bar{\sigma}(P)$ is the largest singular value of P.

Proof. We need only to show that for each $\eta(0) \in \Omega$, $\eta(k) \in \Omega$ for all $k \geq 1$. Suppose for some integer $k_0 > 0$, we have $\|\eta(k_0)\|_2 \leq r_1$, and $\|\eta(k_0+1)\|_2 > r_1$. Because $\Delta v_c(\eta(k_0+1)) < 0$, $\eta'(k_0+2) P \eta(k_0+2) < \eta'(k_0+1) P \eta(k_0+1)$. Furthermore, it is easy to show that the trajectory will eventually fall into the set $\left\{ \eta \left| \eta'(k) P \eta(k) \leq \bar{\sigma}(P) r_1^2 \right. \right\}$. Therefore it suffices to show $\eta(k_0+1) \in \Omega$. Observing that

$$\|\eta(k_0+1)\|_2 \leq \left\| \check{A} \right\|_\infty r_1 + \left\| \check{B} \right\|_\infty \bar{\delta},$$

one has

$$\eta'(k_0+1) P \eta(k_0+1) \leq \bar{\sigma}(P) r_2^2,$$

which gives $\eta(k_0+1) \in \Omega$. ■

The preceding result ascertains the existence of a positively invariant set for the system shown in Figure 3.2; the system behavior inside this invariant set may be very complex (however we will save the discussion on it for the succeeding chapters). The next result gives an upper bound for all fixed points (to be addressed in the next chapter) of system (3.7).

Defining

$$\Phi := - \begin{bmatrix} I & -C_d (I - A_d)^{-1} B_d + D_d \\ -C (I - A)^{-1} B & I \end{bmatrix}, \tag{3.9}$$

then we have:

Corollary 3.1 *For system (3.7), supposing both G and C are stable, if the matrix $\left(C_d (I - A_d)^{-1} B_d - D_d \right) C (I - A)^{-1} B$ has no eigenvalue at $-1 + j0$, then $\left\| \left(I - \tilde{A} \right)^{-1} \check{B} \right\|_1 \cdot \left\| \Phi^{-1} \right\|_1 \bar{\delta}$ is an upper bound for all fixed points of this system.*

Proof. Suppose $\bar{x}$ is a fixed point of system (3.7), then there are an integer $K > 0$ and some vector ϖ such that

$$\eta(k+1) = \tilde{A}\eta(k) + \begin{bmatrix} B & 0 \\ 0 & B_d \end{bmatrix} \varpi \tag{3.10}$$

for all $k > K$. Letting $k \to \infty$, we get

$$\bar{x} = \tilde{A}\bar{x} + \begin{bmatrix} B & 0 \\ 0 & B_d \end{bmatrix} \varpi,$$

then

$$\bar{x} = \left(I - \tilde{A}\right)^{-1} \begin{bmatrix} B & 0 \\ 0 & B_d \end{bmatrix} \varpi,$$

and

$$\left\| \tilde{C}\bar{x} + \begin{bmatrix} 0 & D_d \\ 0 & 0 \end{bmatrix} \varpi - \varpi \right\|_\infty = \|-\Phi\varpi\|_\infty .$$

Because the matrix $\left(C_d(I - A_d)^{-1} B_d - D_d\right) C(I - A)^{-1} B$ has no eigenvalue at $-1 + j0$, Φ is invertible. Furthermore, because

$$\left\| \tilde{C}\bar{x} + \begin{bmatrix} 0 & D_d \\ 0 & 0 \end{bmatrix} \varpi - \varpi \right\|_\infty \le \bar{\delta},$$

and

$$\|\varpi\|_\infty \le \left\|\Phi^{-1}\right\|_1 \|\Phi\varpi\|_\infty \le \bar{\delta},$$

we have

$$\|\bar{x}\|_\infty \le \left\| \left(I - \tilde{A}\right)^{-1} \tilde{B} \right\|_1 \cdot \left\|\Phi^{-1}\right\|_1 \bar{\delta}. \tag{3.11}$$

Since $\bar{x}$ is arbitrarily chosen, the result follows. ■

In particular, assume we have a scalar system with a static state feedback:

$$\begin{aligned} x(k+1) &= ax(k) + bv(k), \\ u(k) &= -fx(k), \\ v(k) &= H_1(u(k), v(k-1)), \end{aligned} \tag{3.12}$$

where $|a - bf| < 1$. Then following the above procedure, one has

$$|\bar{x}| \le (\delta |bf|) / (1 - |a - bf|),$$

where $\bar{x}$ can be any fixed point.

An upper bound has been found for all fixed points. Will any of these fixed points be stable if either G or C is unstable? We have a result reminiscent of that of [16].

Theorem 3.2 *Assume either G or C is unstable, and $\check{A}$ is invertible. Then the set of all initial points η_0 whose closed-loop trajectories tend to a fixed point as $k \to \infty$ has Lebesgue measure zero.*

Proof. Denote this set by U. Let E^s be the generalized stable eigenspace of system (3.7). Then the Lebesgue measure of E^s is zero for system (3.7) is unstable. Suppose $\eta(0) \in U$, following the process in the proof of Corollary 3.1, there exist $K > 0$ and some vector ϖ such that

$$\eta(K) = \begin{bmatrix} A - BD_dC & BC_d \\ -B_dC & A_d \end{bmatrix} \varpi, \tag{3.13}$$

and Eq. (3.10) holds for all $k > K$. Since $\tilde{A}$ is unstable, $\eta(k) \in E^s$ for all $k \geq K$. Furthermore, the invertibility of $\check{A}$ implies that ϖ is uniquely determined by $\eta(K)$. Due to the uniqueness of the state trajectory of system (3.7), note also that this system is essentially a system with a unit time delay, the trajectory starting from $(\eta(-1) = 0, \eta(0))$ is identical to that starting from $(\varpi, \eta(K))$. Define a mapping F as

$$\begin{aligned} F \quad &: \quad U \to E^s, \\ &\eta(0) \longmapsto \eta(K), \end{aligned} \tag{3.14}$$

where $\eta(0)$ and $\eta(K)$ satisfy Eqs. (3.13) and (3.10), then F is injective. Therefore the Lebesgue measure of U is zero. ■

3.3 An example

In this section, one example will be used to illustrate the effectiveness of the scheme proposed in this paper. In this example, the networked control system consists of two subsystems, each composed of a system and its controller, the outputs of the controllers will be sent respectively to controlled systems via a communication channel (see Figure 3.3). For the ease of notation, we denote the two systems, their controllers and their outputs by G_{d1}, G_{d2}, C_{d1}, C_{d2}, y_1 and y_2 respectively. Here two transmission methods will be compared. One is just to let the outputs transmitted sequentially, i.e., the communication sequence is $[u_1(0), u_2(0), u_1(1), u_2(1), \cdots]$. Another method is to add the nonlinear constraint H_2 to the subsystem composed

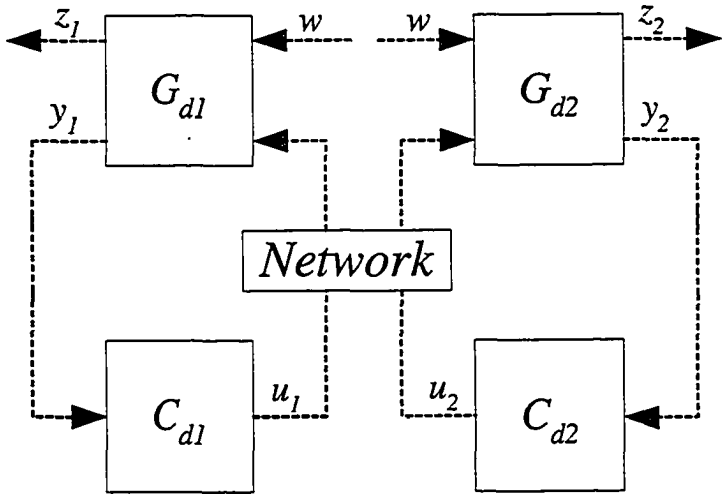

Figure 3.3: A networked control system

of G_{d1} and C_{d1}; if the difference between the two adjacent signals is greater than $\delta_2 = 0.01$, then this subsystem gets access to the network; otherwise the other gets access. Here, we will compare the tracking errors produced under these two schemes respectively. For convenience, we call the first method the *regular static scheduler* and the second the *modified static scheduler*.

The controlled system G_{d1} is:

$$
\begin{aligned}
x_1(k+1) &= \begin{bmatrix} 1.0017 & 0.1000 & 0.0250 & 0.0009 \\ 0.0500 & 1.0000 & 0.5000 & 0.0259 \\ 0.2000 & -0.0003 & 1.0000 & 0.1052 \\ -0.0034 & -0.2103 & -0.0517 & 1.1034 \end{bmatrix} x_1(k) \\
&\quad + \begin{bmatrix} 0.0050 \\ 0.0991 \\ -0.0052 \\ -0.1155 \end{bmatrix} w(k) + \begin{bmatrix} -0.0050 & -0.0000 \\ -0.1000 & -0.0001 \\ 0.0000 & -0.0005 \\ 0.0103 & -0.0105 \end{bmatrix} u_1(k), \\
z_1(k) &= \begin{bmatrix} 1 & 0 & 0 & 0 \\ 1 & 0 & -1 & 0 \end{bmatrix} x_1(k) + \begin{bmatrix} -1 \\ 0 \end{bmatrix} w(k), \\
y_1(k) &= \begin{bmatrix} 1 & 0 & 0 & 0 \\ 0 & 0 & 1 & 0 \end{bmatrix} x_1(k);
\end{aligned}
$$

and G_{d2} is:

$$
\begin{aligned}
x_2(k+1) &= \begin{bmatrix} 1.0000 & 0.0100 & 0.0002 & 0.0000 \\ 0.0005 & 1.0000 & 0.0500 & 0.0003 \\ 0.0200 & -0.0000 & 1.0000 & 0.0101 \\ -0.0000 & -0.0201 & -0.0005 & 1.0100 \end{bmatrix} x_2(k) \\
&\quad + \begin{bmatrix} 0.0000 \\ 0.0100 \\ -0.0001 \\ -0.0102 \end{bmatrix} w(k) + \begin{bmatrix} -0.0000 & -0.0000 \\ -0.0100 & -0.0000 \\ 0.0000 & -0.0000 \\ 0.0001 & -0.0010 \end{bmatrix} u_2(k), \\
z_2(k) &= \begin{bmatrix} 1 & 0 & 0 & 0 \\ 1 & 0 & -1 & 0 \end{bmatrix} x_2(k) + \begin{bmatrix} -1 \\ 0 \end{bmatrix} w(k), \\
y_2(k) &= \begin{bmatrix} 1 & 0 & 0 & 0 \\ 0 & 0 & 1 & 0 \end{bmatrix} x_2(k),
\end{aligned}
$$

where w is a unit step, z_1 and z_2 are tracking errors. Controllers C_{d1} and C_{d2} can be obtained using the technique in [11]. One state space realization of C_{d1} is:

$$
\begin{aligned}
x_{1d}(k+1) &= \begin{bmatrix} 0.4172 & 0.0760 & -0.1735 & 0.0515 \\ 1.9913 & 0.5206 & -3.3773 & 1.0386 \\ 0.0678 & 0.0004 & 0.1875 & 0.1008 \\ -0.6959 & -0.1471 & 0.2780 & 0.9112 \end{bmatrix} x_{1d}(k) \\
&\quad + \begin{bmatrix} 0.6226 & 0.1845 \\ -1.1792 & 3.5968 \\ 0.1272 & 0.8106 \\ 0.5128 & -0.3390 \end{bmatrix} y_1(k), \\
u_1(k) &= \begin{bmatrix} -25.5750 & 4.7948 & 34.7746 & -10.1349 \\ 114.8615 & -1.2995 & -183.9153 & 8.3132 \end{bmatrix} x_{1d}(k) \\
&\quad + \begin{bmatrix} 17.9463 & -31.9727 \\ -105.2714 & 187.5488 \end{bmatrix} y_1(k);
\end{aligned}
$$

and that of C_{d2} is:

$$
\begin{aligned}
x_{2d}(k+1) &= \begin{bmatrix} 0.3810 & 0.0097 & -0.0075 & 0.0007 \\ 0.9331 & 0.9454 & -1.8171 & 0.1305 \\ 0.0059 & 0.0000 & 0.3608 & 0.0100 \\ -0.7141 & -0.0182 & -0.1263 & 0.9999 \end{bmatrix} x_{2d}(k) \\
&\quad + \begin{bmatrix} 0.6195 & 0.0077 \\ -0.8259 & 1.8477 \\ 0.0140 & 0.6392 \\ 0.7027 & 0.1220 \end{bmatrix} y_2(k), \\
u_2(k) &= \begin{bmatrix} -143.7379 & 5.4551 & 215.1570 & -13.0276 \\ 1082.1 & -1.3339 & -1713.7 & 8.8012 \end{bmatrix} x_{2d}(k) \\
&\quad + \begin{bmatrix} 133.0660 & -213.2245 \\ -1071.9 & 1717.6 \end{bmatrix} y_2(k).
\end{aligned}
$$

The simulation results are shown in Figure 3.4 and Figure 3.5.

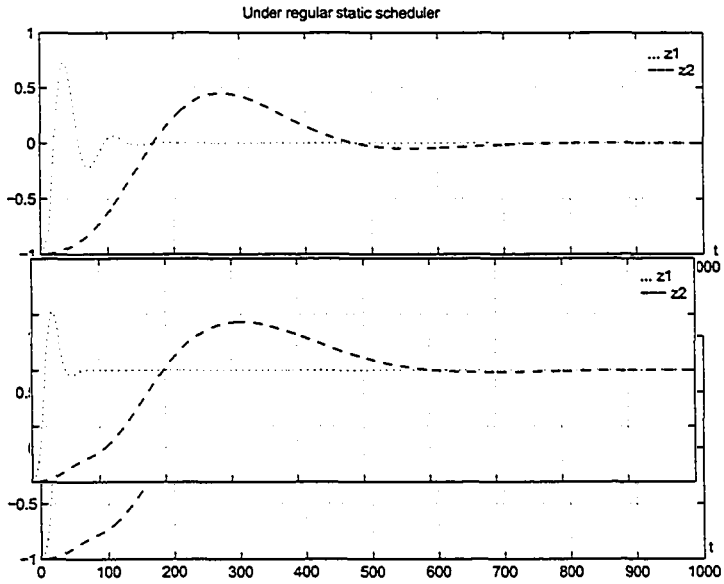

Figure 3.4: The first elements of z_1 and z_2

From these two figures, one sees that the tracking error approaches zero faster under the modified static schedular than under the regular one. Note that both G_{d1} and G_{d2} are unstable. If one of the two systems is stable, one can expect better convergence rates under the modified static scheduler. In essence, our scheme is based on the following principle: Allocate access to the network to the systems with faster dynamics first, then take care of the systems of slower dynamics. In this way, we hope we can improve system performance.

3.4 Conclusions

In this chapter, a new networked control technique is proposed and its effectiveness is illustrated via simulations. The dynamics of the system in Figure 3.2 will be discussed in the next several chapters. More discussions on the controller design based on this transmission strategy will also be discussed later in Chapter 9.

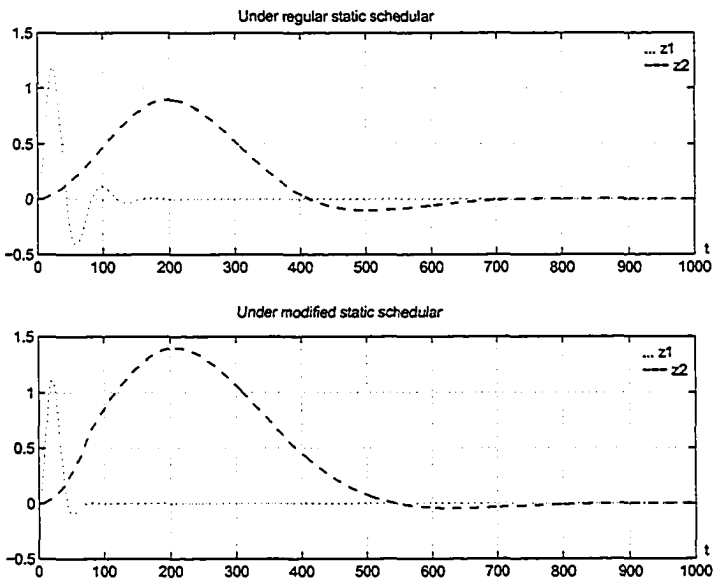

Figure 3.5: The second elements of z_1 and z_2

Chapter 4

Chaos: one-dimensional case I

The behavior of the system shown in Figure 3.2 will be studied in considerable detail in this and several successive chapters. This chapter concentrates on the scalar case. It turns out that this nonlinear system exhibits very interesting dynamical behaviors: in addition to local stability, its trajectories may converge to a non-origin fixed point or be periodic or just be oscillatory. Furthermore this system shows sensitive dependence on initial conditions — an indication of chaos.

4.1 Examples

To get a flavor of the complexity that the system shown in Figure 3.2 may exhibit, let us first look at a simple one-dimensional case:

$$\begin{aligned} x(k+1) &= ax(k) + bv(k), \\ u_c(k) &= x(k), \end{aligned} \tag{4.1}$$

with $v(-1) \in \mathbb{R}$ instead of fixing it to be 0; and for $k \geq 0$,

$$v(k) = H_1\left(u_c(k), v(k-1)\right) = \begin{cases} u_c(k), & \text{if } |u_c(k) - v(k-1)| > \delta_1, \\ v(k-1), & \text{otherwise,} \end{cases}$$

where $\delta_1 = 0.01$. System (4.1) is a static state feedback system with the feedback gain equal to -1. Note that in this example there is no constraint on the output of the system G. Now let $a = 9/10$ and $b = -3/10$. By choosing different initial values $(v(-1), x(0))$, Figures 4.1–4.2 are obtained. In these two figures, the horizontal

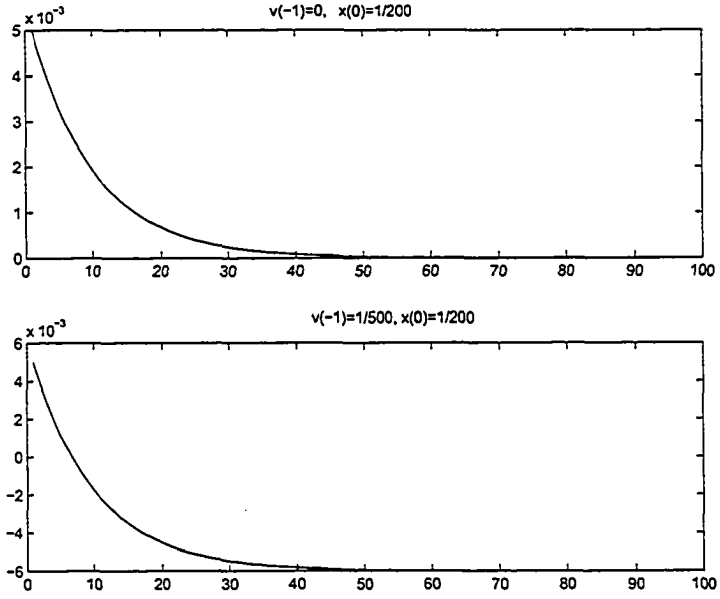

Figure 4.1: Two trajectories converging to different fixed points

axis stands for the iteration time k, and the vertical axis denotes the value of x. It is clear from these two figures that different initial conditions give rise to significantly different types of trajectories: the first converging to the origin while the second converging to a non-origin point and the last just oscillating. Furthermore, system

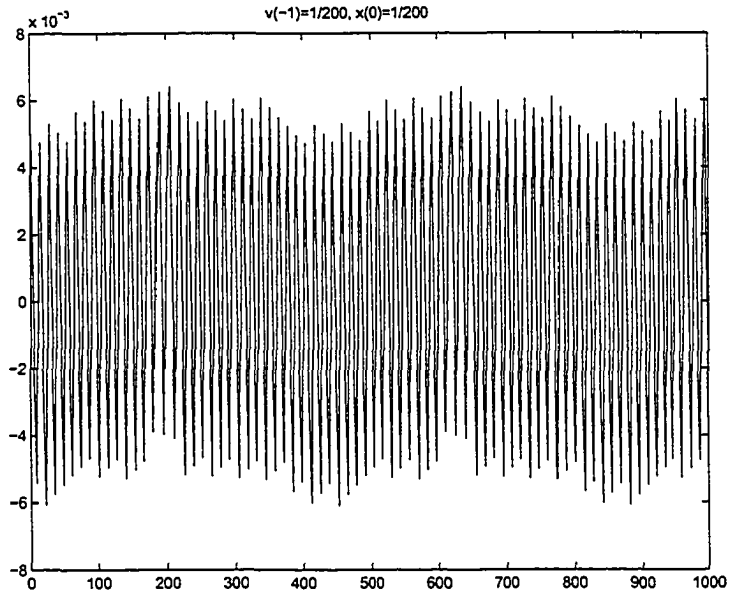

Figure 4.2: An aperiodic trajectory

(4.1) is actually able to exhibit "chaotic" behavior, namely, sensitive dependence on initial conditions. Figure 4.3 reveals this phenomenon clearly. Is the trajectory in the lower part of Figure 4.3 aperiodic? Figure 4.4 is its spectrum produced using the function "pmtm" in Matlab. One can see that this trajectory contains a broad band of frequencies.

Next let $a = 1$ and $b = -3/10$, and one gets Figures 4.5–4.6 where the horizontal axis denotes $v(k-1)$ and the vertical axis stands for $x(k)$. The first two (in Figure 4.5) are eventually periodic orbits of different periods, the third one (in Figure 4.6) is aperiodic.

The complicated behavior of the system shown in Figure 3.2 is due to its nonlinearity induced by the switching law. To some extent, invariant sets provide some measure of how complex the dynamics of a system is. According to the above examples, the invariant sets of system (4.1) may consist of not only the origin, non-origin fixed points (Figure 4.1), but also periodic (Figure 4.5) and aperiodic orbits (Figure 4.6). Furthermore, it may contain a strange attractor if chaos is indeed present in the system. In the rest of this chapter, we will analyze the dynamics of this system. We always assume that $|a+b| < 1$ which guarantees the boundedness of trajectories

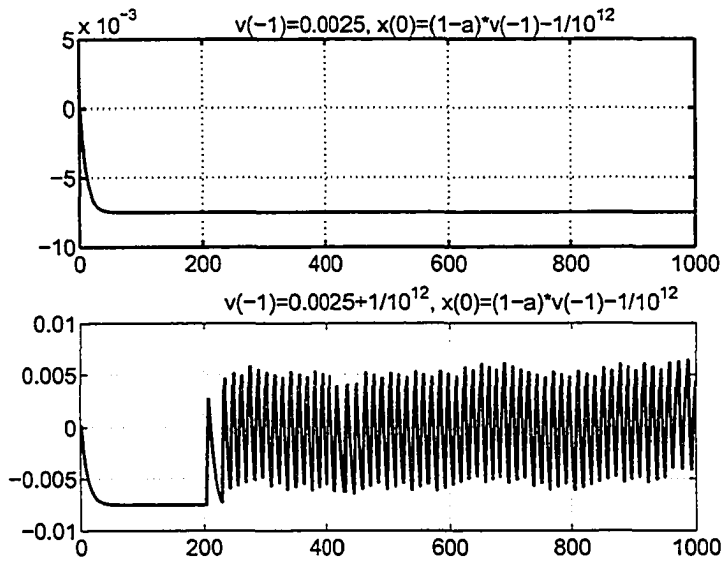

Figure 4.3: Sensitive dependence on initial conditions

of the system.

4.2 The case with $|a| < 1$

For convenience, define

$$\xi(k) := \begin{bmatrix} v(k-1) \\ x(k) \end{bmatrix},$$

then system (4.1) can be written as

$$\begin{aligned} \xi(k+1) &= \begin{bmatrix} 1 & 0 \\ b & a \end{bmatrix} \xi(k) + s_k \begin{bmatrix} -1 & 1 \\ -b & b \end{bmatrix} \xi(k) \\ &:= (A + s_k B)\,\xi(k) := F(\xi(k)),\ \forall k \geq 0, \end{aligned} \tag{4.2}$$

where

$$\begin{aligned} s_k &= 1 \text{ if } |x(k) - v(k-1)| > \delta; \\ s_k &= 0 \text{ if } |x(k) - v(k-1)| \leq \delta. \end{aligned} \tag{4.3}$$

Based on this representation, the fixed points of the system constitute a line segment:

$$x = \frac{b}{1-a} v_-, \tag{4.4}$$

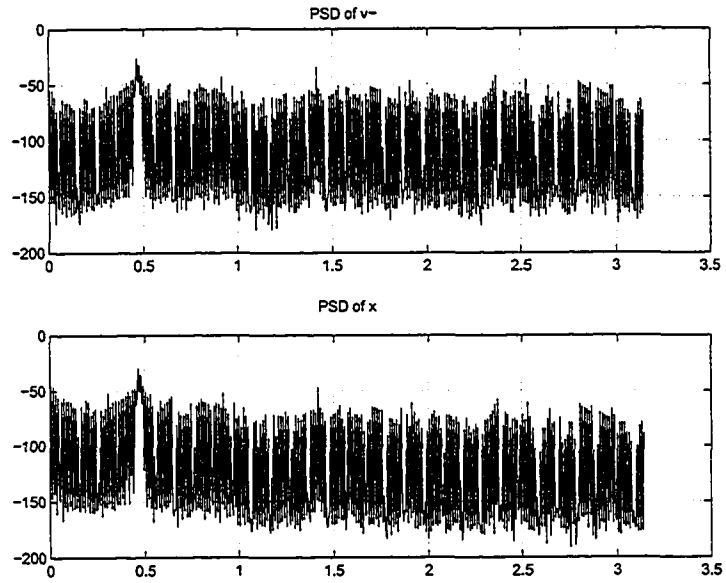

Figure 4.4: Spectrum of an aperiodic orbit

which lies in the region:

$$|x - v_-| \leq \delta. \tag{4.5}$$

(Note that v_- indicates that v is one step behind x.) For local stability of fixed points, we have the following result.

Proposition 4.1 *For system (4.2) with $|a| < 1$, a local stability region, denoted by $R_{loc} \subset \mathbb{R}^2$, of its fixed points is the region encircled by*

$$|x - v_-| = \delta, \tag{4.6}$$

and

$$|v_-| = \frac{1 - |a|}{1 - (a + b)}\delta. \tag{4.7}$$

Proof. Given an initial point $(v(-1), x(0)) \in R_{loc}$, we have

$$x(1) = ax(0) + bv(-1).$$

In general,

$$x(k) = a^k x(0) + \sum_{i=0}^{k-1} a^i bv(-1), \tag{4.8}$$

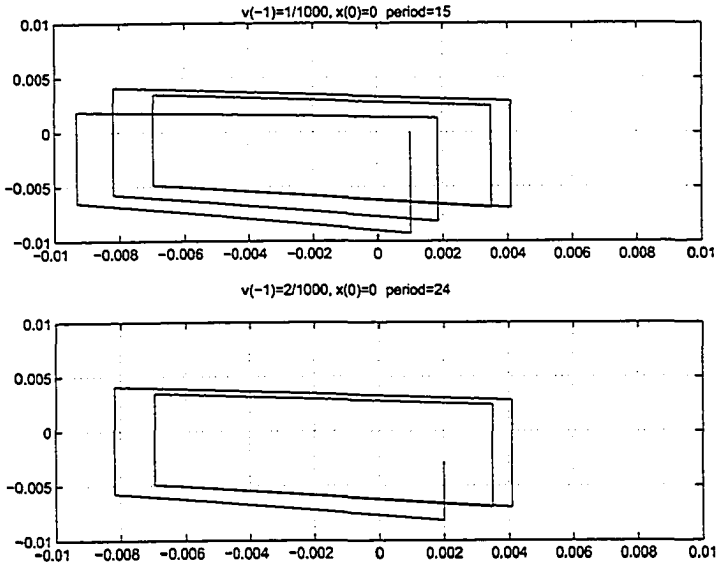

Figure 4.5: Two periodic orbits

provided that

$$|x(k) - v(-1)| \leq \delta, \ \forall k > 0. \tag{4.9}$$

Now we show that Eq. (4.9) indeed holds.

Note that

$$\begin{aligned} x(k) - v(-1) &= a^k x(0) + \sum_{i=0}^{k-1} a^i b v(-1) - v(-1) \\ &= a^k (x(0) - v(-1)) + \left(1 - a^k\right) \frac{b + a - 1}{1 - a} v(-1), \end{aligned}$$

one has

$$|x(k) - v(-1)| \leq \left|a^k\right| |x(0) - v(-1)| + \left(1 - a^k\right) \frac{1 - (a+b)}{1 - a} |v(-1)|.$$

If $0 \leq a < 1$, then

$$|x(k) - v(-1)| \leq a^k \delta + \left(1 - a^k\right) \frac{1 - (a+b)}{1 - a} \frac{1 - a}{1 - (a+b)} \delta = \delta.$$

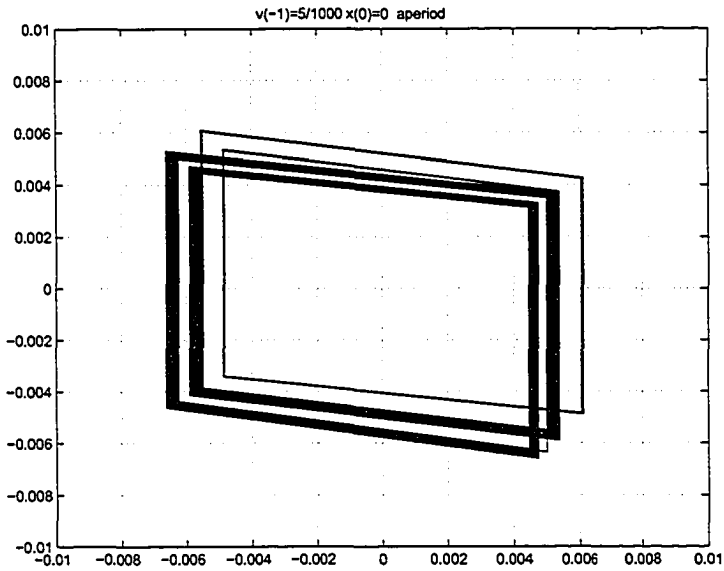

Figure 4.6: An aperiodic orbit

If $-1 < a < 0$ and $a^k > 0$, then

$$\begin{aligned} |x(k) - v(-1)| &\leq a^k\delta + \left(1 - a^k\right)\frac{1-(a+b)}{1-a}\frac{1+a}{1-(a+b)}\delta \\ &= \left(a^k + \left(1-a^k\right)\frac{1+a}{1-a}\right)\delta \\ &\leq \left(a^k + \left(1-a^k\right)\right)\delta = \delta. \end{aligned}$$

If $-1 < a < 0$ and $a^k < 0$, then

$$\begin{aligned} |x(k) - v(-1)| &\leq -a^k\delta + \left(1 - a^k\right)\frac{1-(a+b)}{1-a}\frac{1+a}{1-(a+b)}\delta \\ &= \left(-a^k + \left(1-a^k\right)\frac{1+a}{1-a}\right)\delta \\ &= \frac{1+a-2a^k}{1-a}\delta. \end{aligned}$$

Therefore it suffices to show that

$$\frac{1+a-2a^k}{1-a} \leq 1. \tag{4.10}$$

However, Eq. (4.10) is equivalent to

$$a \leq a^k,$$

which certainly holds for $-1 < a < 0$ and $a^k < 0$. By taking limit in Eq. (4.8) with respect to k, $(v(k-1), x(k))$ converges to a fixed point defined by Eqs. (4.4)-(4.5). The proof is completed. ■

Having identified a local stability region, next we will study the following problem: Can the exact stability region of the fixed points be larger than the region given in Proposition 4.1? We will see that this problem is actually a difficult one in that it depends on system parameters in a complicated manner. Before doing so, we first concentrate on the "one-dimensional case", namely, the dynamics of x instead of both x and v, and get one of its global attracting regions.

Proposition 4.2 *A global attracting region of x is given by*

$$|x| \leq \frac{|b|}{1-|a+b|}\delta. \tag{4.11}$$

Furthermore, it is positively invariant.

Proof. According to Eq. (4.1),

$$\begin{aligned}
x(1) &= ax(0) + bv(0) = (a+b)x(0) + b(v(0) - x(0)), \\
x(2) &= ax(1) + bv(1) \\
&= (a+b)^2 x(0) + (a+b)b(v(0) - x(0)) + b(v(1) - x(1)), \\
&\vdots \\
x(k) &= (a+b)^k x(0) + \sum_{i=0}^{k-1} (a+b)^i b(v(k-1-i) - x(k-1-i)),
\end{aligned}$$

hence

$$|x(n)| \leq |a+b|^n |x(0)| + \frac{1-|a+b|^n}{1-|a+b|}|b|\delta, \ \forall n \geq 1. \tag{4.12}$$

By taking limit on both sides, one gets a global attracting region given by Eq. (4.11). Moreover, if

$$|x(0)| \leq \frac{|b|}{1-|a+b|}\delta,$$

then

$$|x(n)| \leq \frac{|b|}{1-|a+b|}\delta, \quad \forall n \geq 1,$$

implying that the region given by Eq. (4.11) is positively invariant. ■

Based on this observation, we are ready to derive a global positive invariant set for system (4.2).

Theorem 4.1 *For system (4.2), if*

$$\frac{|b|}{1-|a+b|} > \frac{1-|a|}{1-(a+b)},$$

then the region defined by

$$|x| \leq \frac{|b|}{1-|a+b|}\delta,$$

and

$$|v_-| \leq \frac{|b|}{1-|a+b|}\delta$$

is a global positively invariant set. Otherwise, the region defined by

$$|x| \leq \frac{1-|a|}{1-(a+b)}\delta,$$

and

$$|v_-| \leq \frac{1-|a|}{1-(a+b)}\delta$$

is globally attracting, which indicates that the set of fixed points given by Eqs. (4.4)-(4.5) is the unique invariant set of the system (For convenience, we call such a system a generic one).

Proof. It readily follows from Propositions 4.1 and 4.2. ■

Remark 4.1 It is easy to show that Proposition 4.2 and Theorem 4.1 hold for all systems of the form of Eq. (4.1) satisfying $|a+b| < 1$.

The following result is an immediate consequence of Theorem 4.1.

Corollary 4.1 *If system (4.2) satisfies either of*

- $a > 0$ *and* $b > 0$;
- $a < 0$ *and* $b < 0$,

then it is a generic system.

Proof. Suppose $a > 0$ and $b > 0$. Then

$$\frac{|b|}{1-|a+b|} = \frac{b}{1-(a+b)} \leq \frac{1-a}{1-(a+b)} = \frac{1-|a|}{1-(a+b)}.$$

Hence the system is generic. On the other hand, given $a < 0$ and $b < 0$,

$$\frac{|b|}{1-|a+b|} = \frac{-b}{1+(a+b)}, \quad \frac{1-|a|}{1-(a+b)} = \frac{1+a}{1-(a+b)}.$$

Observe that

$$\frac{-b}{1+(a+b)} \leq \frac{1+a}{1-(a+b)}$$

is equivalent to

$$a^2 \leq 1+b^2,$$

which says

$$\frac{|b|}{1-|a+b|} \leq \frac{1-|a|}{1-(a+b)},$$

therefore, the system is generic. ■

Theorem 4.1 tells us that, in order to have complex dynamics,

$$\frac{|b|}{1-|a+b|} > \frac{1-|a|}{1-(a+b)} \tag{4.13}$$

must be satisfied. However, this is *not* a sufficient condition. For the case when

$$a = \frac{9}{10}, \; b = -\frac{3}{10},$$

(which satisfies Eq. (4.13)), we have already known that the system exhibits complicated dynamics (see Figures 4.1–4.4). However, for the case when

$$a = \frac{3}{10}, \; b = -\frac{9}{10},$$

which also satisfies Eq. (4.13), there is no complex dynamic behavior, i.e., the system is generic. The following argument provides a simple interpretation for this specific system.

Given $(v(-1), x(0))$ satisfying

$$|x(0) - v(-1)| > \delta,$$

one has

$$\begin{aligned} x(1) &= (a+b)x(0), \\ v(0) &= x(0). \end{aligned}$$

Suppose

$$|x(1) - v(0)| > \delta,$$

then

$$|x(0)| > \frac{\delta}{1-(a+b)}, \tag{4.14}$$

and

$$\begin{aligned} x(2) &= (a+b)\,x(1) = (a+b)^2 x(0), \\ v(1) &= x(1) = (a+b)\,x(0). \end{aligned}$$

If

$$|x(2) - v(1)| \leq \delta, \tag{4.15}$$

and

$$|v(1)| \leq \frac{1-|a|}{1-(a+b)}\delta,$$

then the trajectory will converge to some fixed point. Meanwhile,

$$|x(0)| \leq \frac{1-|a|}{1-(a+b)}\frac{1}{|a+b|}\delta. \tag{4.16}$$

Note that Eq. (4.15) naturally holds if Eq. (4.14) is satisfied. Therefore, only

$$\frac{\delta}{1-(a+b)} \leq \frac{1-|a|}{1-(a+b)}\frac{1}{|a+b|}\delta \tag{4.17}$$

is required. Moreover, Eq. (4.17) is equivalent to

$$-b \leq 1. \tag{4.18}$$

Systems with

$$a = \frac{3}{10},\ b = -\frac{9}{10}, \tag{4.19}$$

and

$$a = \frac{8}{10},\ b = -\frac{9}{10}, \tag{4.20}$$

both satisfy Eq. (4.18). However, for a sufficiently large time k, any trajectory $(v(k-1), x(k))$ governed by Eq. (4.19) will satisfy

$$|x(k) - v(k-1)| > \delta,$$

and

$$|x(k)| > \frac{\delta}{1-(a+b)}.$$

Consequently, in view of the foregoing discussions, it will converge to a certain fixed point. On the other hand, some trajectories $(v(k-1), x(k))$ governed by Eq. (4.20) violates these two conditions, predicting complex dynamics, see Figure 4.9 for one trajectory of this system.

We have already analyzed three cases:

- $a > 0$ and $b > 0$;
- $a < 0$ and $b < 0$;
- $a > 0$ and $b < 0$.

What about the case that $a < 0$ and $b > 0$? Next we will prove that such a system is generic. It is easy to see that the transition matrix of the system in Eq. (4.1) is some combination of $(a+b)^k$ and $\left(a^m + \sum_{i=0}^{m-1} a^i b\right)$ with the scalar multiplication as the involved operation, where $k \geq 0$ and $m > 1$. Because $|a+b| < 1$, if

$$\left| a^m + \sum_{i=0}^{m-1} a^i b \right| < 1 \tag{4.21}$$

for all $m > 1$, the state x will tend to the origin unless it reaches another fixed point. In this case, the system is generic. A direct calculation shows that Eq. (4.21) is equivalent to

$$0 \leq (1-a^m)\frac{1-(a+b)}{1-a} \leq 2. \tag{4.22}$$

Given $a < 0$ and $b > 0$, define

$$f(m) := (1-a^m)\frac{1-(a+b)}{1-a}, \quad \forall m > 1,$$

then

$$f(m) \geq 0, \quad \forall m > 1,$$

and

$$f(3) = \max_{m>1} f(m).$$

However,

$$\begin{aligned} f(3)-2 &= \left(1-a^3\right)\frac{1-(a+b)}{1-a}-2 \\ &= \left(1+a+a^2\right)(1-(a+b))-2 \\ &\leq 0. \end{aligned}$$

Hence, Eq. (4.22) (then Eq. (4.21)) holds for all $m > 1$, indicating the system is generic.

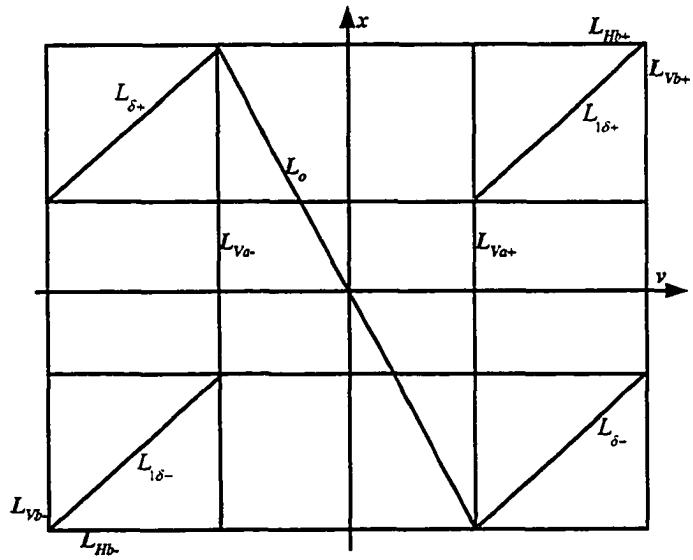

Figure 4.7: Diagram for the case when $a = 0.9$ and $b = -0.3$

In the rest of this section, we will concentrate on a specific system and study its complex dynamics. For the ease of presentation, we rewrite system (4.1):

$$\begin{aligned} x(k+1) &= ax(k)+bv(k), \\ u_c(k) &= x(k). \end{aligned} \tag{4.23}$$

Fix $a = 9/10$, $b = -3/10$, $v(-1) \in \mathbb{R}$, and for $k \geq 0$,

$$v(k) = H_1\left(u_c(k), v(k-1)\right) = \begin{cases} u_c(k), & \text{if } |u_c(k)-v(k-1)| > \frac{1}{100}, \\ v(k-1), & \text{otherwise.} \end{cases}$$

We make the following definitions (Figure 4.7):

$$
\begin{aligned}
L_{Hb+} &:= \left\{\left(v_-, \frac{-b}{1-|a+b|}\delta\right) : |v_-| \le \frac{-b}{1-|a+b|}\delta\right\},\\
L_{Hb-} &:= \left\{\left(v_-, \frac{b}{1-|a+b|}\delta\right) : |v_-| \le \frac{-b}{1-|a+b|}\delta\right\},\\
L_{Vb+} &:= \left\{\left(\frac{-b}{1-|a+b|}\delta, x\right) : |x| \le \frac{-b}{1-|a+b|}\delta\right\},\\
L_{Vb-} &:= \left\{\left(\frac{b}{1-|a+b|}\delta, x\right) : |x| \le \frac{-b}{1-|a+b|}\delta\right\},\\
I_b &:= \left\{(v_-, x) : |v_-| \le \frac{-b}{1-|a+b|}\delta,\ |x| \le \frac{-b}{1-|a+b|}\delta\right\}.
\end{aligned}
$$

$$
\begin{aligned}
L_{Va+} &:= \left\{\left(\frac{1-|a|}{1-(a+b)}\delta, x\right) : |x| \le \frac{-b}{1-(a+b)}\delta\right\},\\
L_{Va-} &:= \left\{\left(-\frac{1-|a|}{1-(a+b)}\delta, x\right) : |x| \le \frac{-b}{1-(a+b)}\delta\right\},\\
I_a &:= \left\{(v_-, x) \in I_b : |v_-| \le \frac{1-|a|}{1-(a+b)}\delta,\ |x| \le \frac{-b}{1-|a+b|}\delta\right\}.
\end{aligned}
$$

$$
\begin{aligned}
L_o &:= \left\{(v_-, x) \in I_a : x = \frac{b}{1-a}v_-\right\},\\
L_{\delta+} &:= \{(v_-, x) \in I_b : x - v_- = \delta\},\\
L_{\delta-} &:= \{(v_-, x) \in I_b : x - v_- = -\delta\},\\
L_{1\delta+} &:= \left\{(v_-, x) \in I_b : x = (a+b)\,v_-,\ v_- > \frac{1-|a|}{1-(a+b)}\delta\right\},\\
L_{1\delta-} &:= \left\{(v_-, x) \in I_b : x = (a+b)\,v_-,\ v_- < -\frac{1-|a|}{1-(a+b)}\delta\right\}.
\end{aligned}
$$

Clearly, L_o is the set of fixed points, I_a is a local stability region of L_o, and I_b is a global attracting region and is also positively invariant. Denote the two endpoints of L_o by E^+ and E^-, namely, $E^+ = \left(-\frac{1-|a|}{1-(a+b)}\delta, -\frac{1-|a|}{1-(a+b)}\delta + \delta\right)$ and $E^- = \left(\frac{1-|a|}{1-(a+b)}\delta, \frac{1-|a|}{1-(a+b)}\delta - \delta\right)$. Define

$$
E_s := L_o \backslash \{E^+, E^-\} = \{(v_-, x) \in L_o : (v_-, x) \notin \{E^+, E^-\}\}.
$$

Then each point in E_s is stable in the sense of Lyapunov, however it is *not* asymptotically. As for the stability of E^+ (resp. E^-), each trajectory starting from a point in I_b on the line $v_- = -\frac{1-|a|}{1-(a+b)}\delta$ (resp. the line $v_- = \frac{1-|a|}{1-(a+b)}\delta$) will converge to E^+ (resp. E^-). What about trajectories starting from points in $I_b \backslash I_a$ which

are sufficiently close to E^+ (resp. E^-)? More generally. can a trajectory starting within $I_b \backslash I_a$ somehow wander off into I_a, thus converging to a certain fixed point on L_o? It turns out this will never happen. Therefore the two fixed points E^+ (resp. E^-) are *not* stable. To wit, we need some preparations.

For convenience, we regard system (4.23) as a map, i.e., adopt the notation defined in Eq. (4.2):

$$\xi(k+1) = F(\xi(k)).$$

Given a set $\Omega \subset I_b$, define

$$\mathrm{pre}^n(\Omega) := \{(v_-, x) \in I_b : F^n((v_-, x)) \subset \Omega\}, \quad \forall n \geq 0, \tag{4.24}$$

where $F^0((v_-, x)) := (v_-, x)$; iteratively

$$F^n((v_-, x)) = F^{n-1}((v_-, x)) \text{ for } n \geq 1.$$

Then it is easy to show that

$$\begin{aligned} L_{\delta-} \backslash \left\{ \left(\frac{1-|a|}{1-(a+b)}\delta, \frac{1-|a|}{1-(a+b)}\delta - \delta \right) \right\} &\subset \mathrm{pre}^2(L_{1\delta-}), \\ L_{\delta+} \backslash \left\{ \left(-\frac{1-|a|}{1-(a+b)}\delta, -\frac{1-|a|}{1-(a+b)}\delta + \delta \right) \right\} &\subset \mathrm{pre}^2(L_{1\delta+}). \end{aligned}$$

Based on this observation, one has

$$F(I_b \backslash \{L_{Va-} \cup L_{Va+}\}) \subset I_b \backslash \{L_{Va-} \cup L_{Va+}\},$$

i.e., $I_b \backslash \{L_{Va-} \cup L_{Va+}\}$ is positively invariant. As a consequence, in particular, trajectories starting from points in $I_b \backslash \{L_{Va-} \cup L_{Va+}\}$, no matter how close to E^+ (resp. E^-) initially, will *not* converge to E^+ (resp. E^-), indicating that neither E^+ nor E^- is locally stable.

Moreover, for a given set $\Omega \subset I_b \backslash \{L_{Va-} \cup L_{Va+}\}$, define

$$\begin{aligned} \mathrm{Img}^n(\Omega) &:= \{F^n(\Omega)\}, \\ \Psi(\Omega) &:= \cup_{n=0}^{\infty} \mathrm{Img}^n(\Omega). \end{aligned}$$

Then it is easy to verify that

$$\begin{aligned} F(\Psi(L_{1\delta+})) &\subset \Psi(L_{1\delta+}), \\ F(\Psi(L_{1\delta-})) &\subset \Psi(L_{1\delta-}), \end{aligned}$$

which furthermore imply all trajectories starting within $I_b \backslash \{L_{Va-} \cup L_{Va+}\}$ will eventually move along the line segments $\Psi(L_{1\delta+}) = \Psi(L_{1\delta-})$. For a point $\xi \in I_b \backslash I_a$, let $\omega(x)$ denote its $\omega-$limit set. Define

$$\omega(I_b \backslash I_a) := \cup_{\xi \in I_b \backslash I_a} \omega(\xi),$$

then

$$\omega(\in I_b \backslash I_a) \subset \Psi(L_{1\delta+}).$$

Obviously

$$\omega(I_a) = L_o.$$

Thus we get a characterization of the $\omega-$limit sets of system (4.23). However, we have to admit that this characterization is crude because all trajectories starting within $I_b \backslash I_a$ will eventually move along merely a part of each line segment in $\Psi(L_{1\delta+})$ instead of the whole line segment. Figure 4.8 given later will visualize this observation. Now the problem of finding the exact $\omega-$limit sets of the system is still under our study. Nevertheless, adopting the argument on pp. 24 in [85], it is easy, though not straightforward due to the nature of the map F, to show that these $\omega-$limit sets are indeed *invariant*. Based on extensive simulations, it is speculated that these $\omega-$limit sets are also *topologically transitive*. However, up to now there still lacks solid theoretic background to support this conjecture.

Based on the above analysis, it is fair to say that the dynamics of system (4.23) is remarkably complicated: It indeed exhibits the feature of sensitive dependence on initial conditions, this sensitivity locates only on $\cup_{n=0}^{\infty}(\text{pre}^n(L_{\delta-}) \cup \text{pre}^n(L_{\delta+}))$, a subset of $\cup_{n=0}^{\infty}(\text{pre}^n(L_{1\delta-} \cup L_{1\delta+}))$. Hence it is weakly chaotic. Next we will calculate its generalized topological entropy discussed in [40] and [25].

Denote by I_{binv+} the region encircled by the lines L_{Va+}, L_{Vb+}, $L_{1\delta+}$ and $\text{Img}^1(L_{\delta-})$. Similarly denote the region encircled by the lines L_{Va-}, L_{Vb-}, $L_{1\delta-}$ and $\text{Img}^1(L_{\delta+})$ by I_{binv-}. In view of the foregoing argument, we have the following claim:

Claim 4.1 The steady state of the system will settle in the region $I_{binv+} \cup I_{binv-}$.

This claim is a straightforward application of the preceding analysis, however it plays an important role in the calculation of the topological entropy of the system.

For the definition of the topological entropy for piecewise monotone maps with discontinuities, please refer to [40]. Now we will give a construction in order to compute the topological entropy for our system, which is clearly piecewise monotone (under some metric defined on the system rather than under the usual Euclidean metric; however, this is not essential.) with discontinuities.

Define

$$\begin{aligned} \mathrm{Pim}_F(0) &:= \{L_{\delta-}, L_{\delta+}\}, \\ \mathrm{Pim}_F(1) &:= \{L : L \cap \mathrm{Pim}_F(0) = \phi, F(L) \subset \mathrm{Pim}_F(0)\}, \\ &\vdots \\ \mathrm{Pim}_F(m) &:= \left\{L : L \cap \left(\cup_{i=0}^{m-1} \mathrm{Pim}_F(0)\right) = \phi, F^m(L) \subset \mathrm{Pim}_F(0)\right\}, \quad m \geq 1, \end{aligned} \tag{4.25}$$

where ϕ stands for the empty set. Note that the elements in each $\mathrm{Pim}_F(m)$ are line segments.

Denote by $\#(\mathrm{Pim}_F(m))$ the number of elements in $\mathrm{Pim}_F(m)$.

Before calculating the topological entropy, one has to pay a bit more attention to the map F. Clearly, according to Figure 4.7 there exists a positive integer M such that

$$\begin{aligned} \mathrm{pre}^{M+l}(L_{\delta+}) \cap L_{1\delta-} &\neq \phi, \\ \mathrm{pre}^{M+l}(L_{\delta-}) \cap L_{1\delta+} &\neq \phi, \quad \forall l \geq 1. \end{aligned} \tag{4.26}$$

In fact, each set of intersections contains exactly one element (one line segment). For each given integer $n > 0$, define

$$\#F(n) := \sum_{m=0}^{n} \#(\mathrm{Pim}_F(m)),$$

and define the *topological entropy* of F as

$$\aleph(F) := \lim_{n \to \infty} \frac{\log \#F(n)}{n}, \tag{4.27}$$

which turns out to be well-defined (see the proof below). Then we have

Theorem 4.2 *For system (4.23), the following statements hold:*

- *For $m \leq M$,*

$$\#(\mathrm{Pim_F(m)}) = 2. \tag{4.28}$$

- *For $m > M$,*

$$\#\left(\mathrm{Pim_F\,(m)}\right) = 2 + 2 \cdot (m - M)\,, \tag{4.29}$$

and

$$\aleph\,(F) = 0. \tag{4.30}$$

Proof. Eq. (4.28) is self-evident, Eq. (4.29) follows from Claim 1 by restricting $\#\left(\mathrm{Pim}_F\,(m)\right)$ on $I_{binv+} \cup I_{binv-}$ for $m > M$ and the analysis above. Then for sufficiently large n $(n \geq M)$,

$$\#F(n) = 2\,(M+1) + 2\frac{(n-M)\,(n-M+1)}{2},$$

thus

$$\begin{aligned} \aleph\,(F) &:= \lim_{n\to\infty} \frac{\log \#F(n)}{n} \\ &= \lim_{n\to\infty} \frac{\log\left(2\,(M+1) + (n-M)\,(n-M+1)\right)}{n} \\ &= 0. \end{aligned}$$

The proof is completed. ∎

Remark 4.2 In light of this result, from the perspective of topological entropies, our system is weakly chaotic.

The above discussion is mainly for the case that $|b| < a$. For example, given $a = 0.9$ and $b = -0.3$, Figure 4.8 plots the steady state of a trajectory, namely, its asymptotic behavior, where the horizontal axis is v_- and the vertical one stands for x. Now consider the case that $a = 0.8$ and $b = -0.9$, hence $|b| > a$, and we also draw its asymptotic behavior, as shown in Figure 4.9, starting from the same initial point as the above. We observe that their asymptotic behaviors are vastly different. The underlying reason is still unclear up to now.

Having done the above analysis, maybe it is time now to pose some problems.

Problem 4.1 *Given a, b and δ, how to find the exact ω−limit set of system Eq. (4.1)?*

Problem 4.2 *Why are the asymptotic behaviors of the systems with $|b| < a$ and $|b| > a$ dramatically different?*

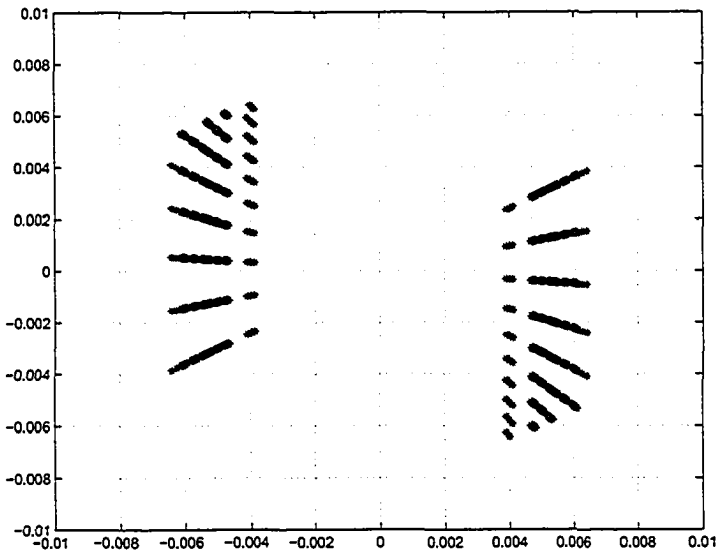

Figure 4.8: The asymptotic behavior of a trajectory for $|b| < a$

4.3 The case with $a = 1$

Let $a = 1$. Then system (4.1) becomes

$$\begin{aligned} x(k+1) &= x(k) + bv(k), \\ u_c(k) &= x(k), \end{aligned} \tag{4.31}$$

where $|1 + b| < 1$. Let $v(-1) \in \mathbb{R}$, and for $k \geq 0$,

$$v(k) = H_1\left(u_c\left(k\right), v(k-1)\right) = \begin{cases} u_c(k), & \text{if } |u_c\left(k\right) - v\left(k-1\right)| > \frac{1}{100}, \\ v(k-1), & \text{otherwise.} \end{cases}$$

In this case, Figure 4.7 is now Figure 4.10. We note that here the two lines $L_{1\delta+}$ and $L_{1\delta-}$ merge at the origin. L_o, the line segment of fixed points, coincides with the vertical axis, so do L_{Va+} and L_{Va-}.

Figures 4.5–4.6 show that the dynamics of system (4.31) can be fairly complicated. The rest of this section studies the problem when the system will have periodic orbits. From now on, assume

$$-1 \leq b < 0.$$

Define

$$\Gamma_{in} := \{(v_-, x) \in I_b : |x - v_-| \leq \delta\}, \tag{4.32}$$

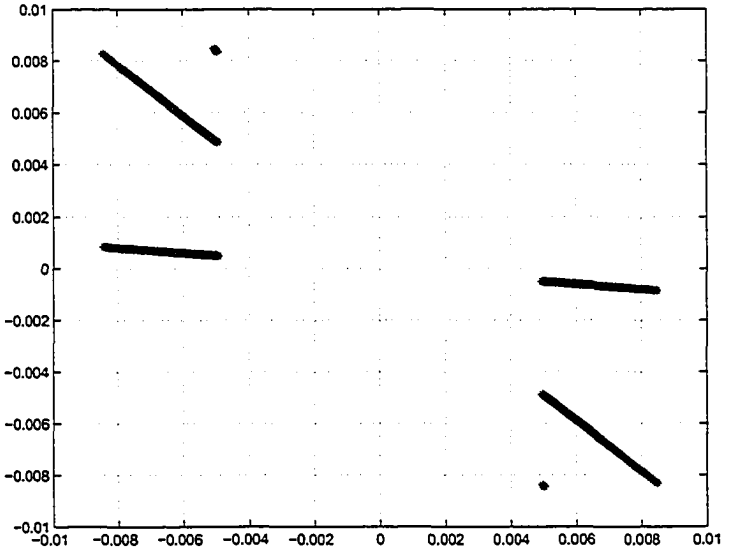

Figure 4.9: The asymptotic behavior of a trajectory for $|b| > a$

and

$$\Gamma_{ex} := I_b \backslash \Gamma_{in}. \tag{4.33}$$

The following is a necessary condition for the existence of periodic orbits.

Theorem 4.3 *If system (4.31) has periodic orbits, then there exist an even integer $n > 0$ and integers $K_i > 0$ such that*

$$\prod_{i=1}^{n} (1 + K_i b) = 1. \tag{4.34}$$

Without loss of generality, we only prove the case when $n = 2$. The following Lemma is used in the proof of Theorem 4.3.

Lemma 4.1 *Suppose $\xi_0 \in \Gamma_{ex}$ is a point on a periodic orbit at time K_0, it will be inside Γ_{in} at $K_0 + 1$.*

Proof. Let $\xi_0 = \begin{bmatrix} v_- \\ x \end{bmatrix}$. Then

$$\xi_1 = \begin{bmatrix} v_1 \\ x_1 \end{bmatrix},$$

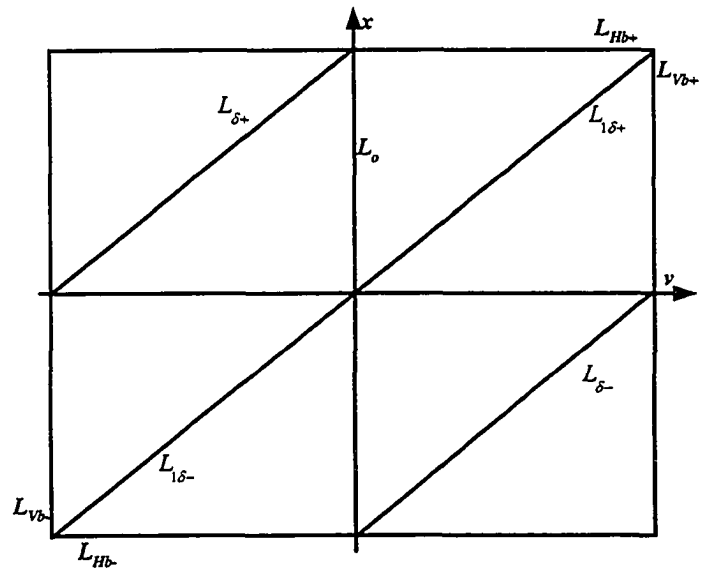

Figure 4.10: Diagram for the case of $a = 1$

where

$$\begin{aligned} x_1 &= (a+b)\,x, \\ v_1 &= x. \end{aligned}$$

Hence

$$|x_1 - v_1| = |1-(a+b)|\,|x| = |b|\,|x|\,.$$

Since $\begin{bmatrix} v_- & x \end{bmatrix}'$ is a periodic point, in view of Remark 4.1, one has

$$|x| \le \frac{|b|\,\delta}{1-(a+b)} = \delta.$$

Consequently,

$$|x_1 - v_1| = |1-(a+b)|\,|x| \le |b|\,\delta \le \delta,$$

i.e., $\xi_1 \in \Gamma_{in}$. ■

Note that Lemma 4.1 is nontrivial because there are systems such as the case that $a = 3/10$ and $b = -9/10$ violating this property.

Proof of Theorem 4.3. Without loss of generality, suppose there is a periodic orbit starting from $\xi_0 \in \Gamma_{ex}$. By Lemma 4.1,

$$\xi_1 = A_1\xi_0 \in \Gamma_{in}, \tag{4.35}$$

where

$$A_1 = \begin{bmatrix} 0 & 1 \\ 0 & 1+b \end{bmatrix}.$$

Assume after a time K_1 the state

$$\xi_2 = (A_1 + A_2)^{K_1 - 1} \xi_1$$

is in Γ_{ex}, where

$$A_2 = \begin{bmatrix} 1 & -1 \\ b & -b \end{bmatrix}.$$

Then

$$\xi_3 = A_1 \xi_2 \in \Gamma_{in}.$$

After a time K_2 the state

$$\xi_4 = (A_1 + A_2)^{K_2 - 1} \xi_3$$

returns to ξ_0. Hence

$$(A_1 + A_2)^{K_2 - 1} A_1 (A_1 + A_2)^{K_1 - 1} A_1 \xi_0 = \xi_0. \tag{4.36}$$

By straightforward algebraic computations, one gets

$$\begin{aligned} dcx &= x, \\ dx &= v_-, \end{aligned} \tag{4.37}$$

where

$$d = 1 + K_2 b, \; c = 1 + K_1 b.$$

Since $\xi_0 \in \Gamma_{ex}$,

$$|x - v_-| > \delta.$$

According to Eq. (4.37), note that $c \neq 0$, $d \neq 0$,

$$cd = 1. \tag{4.38}$$

Given $a = 1$,

$$K_1 + K_2 = K_1 K_2 (-b), \tag{4.39}$$

which is equivalent to Eq. (4.34) for $n = 2$. ■

Remark 4.3 Theorem 4.3 provides a necessary condition for having periodic orbits. Interestingly for the case when $n = 2$, extensive experiments imply that there are periodic orbits of period $K_1 + K_2$ if K_1 and K_2 satisfy Eq. (4.34), and there are no periodic orbits if there are no such K_1 and K_2. Based on this observation, Theorem 4.3 is not severely conservative. A necessary and sufficient condition of the existence of periodic orbits will be given in Sec. 4.5 with resort to first return maps, which generalizes Theorem 4.3.

Following the previous analysis, one immediately has

Corollary 4.2 *Suppose a is rational and b is irrational in Eq. (4.2), then there are no periodic orbits.*

Proof: Following the proof above, it suffices to show that

$$\prod_{i=1}^{n} \left(a^{K_i} + \sum_{j=0}^{K_i-1} a^j b \right) = 1 \tag{4.40}$$

has no positive integer solutions for any given even number $n > 0$. This can be easily verified. ■

Though the above result is simple, its significance can not be underestimated: If a system has periodic orbits, then it is *not* structurally stable.

Now suppose a system has periodic orbits, how to determine their periods? To give a partial answer to that, let us first consider an example.

Example 4.1 In the case that $a = 1$ and $b = -3/10$, there are two types of periodic solutions (refer to Figure 4.5). One is of period 24 corresponding to $K_1 = 4$ and $K_2 = 20$, the other is of period 15 corresponding to $K_1 = 5$ and $K_2 = 10$. Observe that

$$-b = \frac{3}{10} = \frac{3}{2 \cdot 5} := \frac{p}{q_1 \cdot q_2},$$

where $p = 3$, $q_1 = 2$, $q_2 = 5$, interestingly, one has

$$4 = \frac{q_2 + 1}{p} q_1, \; 20 = \frac{q_2 + 1}{p} q_1 \cdot q_2,$$

$$5 = \frac{q_1 + 1}{p} q_2, \; 10 = \frac{q_1 + 1}{p} q_1 \cdot q_2.$$

Based on this observation, we propose a necessary condition for Theorem 4.3 for the case that $n = 2$.

Theorem 4.4 *Given*

$$a = 1 \quad \textit{and} \quad b = -\frac{p}{q}.$$

Suppose positive integers p and q satisfy $1 < p < q$, $p \neq 2$ ($p = 2$ is a trivial case), and $\gcd(p, q) = 1$, i.e., the greatest common divisor of p and q is 1. Define

$$\Delta := \{q_i : q_i \textit{ is a prime number, } q_i | q\}. \tag{4.41}$$

Then if $p | (q_i + 1)$, where $q_i \in \Delta$,

$$\left(\frac{q_i + 1}{p}\frac{q}{q_i}, \ \frac{q_i + 1}{p}q\right)$$

is a solution to Eq. (4.34).

Proof. Obviously, given $p | (q_i + 1)$, $\left(\frac{q_i+1}{p}\frac{q}{q_i}, \frac{q_i+1}{p}q\right)$ is a solution to Eq. (4.34). Now we show how the set Δ is constructed in the above way. Given $q_i \in \Delta$. If there are two positive numbers m and n satisfying

$$\frac{1}{m} + \frac{1}{n} = \frac{p}{q_i}, \tag{4.42}$$

then $\left(m\frac{q}{q_i}, mq\right)$ is a solution to Eq. (4.34). Hence we need only to focus on solutions to Eq. (4.42). Suppose (m, n) is a solution of Eq. (4.42), then either $\gcd(m, q_i) = 1$ or $\gcd(n, q_i) = 1$ (otherwise, $p = 2$ or does not exist). For convenience, and with no loss of generality, we always assume $\gcd(m, q_i) = 1$. According to Eq. (4.42),

$$\frac{m + n}{nm} = \frac{p}{q_i},$$

i.e.,

$$(m + n)\, q_i = pmn.$$

Then $q_i | pmn$. Since $\gcd(p, q_i) = \gcd(m, q_i) = 1$, $q_i | n$. Let

$$n = kq_i, \tag{4.43}$$

which leads to

$$\frac{1}{m} + \frac{1}{kq_i} = \frac{p}{q_i}.$$

Consequently,

$$m(pk - 1) = kq_i,$$

hence $m|kq_i$. Since $\gcd(m, q_i) = 1$, $m|k$. In light of Eq. (4.43), one has

$$n = ml \text{ for some interger } l > 0.$$

Substituting it into Eq. (4.42), one has

$$\frac{1}{m} + \frac{1}{ml} = \frac{p}{q_i},$$

equivalently,

$$mpl = q_i(l+1),$$

indicating that $q_i|mpl$, i.e., $q_i|l$. Similarly, $l|q_i(l+1)$. Hence $l = q_i$. As a result,

$$m = \frac{q_i + 1}{p}.$$

If $p|(q_i + 1)$, then

$$\left(\frac{q_i+1}{p}, \frac{q_i+1}{p}q_i\right)$$

solves Eq. (4.42), and

$$\left(\frac{q_i+1}{p}\frac{q}{q_i}, \frac{q_i+1}{p}q\right)$$

is a solution to Eq. (4.34). ■

The above theorem provides a construction for the solutions to Eq. (4.34). Unfortunately it is not always effective. For example, for $a = 1$ and $b = -3/7$, the set Δ is empty. There are no positive integers satisfying Eq. (4.34) for $n = 2$ either. This is good for us. However for $a = 1$ and $b = -3/(2 \cdot 5 \cdot 11)$, we have the following observations (Table 4.1):

Table 4.1: Some periodic orbits

(v_-, x_0)	$(\frac{1}{1000}, 0)$	$(\frac{2}{1000}, 0)$	$(\frac{1}{1000}, 0)$	$(\frac{1}{2000}, 0)$
Periods	165	147	243	480
(v_-, x_0)	$(\frac{1}{2000}, \frac{1}{2000})$	$(\frac{1}{2000}, \frac{1}{8000})$	$(\frac{1}{2000}, \frac{1}{8500})$	$(\frac{1}{3000}, 0)$
Periods	264	480	243	1083

Periods 165, 264 and 480 can be obtained via Theorem 4.4, however, others can not. Actually there are more periodic and aperiodic orbits (Table 4.2).

Table 4.2: More periodic orbits and aperiodic orbits

(v_-, x_0)	$\left(\frac{\delta}{1000}, \frac{(a+b)\delta}{1000}\right)$	$\left(\frac{\delta}{100}, \frac{(a+b)\delta}{100}\right)$	$\left(\frac{\delta}{10}, \frac{(a+b)\delta}{10}\right)$	$\left(\frac{2\delta}{10}, \frac{2(a+b)\delta}{10}\right)$
Periods	4107	264	243	165
(v_-, x_0)	$\left(\frac{4\delta}{10}, \frac{4(a+b)\delta}{10}\right)$	$\left(\frac{9\delta}{20}, \frac{9(a+b)\delta}{20}\right)$	$\left(\frac{5\delta}{10}, \frac{5(a+b)\delta}{10}\right)$	$\left(\frac{6\delta}{10}, \frac{6(a+b)\delta}{10}\right)$
Periods	aperiodic	aperiodic	147	aperiodic
(v_-, x_0)	$\left(\frac{7\delta}{10}, \frac{7(a+b)\delta}{10}\right)$	$\left(\frac{8\delta}{10}, \frac{8(a+b)\delta}{10}\right)$	$\left(\frac{9\delta}{10}, \frac{9(a+b)\delta}{10}\right)$	$\left(\frac{10\delta}{10}, \frac{10(a+b)\delta}{10}\right)$
Periods	165	165	243	4107

Furthermore, we observed that there are at least 55 solutions to Eq. (4.34) for $n = 4$.

The foregoing analysis tells us:

- There may exist periodic orbits of very large periods.
- There are always aperiodic orbits.

Inspired by the proof of Corollary 4.2, especially by Eq. (4.40), now we attempt to construct systems with $|a| < 1$ that have periodic orbits. First choose $n = 2$, $a = 9/10$, $K_1 = 15$ and $K_2 = 7$. Then

$$b = -\frac{9015229097816388767119}{41428905812371212328810}$$

solves Eq. (4.40). Surprisingly the trajectory starting from

$$(v_-, x_0) = \left(\frac{-b * \delta}{1 - |a + b|} - \frac{1}{10^4}, 0\right)$$

will become a periodic orbit of period $22(= K_1 + K_2)$ after some iterations, i.e., it is an eventually periodic orbit. It can be shown that this periodic orbit is locally stable. However, a trajectory starting outside the stability region, say, from

$$(v_-, x_0) = \left(\frac{-b * \delta}{1 - |a + b|} - \frac{1}{10^4}, \frac{1}{10^3}\right)$$

is aperiodic. For the case when $|a| > 1$, suppose $a = 11/10$. choose $K_1 = 7$ and $K_2 = 5$. Then

$$b = -\frac{2138428376721}{5792012767210}$$

solves Eq. (4.40). And the trajectory starting from

$$(v_-, x_0) = \left(\frac{\delta}{10^5}, \frac{(a+b)*\delta}{10^5}\right)$$

is an eventually periodic orbit of period $12(= K_1 + K_2)$. It can be shown this periodic orbit is also locally stable and nearby are aperiodic orbits too.

Remark 4.4 From this construction, one finds out that most systems with $|a| < 1$ or $|a| > 1$ will be unlikely to have periodic orbits.

4.4 The case with $a > 1$

This case is analogous to that of $|a| < 1$ except that all the fixed points are unstable. In this case, Figure 4.7 is now Figure 4.11. Figure 4.12 is a plot of the steady state

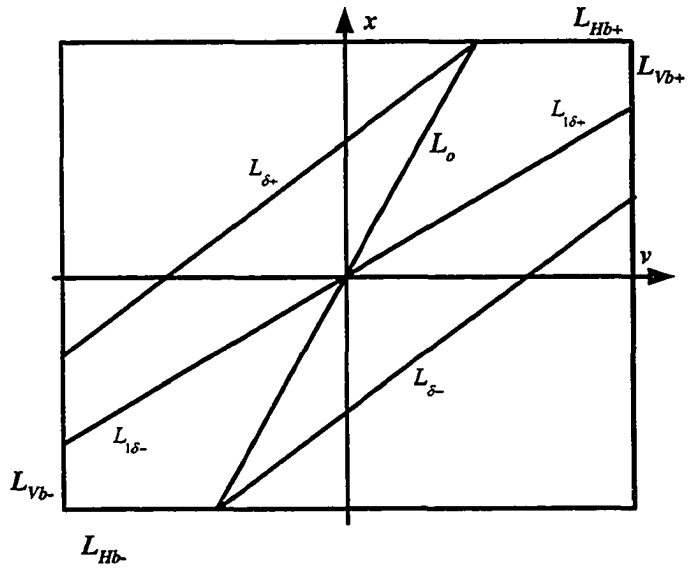

Figure 4.11: Diagram for the case of $a > 1$

of one trajectory.

4.5 First return maps

To simplify the following discussions, suppose that the system G shown in Figure 3.2 is a scalar system, the controller C is simply -1, there is no H_2 involved, and

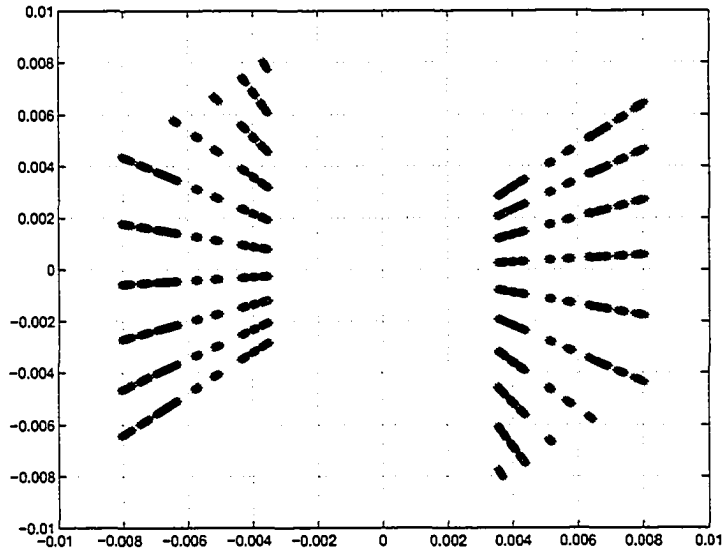

Figure 4.12: The asymptotic behavior of a trajectory for $a > 1$

$r = 0$. That is, in this part we consider the following simplified system:

$$x(k+1) = ax(k) + bv(k), \tag{4.44}$$

with $v(-1) \in \mathbb{R}$, and for $k \geq 0$,

$$\begin{aligned} v(k) &= H_1(x(k), v(k-1)) \\ &:= \begin{cases} x(k), & \text{if } |x(k) - v(k-1)| > \delta, \\ v(k-1), & \text{otherwise,} \end{cases} \end{aligned} \tag{4.45}$$

where $|a+b| < 1$ and δ is a positive number.

For the system composed of Eqs. (4.44)-(4.45), Theorem 4.3 gives a necessary condition for the existence of periodic orbits. We now generalize it and provide a necessary and sufficient condition and give a characterization of periodic orbits based on it. This analysis is important: To achieve good control, a nonlinear system may be desired to work near an equilibrium point or a limit cycle. In the case that a limit cycle is preferred, this result will reveal under what condition limit cycles may exist and starting from where a trajectory may converge to the desired limit cycle. In the case that an equilibrium is desirable, this result will provide the designer with some information as how to design controllers to prevent trajectories from being stuck into a limit cycle. Hence, this analysis will provide useful insights into the design

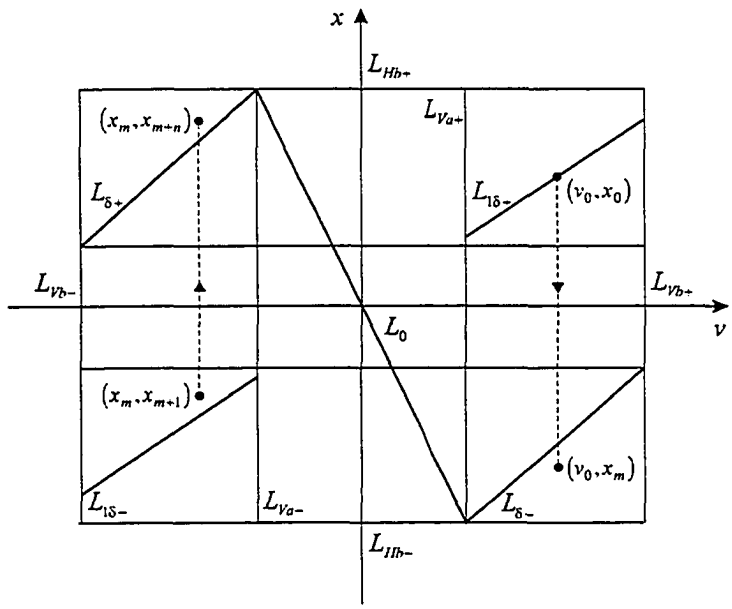

Figure 4.13: Diagram for the case $0 < a < 1$ and $b < 0$

of control systems under the data transmission strategy proposed in Chapter 3. We now investigate this important problem case by case.

4.5.1 Case 1: $0 < a < 1$, $b < 0$

For convenience, we present Figure 4.13 which is obtained by adding one typical trajectory to Figure 4.7. Assume that an initial condition (v_0, x_0) is located on the line $L_{1\delta+}$ satisfying

$$x_0 = (a+b)v_0.$$

Moreover, suppose that the trajectory starting from it does not converge to a fixed point (see Sec. 4.2 for details). Hence, the successive iterations are given by

$$\begin{aligned} x_1 &= ax_0 + bv_0 = \left(a^2 + ab + b\right) v_0 = \left(a^2 + \sum_{i=0}^{1} a^i b\right) v_0, \\ v_1 &= v_0, \end{aligned}$$

$$\begin{aligned} x_2 &= ax_1 + bv_0 = \left(a^3 + \sum_{i=0}^{2} a^i b\right) v_0, \\ v_2 &= v_0, \end{aligned}$$

$$\vdots$$

$$
\begin{aligned}
x_m &= a x_{m-1} + b v_0 = \left(a^{m+1} + \sum_{i=0}^{m} a^i b \right) v_0, \\
v_m &= v_0.
\end{aligned}
$$

Accordingly,

$$
v_m - x_m = \left(1 - a^{m+1} - \sum_{i=0}^{m} a^i b \right) v_0.
$$

As indicated in Figure 4.13, the orbit moves downward following the line $v = v_0$ on the right part of the region. In this way, there will exist a value of m such that the trajectory crosses the line segment $L_{\delta-}$, i.e.,

$$
|x_m - v_m| > \delta, \tag{4.46}
$$

and note that such an m always exists. Thus

$$
\begin{aligned}
\left(1 - a^{m+1} - \sum_{i=0}^{m} a^i b \right) v_0 > \delta \quad &\Leftrightarrow \quad \frac{(1-a)\,\delta}{(1-(a+b))v_0} < 1 - a^{m+1} \\
&\Leftrightarrow \quad a^{m+1} < 1 - \frac{(1-a)\,\delta}{(1-(a+b))v_0} \\
&\Leftrightarrow \quad m > \frac{\ln\left(1 - \frac{(1-a)\delta}{(1-(a+b))v_0}\right)}{\ln a} - 1.
\end{aligned}
$$

Hence, the smallest m is given by

$$
m = \left\lceil \frac{\ln\left(1 - \frac{(1-a)\delta}{(1-(a+b))v_0}\right)}{\ln a} \right\rceil - 1, \tag{4.47}
$$

where $\lceil r \rceil$ is the least integer bigger than r. Note that

$$
\begin{aligned}
x_{m+1} &= (a+b)\, x_m, \\
v_{m+1} &= x_m.
\end{aligned}
$$

Since $x_m < 0$, this point is located on the left part of Figure 4.13, and also

$$
|x_{m+1} - v_{m+1}| < \delta.
$$

Hence

$$
\begin{aligned}
x_{m+2} &= a x_{m+1} + b v_m = \left(a^2 + \sum_{i=0}^{1} a^i b \right) x_m, \\
v_{m+2} &= x_m,
\end{aligned}
$$

$$\vdots$$

$$\begin{aligned} x_{m+n} &= \left(a^n + \sum_{i=0}^{n-1} a^i b\right) x_m, \\ v_{m+n} &= x_m, \end{aligned}$$

$$x_{m+n} - v_{m+n} = \left(a^n + \sum_{i=0}^{n-1} a^i b - 1\right) x_m.$$

The orbit now moves upward along the line $v = x_m$ (see Fig 4.13). Then, there will exist a value of n such that the trajectory crosses $L_{\delta+}$, i.e.,

$$|x_{m+n} - v_{m+n}| > \delta.$$

Note that

$$v_{m+n} = x_m < 0.$$

Then

$$\begin{aligned} \left(a^n + \sum_{i=0}^{n-1} a^i b - 1\right) x_m &= \left(a^n + \sum_{i=0}^{n-1} a^i b - 1\right)\left(a^{m+1} + \sum_{i=0}^{m} a^i b\right) v_0 > \delta \\ &\Leftrightarrow \quad 1 - a^n > \frac{(1-a)\,\delta}{(a+b-1)\left(\left(1-a^{m+1}\right)\frac{a+b-1}{1-a} + 1\right) v_0} \\ &\Leftrightarrow \quad n > \frac{\ln\left(1 - \frac{(1-a)\delta}{(a+b-1)\left(\left(1-a^{m+1}\right)\frac{a+b-1}{1-a}+1\right)v_0}\right)}{\ln a}. \end{aligned}$$

Hence, the smallest n is

$$n = \left\lceil \frac{\ln\left(1 - \frac{(1-a)\delta}{(a+b-1)\left(\left(1-a^{m+1}\right)\frac{a+b-1}{1-a}+1\right)v_0}\right)}{\ln a} \right\rceil. \tag{4.48}$$

The switching law (Eq. 4.45) provokes that the new iteration point

$$\begin{aligned} x_{m+n+1} &= (a+b)\, x_{m+n}, \\ v_{m+n+1} &= x_{m+n}, \end{aligned}$$

returns to the zone where the trajectory was originated. In particular, if

$$(v_{m+n+1}, x_{m+n+1}) = (v_0, x_0),$$

then one gets a closed orbit. This motivates us to define the first-return map

$$\begin{aligned} \varphi \ : \ & L_1 \to L_1 \\ & v \mapsto \left(a^n + \sum_{i=0}^{n-1} a^i b\right)\left(a^{m+1} + \sum_{i=0}^{m} a^i b\right) v, \end{aligned} \tag{4.49}$$

where L_1 is the projection of $L_{1\delta+}$ onto the v axis, and m and n satisfy Eqs. (4.47) and (4.48) respectively.

Definition 4.1 *(Type 1 periodic orbits) A periodic orbit starting from $(v_0, x_0) \in L_{1\delta+}$ is said to be of type 1 if*

$$\varphi(v_0) = v_0, \tag{4.50}$$

where φ is defined by (4.49), and m and n satisfy Eqs. (4.47) and (4.48), respectively. In this case, the period of this orbit starting from (v_0, x_0) is $m + n + 1$.

Remark 4.5 *A periodic orbit is of type 1 if it forms a closed loop right after the first return. There are possibly other periodic orbits that become closed loops after several returns. These orbits can be studied in a similar way, but it is more computationally involved.*

The following result follows immediately from the foregoing discussions.

Theorem 4.5 *The trajectory starting from (v_0, x_0) is periodic of type 1 if and only if Eq. (4.50) holds.*

Actually, we can find all periodic orbits of type 1: If Eq. (4.50) holds, i.e.,

$$\varphi(v_0) = v_0,$$

then

$$\left(a^n + \sum_{i=0}^{n-1} a^i b\right)\left(a^{m+1} + \sum_{i=0}^{m} a^i b\right) = 1,$$

i.e.,

$$\left((1-a^n)\frac{a+b-1}{1-a} + 1\right)\left((1-a^{m+1})\frac{a+b-1}{1-a} + 1\right) = 1 \tag{4.51}$$

for some $m, n > 0$. Given that $0 < a < 1$, $b < 0$ and $|a + b| < 1$, m and n satisfying (4.51) are both finite. Hence, all periodic orbits of type 1 can be found.

Remark 4.6 If (v, x) leads to a periodic orbit of type 1, according to Eqs. (4.47) and (4.48), there exists a neighborhood of (v, x) on $L_{1\delta+}$ such that each point of which will lead to a periodic orbit of type 1, so all such orbits together are dense.

4.5.2 Case 2: $a = 1$

Assume that an initial condition (v, x) satisfies

$$x = (1+b)\,v,\ v > 0.$$

Then

$$\begin{aligned} x_1 &= x + bv = (1+2b)\,v, \\ v_1 &= v, \\ &\vdots \\ x_m &= x_1 + bv_1 = (1+(m+1)\,b)\,v, \\ v_m &= v. \end{aligned}$$

Suppose that

$$v_m - x_m = -(m+1)\,bv > \delta.$$

Then

$$m+1 > \frac{\delta}{(-b)\,v}.$$

Hence, the least m is given by

$$m = \left\lceil \frac{\delta}{(-b)\,v} \right\rceil - 1.$$

Moreover,

$$\begin{aligned} x_{m+1} &= (1+b)\,x_m, \\ v_{m+1} &= x_m < 0, \\ &\vdots \\ x_{m+n} &= (1+nb)\,x_m, \\ v_{m+n} &= x_m. \end{aligned}$$

Suppose that

$$x_{n+m} - v_{n+m} = nbx_m > \delta.$$

Then

$$n > \frac{\delta}{bx_m} = \frac{\delta}{b\left(1+(m+1)\,b\right)v}.$$

Hence, the smallest n is given by

$$n = \left\lceil \frac{\delta}{b\left(1+(m+1)\,b\right)v} \right\rceil.$$

Define

$$\begin{aligned} \varphi \;:\; & L_1 \to L_1 \\ & v \mapsto (1+nb)\left(1+(m+1)\,b\right)v, \end{aligned} \tag{4.52}$$

If

$$\varphi(v) = v,$$

then

$$\frac{1}{m+1} + \frac{1}{n} = -b. \tag{4.53}$$

Theorem 4.6 *The trajectory starting from $(v, (1+b)v)$ is periodic of type 1 if and only if v is a fixed point of the first-return map defined in Eq. (4.52).*

Remark 4.7 This result is a generalization of Theorem 4.3, where the condition is only necessary. For example, given $a = 1$ and $b = -1/2$, the origin is the unique invariant set. It is obvious that $p = q = 4$ is a solution to

$$\frac{1}{p} + \frac{1}{q} = -b.$$

However, there are no periodic orbits. This indicates that the necessary condition given by Theorem 4.3 is not sufficient.

Next we find all periodic orbits of type 1 for the case of $a = 1$. For convenience, here we use m instead of $m+1$ in Eq. (4.53). Suppose

$$b = -\frac{q}{p},$$

where $p > 0$, $q > 0$, $\gcd(p, q) = 1$. According to Eq. (4.53),

$$\frac{1}{m} = -b - \frac{1}{n} = \frac{pn-q}{qn},$$

i.e.,

$$m = \frac{qn}{pn - q}.$$

Obviously,

$$m > \frac{q}{p}.$$

Furthermore, m is a decreasing function of n. By symmetry, let

$$n_0 = \left\lceil \frac{q}{p} \right\rceil.$$

Then

$$\left\lceil \frac{q}{p} \right\rceil \leq m \leq \left\lceil \frac{qn_0}{pn_0 - q} \right\rceil.$$

Similarly,

$$\left\lceil \frac{q}{p} \right\rceil \leq n \leq \left\lceil \frac{qm_0}{pm_0 - q} \right\rceil,$$

where

$$m_0 = \left\lceil \frac{q}{p} \right\rceil.$$

Based on this analysis and Theorem 4.6, all periodic orbits of type 1 can be determined.

4.5.3 Case 3: $a = -1$ and $|a + b| < 1$

For this case, each trajectory is an eventually periodic orbit of period 2.

4.5.4 Case 4: $a > 1$

This is similar to the case of $0 < a < 1$. The only difference is

$$m < \frac{\ln\left(1 - \frac{(1-a)\delta}{(1-(a+b))v}\right)}{\ln a} - 1,$$

due to $\ln a > 0$. The least m is

$$m = \left\lceil \frac{\ln\left(1 - \frac{(1-a)\delta}{(1-(a+b))v}\right)}{\ln a} \right\rceil - 1.$$

4.6 Conclusions

In this chapter, focused on the scalar case, the dynamics of the system induced by the network data transmission strategy proposed in Chapter 3 is investigated in detail. Though appears simple, the system possesses very rich dynamics. More on this type of dynamical systems will be discussed in successive chapters.

Chapter 5

Chaos: one-dimensional case II

This chapter continues the study of the chaotic dynamical systems discussed in Chapter 4. Sec. 5.1 discusses why traditional methods for proving chaos fail as well as difficulties involved in analyzing this type of systems. Though there is no a universally agreed definition for chaos, a chaotic map normally should have an invariant set on which it is topologically transitive and has sensitive dependence on initial conditions. Hence Sec. 5.2 demonstrates topological transitivity and sensitive dependence on initial conditions via numerical examples.

5.1 Why traditional approaches fail?

5.1.1 Traditional methods to prove chaos

The most rigorous way in proving that an autonomous dynamical system is chaotic is to show that there are Smale horseshoes [93, 26]. Clearly, there will be infinitely many periodic orbits if there are Smale horseshoes. Unfortunately, the systems that we are studying here generally do not possess periodic orbits. As a result, this way to prove chaos does not promise much, if any.

A chaotic system normally is ergodic. For a given map, if it is expensive, then it is possible to prove ergodicity with resort to Perron-Frobenius operators [47]. For example, ergodicity of an unstable quantized scalar system is intensively studied in [16]. In essence, results obtained there depend heavily on the affine representation of the system by which it is piecewise expanding, i.e., the absolute value of the derivative of the piecewise affine map in each interval is greater than 1. Based on this crucial property, the main theorem (Theorem 1) in [55] and then that of [56] are employed to show that there exists a unique invariant measure on which the affine map is ergodic. Therefore, ergodicity is established for scalar unstable quantized systems. However, this is not the case for the system we are studying. Though these maps are piecewise linear, they are **singular** with respect to the Lebesgue measure and, furthermore, the derivative of the system along the lines $L_{1\delta-}$ and $L_{1\delta+}$ is $(a+b)$, whose absolute value is strictly less than 1. Consequently the results in [55] and [56] are not applicable here. Another approach to proving ergodicity is by means of the Markov transition. For a piecewise linear map, say Γ, suppose one subinterval, T_1, contains a subset of the image of another interval, T_2, that is, $T_1 \cap \Gamma(T_2)$ is not empty, then it is required that $T_1 \subset \Gamma(T_2)$. If this relation holds for all subintervals, then the Markov transition can be used to study the ergodicity of the map. Unfortunately, systems studied here do not satisfy this condition. Therefore, this method is not applicable either. We comment that a critical point in the existing approaches of proving chaos is that the system or map involved is of some hyperbolic structure [17]. Apparently, systems discussed here lack this key property.

5.1.2 Analysis of difficulties involved

In this part, the complexity of systems studied in the previous chapter is investigated from the point of view of numerical approximations and computational precision.

For convenience we define

$$x_2(k) := v(k-1), \quad k \geq 0.$$

Then the original system defined in Eqs. (4.44)-(4.45) is equivalent to

$$\begin{bmatrix} x_1(k+1) \\ x_2(k+1) \end{bmatrix} = \begin{cases} \begin{bmatrix} a+b & 0 \\ 1 & 0 \end{bmatrix} \begin{bmatrix} x_1(k) \\ x_2(k) \end{bmatrix}, & \text{if } |x_1(k) - x_2(k)| > \delta, \\ \begin{bmatrix} a & b \\ 0 & 1 \end{bmatrix} \begin{bmatrix} x_1(k) \\ x_2(k) \end{bmatrix}, & \text{otherwise,} \end{cases} \tag{5.1}$$

where $|a+b| < 1$. Define

$$A_1 = \begin{bmatrix} a+b & 0 \\ 1 & 0 \end{bmatrix}, \; A_2 = \begin{bmatrix} a & b \\ 0 & 1 \end{bmatrix}, \; C = \begin{bmatrix} 1 & -1 \end{bmatrix},$$

then, system (5.1) can be rewritten as

$$\begin{aligned} x(k+1) &= \frac{1}{2}(A_1 + A_2)x(k) + \frac{1}{2}(A_1 - A_2)(1 - u(k))x(k), \\ y(k) &= Cx(k), \\ u(k) &= 1 - \operatorname{sgn}(y(k)\operatorname{sgn}(y(k)) - \delta). \end{aligned} \tag{5.2}$$

Figure 5.1 is the plot of u as a function of y. Clearly, there are two discontinuous points: one is at $-\delta$ and the other is at δ here $\delta = 1$). Next, we use two different forms to approximate this function u. The first coming to mind is polynomials. We attempt to approximate the discontinuity at the point $y = 1$ up to degree 2. Hence, the polynomial to be used is

$$P(y) := a_3 y^3 + a_2 y^2 + a_1 y + a_0 \tag{5.3}$$

with a_i, $i = 0, \cdots, 3$ to be determined. Choose a small interval, $[1-\gamma, 1+\gamma]$, where $\gamma = 1/10^3$, and set

$$\begin{aligned} P(1+\gamma) = 0, \quad P'(1+\gamma) = 0; \\ P(1-\gamma) = 1, \quad P'(1-\gamma) = 0. \end{aligned}$$

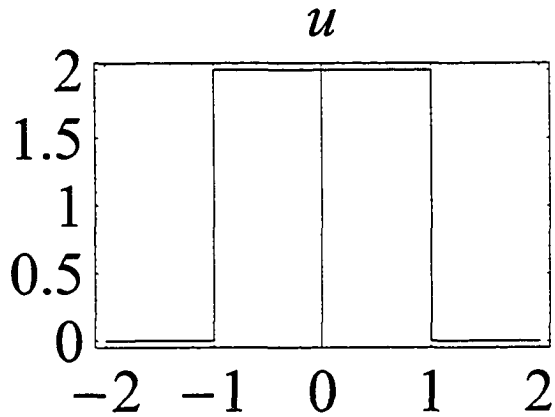

Figure 5.1: u has two discontinuous points: one is at $-\delta = -1$ and the other is at $\delta = 1$

Then, we get the polynomial as

$$P(y) = 500000000y^3 - 1500000000y^2 + 1499998500y - 499998499, \qquad (5.4)$$

whose plot at $[1-\gamma, 1+\gamma]$ is Figure 5.2 and at $[1-\gamma-1/1000, 1+\gamma+1/1000]$ is Figure 5.3. It is evident that the polynomial $P(y)$ defined in Eq. (5.4) is a bad approximation because its parameters are very big, thus very prone to perturbations (that's why Figure 5.3 is quite different from that of the original system). Notice that by using a polynomial approximation we get a *continuous* function approximating the original discontinuous function.

Another way to approximate u is to use hyperbolic tangent functions. In fact, u can be approximated by

$$u(y) = \begin{cases} 2, & -\delta+\rho < y < \delta-\rho, \\ \mathrm{Tanh}(\tau y), & \delta-\rho \le y \le \delta+\rho, \\ 0, & y > \delta+\rho, \\ \mathrm{Tanh}(\tau y), & -\delta-\rho \le y \le -\delta+\rho, \\ 0, & y < -\delta-\rho, \end{cases} \qquad (5.5)$$

where ρ should be sufficiently small. Now, we test the effectiveness of this approximation. First, choose $\tau = 2 * 10^6$, use the function (5.5) to replace the original u, and then plot a trajectory as shown in Figure 5.4. Then choose $\tau = 3 * 10^6$, following the same procedure, we get another trajectory, shown in Figure 5.5. The

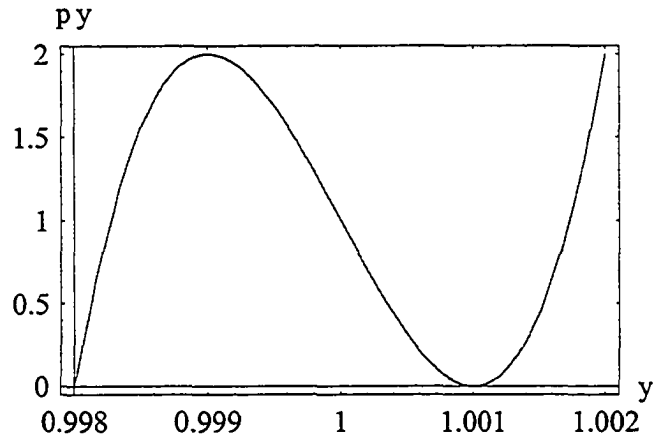

Figure 5.2: One plot of polynomial Eq. (5.4)

second trajectory is consistent with that of the original system. So, to get a good approximation, τ will have to be very big.

Remark 5.1 When ρ is small enough, the system composed of Eqs. (5.2) and (5.5) behaves like the original system. However, no matter how small ρ is, the modified system still has discontinuities, indicating that this approximation is not of much help. Even worse, to get a faithful approximation, τ must be very large, which will inevitably leads to large numerical errors.

Next we consider the problem of numerical precision. In our study we normally use Mathematica to get the exact orbits for each case. The reason to do this is to avoid numerical errors. This is best illustrated by the following examples. Suppose

$$a = \frac{9}{10},\ b = -\frac{3 * 1.4142135623730950}{10},\ \delta = \frac{1}{100},$$

in Eq.(5.1), with initial condition

$$x_1(0) = \frac{-(a+b) * (-\delta)}{2},\ x_2(0) = \frac{-\delta}{2}.$$

Using Mathematica, we get the result shown in Figure 5.6. Now, modify b to be

$$b = -\frac{3 * 14142135623730950}{10^{17}},$$

and fix the numerical precision to be 200 decimal points (the original one was 17). And we get Figure 5.7. Which plot is a faithful representation of the exact plot? By

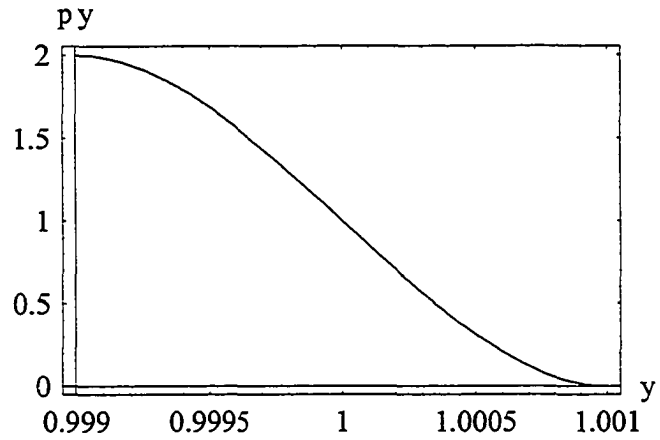

Figure 5.3: Another plot of polynomial Eq. (5.4)

using the exact value of $b = -\frac{3*14142135623730950}{10^{17}}$ to produce the true trajectory. we find it corresponds to Figure 5.6. Now, we see the difficulty: by increasing numerical precision, the result becomes less precise! So, we conclude that one has to be very careful when dealing with this type of systems because of its bewildering complexity.

5.2 Evidence of chaos

In this section, we illustrate the chaotic behavior of system (5.1). Though there is no universally agreed definition of chaos, a chaotic map typically has an invariant set on which it is topologically transitive and has sensitive dependence on initial conditions. So, we first demonstrate the topological transitivity of the map via numerical examples.

Fix parameters to be

$$a = \frac{9}{10},\ b = -\frac{3}{10},\ \delta = \frac{1}{100}.$$

Choose a trajectory $x_1(i), i = 1, ..., N$, starting from

$$x_1(0) = \frac{\delta}{2} + \frac{1.0}{10^8}$$

with $N = 5*10^6$. Here, the numerical precision is set to be 32. Then, choose several points along this trajectory and check the points within each interval of length ϵ centered at each of these chosen points (except itself). The computational result is summarized in Table 1.

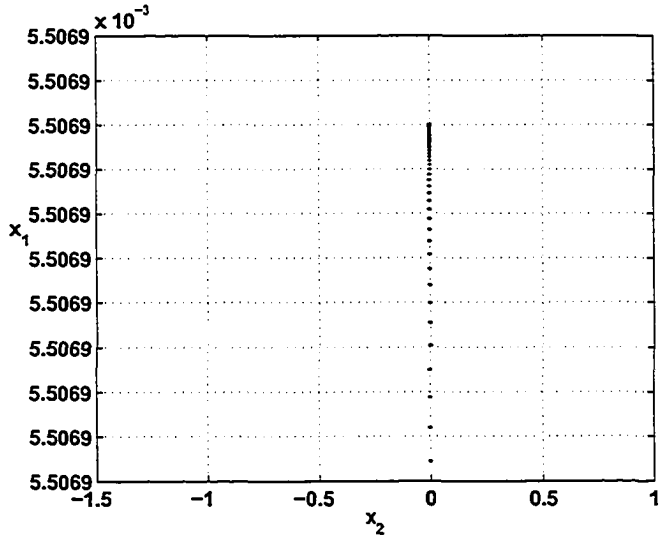

Figure 5.4: A trajectory with $\tau = 2 * 10^6$

Table 5.1: Recurrent behavior of x_1

val	ε	number
$x_1\,(90000)$	10^{-10}	1
$x_1\,(1000006)$	10^{-10}	0
$x_1\,(1000006)$	10^{-9}	14
$x_1\,(N-11)$	10^{-10}	135
$x_1\,(N-11)$	10^{-12}	0
$x_1\,(N-11)$	10^{-11}	1

We clearly see the recurrence of the trajectory to itself. Next, we choose another orbit, $x_2(k)$, starting from

$$x_2(0) = \frac{2 * \delta}{3} + \frac{1.0}{10^8}.$$

Accordingly the following points are obtained:

$$\begin{aligned} x_2(1000006) &= 0.00547824740916866066894384021163160388970261159915826670 2, \\ x_2(N-11) &= 0.00550783341443438496518396349495590987904110696161757567 4, \\ x_2(300006) &= 0.00541143954034974230346636647158607248690322941145375678 1. \end{aligned}$$

We then check the number of points of $x_1(k)$ inside each point above. Table 2 summarizes the result.

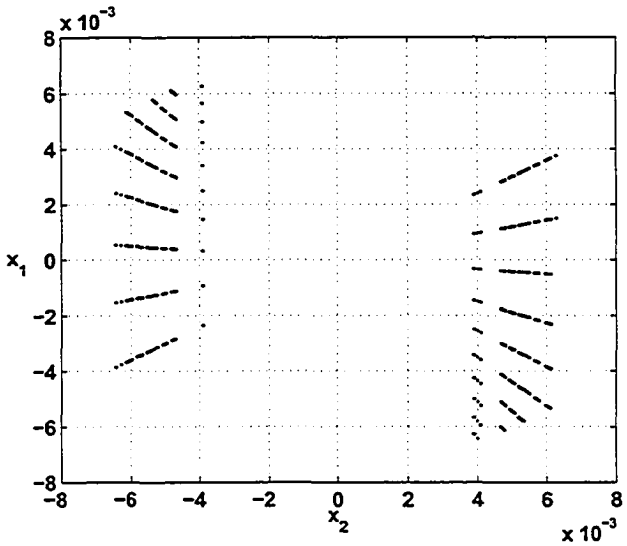

Figure 5.5: A trajectory with $\tau = 3 * 10^6$

Table 5.2: x_1 around x_2

val	ε	number
$x_2(1000006)$	10^{-9}	13
$x_2(1000006)$	10^{-10}	0
$x_2(N-11)$	10^{-10}	2
$x_2(300006)$	10^{-10}	2
$x_2(300006)$	10^{-13}	0

We find that within each small neighborhood of each chosen point in x_2, there are always points of x_1. (Note that the occurrence of 0 in these two tables is due to the limited amount of data we have. By choosing N bigger, ϵ, namely, the neighborhoods, can be smaller.) Since x_1 and x_2 are chosen *arbitrarily*, it is plausible to infer that there must be an invariant set within which almost all the orbits are dense. Such a set, say Λ, can be approximated as

$$\Lambda = \overline{\overline{\lim}\{x_1(k)\}}, \tag{5.6}$$

where x_1 is an oscillating orbit of the map, the outer *overline* denotes the closure, and $\overline{\lim}$ means the upper limit. It is worth pointing out that here the uniqueness of an invariant set in the oscillating region is implicitly assumed. Our extensive

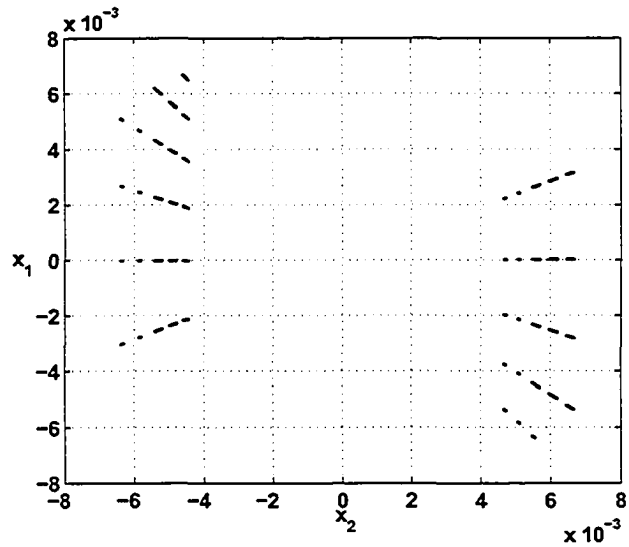

Figure 5.6: One trajectory generated via Mathematica

simulations strongly support this conjecture. Clearly Λ is closed and compact. Moreover, Table 1 tells us that each point in Λ is an accumulating point. As is known, dissipative chaos is always closely related to some Cantor set. To make Λ a Cantor set, we need to show that Λ is nowhere dense, which can be guaranteed if the map involved is dissipative. For a continuously differentiable dynamical system, its dissipativity can be verified quite easily. However, for a nonsmooth dynamical system, there still lack effective tools to do so. We have to admit that it is extremely hard to find the invariant set Λ *analytically*. This is best demonstrated by Figure 5.6, where it is hard to find any explicit pattern.

Problem 5.1 *How to determine if system (5.1) is dissipative?*

Next, we study the sensitive dependence on initial conditions, a defining nature of chaos. Fix

$$a = \frac{11}{10},\ b = -\frac{3}{10},\ \delta = \frac{1}{100}.$$

We then check the maximal distance between two initially-nearby trajectories. In Table 3, there are 4 rows of data. In each row, the first and second columns are the initial points of two trajectories, denoted "traj1" and "traj2", respectively. The third column contains the maximal distance between these two trajectories. The initial

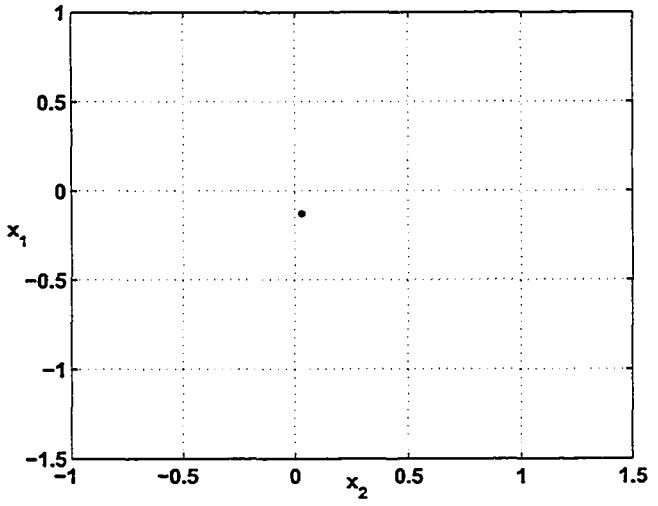

Figure 5.7: Another trajectory generated via Mathematica

differences are tiny, at levels of 10^{-6}, 10^{-7}, 10^{-8}, 10^{-10}, respectively. However, the maximal distances are all around 0.0043888, so the sensitive dependence on initial conditions is clear. As commented before, topological transitivity on an invariant set and sensitive dependence on initial conditions are two characteristic features of a chaotic map. Based on our forgoing simulations, the system discussed here does show chaotic behavior. It is our strong belief that a map is chaotic if it has a Cantor set as an invariant set and on which the map is topologically transitive.

Table 5.3: Sensitive dependence on initial conditions

traj1	traj2	maximal distance
$\frac{\delta}{2}+\frac{2*\delta}{10^6}*\left(\frac{-b-1+a}{1-(a+b)}\right)$	$\frac{\delta}{2}+\frac{3*\delta}{10^6}*\left(\frac{-b-1+a}{1-(a+b)}\right)$	0.004388827490502198
$\frac{\delta}{2}+\frac{2*\delta}{10^7}*\left(\frac{-b-1+a}{1-(a+b)}\right)$	$\frac{\delta}{2}+\frac{3*\delta}{10^7}*\left(\frac{-b-1+a}{1-(a+b)}\right)$	0.004388810010553412
$\frac{\delta}{2}+\frac{2*\delta}{10^8}*\left(\frac{-b-1+a}{1-(a+b)}\right)$	$\frac{\delta}{2}+\frac{3*\delta}{10^8}*\left(\frac{-b-1+a}{1-(a+b)}\right)$	0.004388807107462013
$\frac{\delta}{2}+\frac{2*\delta}{10^{10}}*\left(\frac{-b-1+a}{1-(a+b)}\right)$	$\frac{\delta}{2}+\frac{3*\delta}{10^{10}}*\left(\frac{-b-1+a}{1-(a+b)}\right)$	0.004388806797374203

5.3 Conclusions

In this chapter, extensive simulations have demonstrated the chaotic behavior of system (5.1). Difficulties involved in analyzing this class of systems has also been discussed. Problem 5.1 will be one of our future research lines.

Chapter 6

Structural stability

In Chapter 4, it is proved that given $a = 1$, system (4.1), if there are periodic orbits, then the system is not structurally stable. Loosely speaking, a dynamical system is *structurally stable* if a slight perturbation of its system parameters will not change its phase portrait. In this chapter it is shown that the condition of $a = 1$ is actually unnecessary. Sec. 6.1 proves that the system is not structurally stable by introducing a line of systems. Sec. 6.2 contains a study of local region of convergence. Sec. 6.3 discusses the phase transition of the above-mentioned line of systems. Sec. 6.4 investigates the eigen-structure of the line of systems near a particular parameter point.

6.1 Structural stability

Loosely speaking, a nonlinear system is *structurally stable* if a slight perturbation of its system parameters will not change its phase portrait qualitatively. In Chapter 4, we proved that given $a = 1$ in system (4.44), if there are periodic orbits, then the system is not structurally stable. In this section, we will show that the condition of $a = 1$ is actually unnecessary.

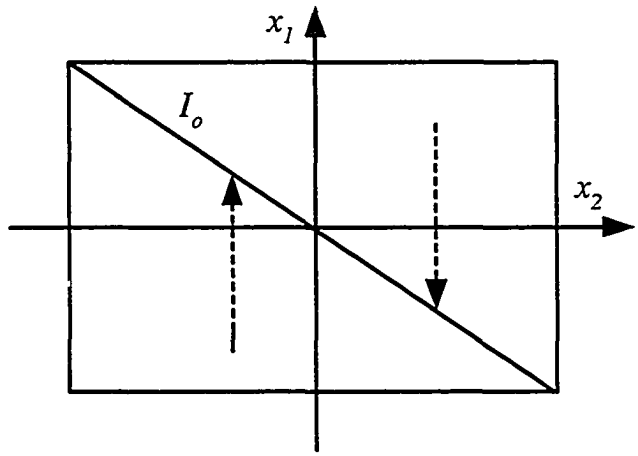

Figure 6.1: A global attracting region of a type-1 generic system

We begin with the simplest case, namely, a generic system, whose unique attractor is the line segment of fixed points. Even such a simple case can still be classified into at least two categories. We proved in Chapter 4 that if the parameters of the system defined by Eqs. (4.44)-(4.45) satisfy

$$\frac{1-|a|}{1-(a+b)} > \frac{|b|}{1-|a+b|} \tag{6.1}$$

with $|a+b| < 1$ and $|a| < 1$, then it is generic. One of whose global attracting regions is shown in Figure 6.1, where I_o is the line segment of fixed points, which runs from the point $(x_2, x_1) = \left(-\frac{(1-|a|)\delta}{1-(a+b)}, \frac{b}{1-a}\frac{(1-|a|)\delta}{1-(a+b)}\right)$ on the left to the point $(x_2, x_1) = \left(\frac{(1-|a|)\delta}{1-(a+b)}, -\frac{b}{1-a}\frac{(1-|a|)\delta}{1-(a+b)}\right)$ on the right. A trajectory will converge *vertically* to a certain point on I_o. On the other hand, we proved that the system with parameters $a = \frac{3}{10}$ and $b = -\frac{9}{10}$, which do not satisfy Eq. (6.1), is also generic, whose typical trajectories are like that shown in Figure 6.2 (the trajectory starting from $(0.005, 0.005)$ around converges to a fixed point close to $(0.0004, 0.004)$ after

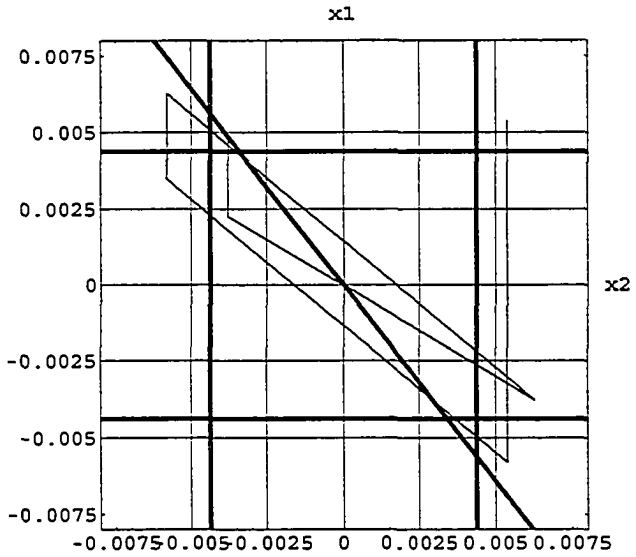

Figure 6.2: A global attracting region of the generic system with $a = 0.3$ and $b = -0.9$

several oscillations). Till now, we have not found a third type of generic systems. Apparently the first generic system is simpler than the second. Hence, we first investigate the structural stability of the first type of systems. For convenience, we call such systems type-1 generic systems, or generic systems of type 1. Observing that each type-1 generic system has a global attracting region as shown in Figure 6.1, thereby we focus on its behavior in this region.

The following result asserts that two generic systems of type 1 are 'identical' in the sense of topology:

Proposition 6.1 *Two type-1 generic systems are homeomorphic, i.e., there exists a bijective map form one to the other, which is continuous and has a continuous inverse.*

Proof. For convenience, define

$$x_2(k) := v(k-1), \quad k \geq 0.$$

Then, the original system defined in Eqs. (4.44)-(4.45) is equivalent to system (5.1)

presented in Chapter 5:

$$\begin{bmatrix} x_1(k+1) \\ x_2(k+1) \end{bmatrix} = \begin{cases} \begin{bmatrix} a+b & 0 \\ 1 & 0 \end{bmatrix} \begin{bmatrix} x_1(k) \\ x_2(k) \end{bmatrix}, & \text{if } |x_1(k) - x_2(k)| > \delta, \\ \begin{bmatrix} a & b \\ 0 & 1 \end{bmatrix} \begin{bmatrix} x_1(k) \\ x_2(k) \end{bmatrix}, & \text{otherwise.} \end{cases}$$

Consider the following two type-1 generic systems whose global attracting regions

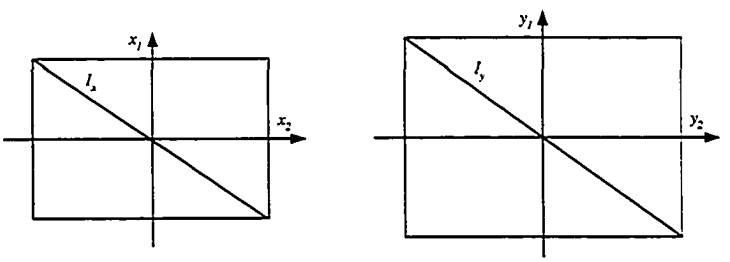

Figure 6.3: Global attracting regions of systems Σ_1 and Σ_2

are shown in Figure 6.3:

$$\Sigma_1: \quad x(k+1) = \begin{cases} B_1 x(k), & \text{if } |x_1(k) - x_2(k)| > \delta, \\ A_1 x(k), & \text{otherwise,} \end{cases}$$

$$\Sigma_2: \quad y(k+1) = \begin{cases} B_2 x(k), & \text{if } |y_1(k) - y_2(k)| > \delta, \\ A_2 x(k), & \text{otherwise,} \end{cases}$$

in which

$$x = \begin{bmatrix} x_1 \\ x_2 \end{bmatrix}, \; y = \begin{bmatrix} y_1 \\ y_2 \end{bmatrix}, \; A_i = \begin{bmatrix} a_i & b_i \\ 0 & 1 \end{bmatrix}, \; B_i = \begin{bmatrix} a_i + b_i & 0 \\ 1 & 0 \end{bmatrix}, \; i = 1, 2.$$

Next, define a map h from I_x to I_y by

$$\begin{aligned} h \;:\; & I_x \longrightarrow I_y, \\ & \left(\frac{b_1}{1-a_1}x_2, x_2\right) \mapsto \left(\frac{b_2}{1-a_2}\frac{\frac{1-|a_2|}{1-(a_2+b_2)}}{\frac{1-|a_1|}{1-(a_1+b_1)}}x_2, \frac{\frac{1-|a_2|}{1-(a_2+b_2)}}{\frac{1-|a_1|}{1-(a_1+b_1)}}x_2\right). \end{aligned} \tag{6.2}$$

Clearly, h is one-to-one, onto and has a continuous inverse.

Next, define

$$\begin{aligned} \tilde{h} \;:\; & \Sigma_1 \longrightarrow \Sigma_2, \\ & (x_1, x_2) \mapsto \left(\frac{\frac{b_2}{1-a_2}}{\frac{b_1}{1-a_1}}\frac{\frac{1-|a_2|}{1-(a_2+b_2)}}{\frac{1-|a_1|}{1-(a_1+b_1)}}x_1, \frac{\frac{1-|a_2|}{1-(a_2+b_2)}}{\frac{1-|a_1|}{1-(a_1+b_1)}}x_2\right). \end{aligned} \tag{6.3}$$

It is easy to see that the projection of $\tilde{h}$ on I_x is exactly h, and furthermore $\tilde{h}$ is a homeomorphism. Actually system Σ_2 can be obtained by stretching (or contracting) system Σ_1, therefore they are topologically equivalent. ■

Two remarks are in order.

Remark 6.1 It is hard to apply the foregoing method to other types of generic systems because they may not have such simple global attracting regions.

Remark 6.2 As can be conjectured, this method is probably not applicable to non-generic systems that have some complex attractors besides the line segment of fixed points (see Chapter 4 for details).

Before investigating the structural stability of generic systems, we first discuss their ω-stability. A dynamical system is ω-stable if there exists a homeomorphism from its *non-wandering* set (here it is I_o) to that of the system obtained by perturbing it slightly [93]. Hence, a structurally stable dynamical system is necessarily ω-stable, but the converse may not be true. Because there always exists a homeomorphism between two given line segments, it seems plausible to infer that a generic system is ω-stable. Unfortunately, it is not true. Observe that Proposition 6.1 holds upon the assumption that two given systems are generic, some other "unusual" types of perturbations may lead to a system that is not generic, thus destroying the ω-stability of generic systems. To that end, a new point of view is required.

Define a family of systems:

$$\begin{bmatrix} x_1(k+1) \\ x_2(k+1) \end{bmatrix} = \begin{cases} A_1 \begin{bmatrix} x_1(k) \\ x_2(k) \end{bmatrix}, & \text{if } |x_1(k) - x_2(k)| > \delta, \\ A_2 \begin{bmatrix} x_1(k) \\ x_2(k) \end{bmatrix}, & \text{otherwise,} \end{cases} \tag{6.4}$$

where

$$A_1 = \begin{bmatrix} a+b & 0 \\ 1 & 0 \end{bmatrix}, \quad A_2 = \begin{bmatrix} a+\lambda b & (1-\lambda)b \\ \lambda & (1-\lambda) \end{bmatrix}. \tag{6.5}$$

Note that when $\lambda = 1$, $A_2 = A_1$, and that the resulting system is a stable linear system. When $\lambda = 0$, $A_2 = \begin{bmatrix} a & b \\ 0 & 1 \end{bmatrix}$, giving system (5.1). Hence, by introducing $\lambda \in [0,1]$, one gets a family of systems.

It is easy to verify the following result:

Theorem 6.1 *For each* $\lambda \in (0, 1]$, *system (6.4) has a unique fixed point* $(0, 0)$.

Consider a perturbation of a system in the form of (5.1) by choosing a λ sufficiently close to but not equal to zero. Theorem 6.1 tells us that the new system has a unique fixed point. Clearly, there are no homeomorphisms between these two systems since there exist no one-to-one maps from a line segment to a single point. Moreover, a non-generic system also has a line segment of fixed point. So, we have the following conclusion:

Theorem 6.2 *System (5.1) is not* ω*-stable.*

The following is an immediate consequence.

Corollary 6.1 *System (5.1) is not structurally stable.*

Remark 6.3 The above investigation tells us that the system with $\lambda = 0$ is a rather ill-conditioned one. Will a system with $\lambda \neq 0$ be ω-stable (or even structurally stable)? We are convinced that this generally holds, but till now we have been unable to prove it.

Remark 6.4 For a generic system, no matter it is of type 1 or not, its non-wandering set is just a line segment of fixed points, therefore its ω-stability is preserved if a perturbation is on a and b, while *not* destroying the structure shown in Eq. (5.1). Consider the discussion in Chapter 3, the system composed of (4.44)-(4.45) is proposed for a new data transmission strategy, hence the perturbation of a and b is reasonable, while the perturbation of the form (6.4)-(6.5) induced by λ does not make sense physically. Based on this, we can say that ω-stability is "robust" with respect to uncertainty which is meaningful (The same argument is proposed in [84] for structural stability). However, it is pretty "fragile" with respect to such rare uncertainty as that in Eqs. (6.4)-(6.5). In other words, it is robust yet fragile. It is argued in [18] that 'robust yet fragile' is the most important property of complex systems.

It is evident that there is clearly a transition process in the family of systems defined by Eqs. (6.4) and (6.5) as λ moves from 1 to 0. Obviously this transition

is very interesting. Next we will demonstrate this transition process by examples in the hope of pinning down the inherent dynamics and thereby learning something about this type of nonsmooth dynamical systems.

In the following, we concentrate on the case that

$$a = 9/10, \quad b = -3/10, \quad \delta = 1/100.$$

6.2 The region of converging orbits

According to Proposition 6.1, there is a neighborhood around the origin $(0, 0)$, each orbit starting within which will converge to the origin. One question is: Is it possible to determine this local stability region analytically? This problem turns out to be difficult. For example, assume $\lambda = 16/100$. Starting from an initial point $(-10, 10)$, the orbit is oscillating (see Figure 6.4). Based on this, one may guess that each

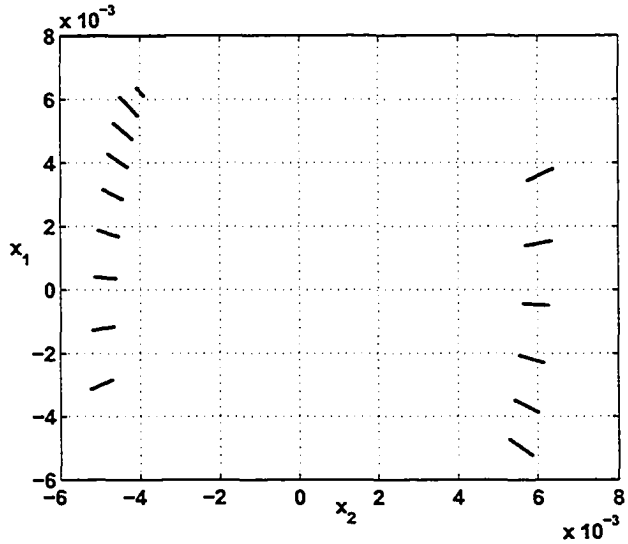

Figure 6.4: An oscillating orbit starting from $(-10, 10)$

orbit starting from an initial point further away from $(0, 0)$ than $(-10, 10)$ will be oscillating. However, this is not true. In fact, the trajectory starting from $(-100, 870)$ converges to the origin (see Figure 6.5). This example tells us that the set of converging orbits is hard to find analytically, even if it is possible. Clearly, this problem is closely related to the problem of computational complexity (see [4] and some references therein).

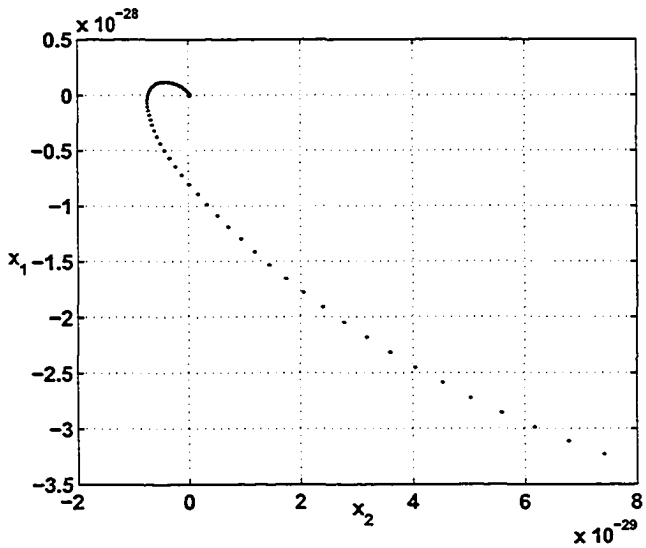

Figure 6.5: A converging orbit starting from $(-100, 870)$

6.3 Phase transition

In this section, we study the transition process as λ moves from 1 to 0. Here, we fix an initial point $(-10, 10)$ and study the evolution of its orbits as λ varies. To be precise, we use Mathematica to find these analytic orbits instead of using numerical ones, for the reason has already been given in chapter 5. We start from $\lambda = 165/10^4$. It is found that the orbit is converging. So, we reduce λ (we expect that the smaller the λ is, the more unstable the system will be) by choosing $\lambda = 162/10^4$, and the orbit oscillates. Then, we choose a bigger λ, $\lambda = 163/10^4$, but in this case the orbit converges to the origin. We then reduce λ again by choosing $\lambda = 1625/10^5$, and the trajectory is oscillating. However, for $\lambda = 1626/10^5$, it converges.

At $\lambda = 1$, we have a stable linear system. When λ is slightly less than 1, the system is nonlinear, but is still globally asymptotically stable. As λ goes further toward 0, the nonlinearity becomes more and more prevalent and ends up with chaos at $\lambda = 0$.

We are now in a position to pose two questions:

Problem 6.1 *Assume parameters a, b, δ are given in the system composed of Eqs. (6.4)-(6.5). As far as a particular orbit is concerned, for instance, the one starting*

from $(-10, 10)$ *in the example studied above, is there a* $\lambda_0 \in (0, 1)$ *such that the orbit converges to the origin for all* $1 \geq \lambda > \lambda_0$*, whereas it oscillates for all* $0 \leq \lambda < \lambda_0$*? If so, what behavior will the orbit starting from* $(-10, 10)$ *run into: converge to the origin or a periodic orbit, oscillate or be periodic?*

Problem 6.2 *Is there a* $\lambda_1 \in (0, 1)$ *such that all orbits will converge for all* $1 \geq \lambda > \lambda_1$*, whereas there is at least one oscillating orbit for each* $0 \leq \lambda < \lambda_1$*? Again, if so, for this* λ_1*, what will trajectories end up with?*

Another interesting question is: Is there any continuous function of λ as it goes from 1 to 0? The first candidate coming to mind is, of course, the system trajectories. However, they are unlikely. For example, Σ_s is a linear stable system, and systems with λ very close to 1 also have the origin as the unique global attractor, whereas Σ_u has an oscillating region. Hence, as λ decreases, aperiodic orbits come into being, which disqualify the continuation of trajectories as a function of λ. The same argument asserts that neither the system attractors nor structural stability are continuous with respect to λ. Then, what about dissipativity? (Here we define that a system is dissipative if the volume of its attractors has Lebesgue measure 0.) One may disprove this by saying that there are dense periodic orbits in the case of $a = 1$ and $b = -3/10$ (please refer to Chapter 4 for details). However, our argument here is that systems with periodic orbits are not typical in this type of systems. As proved in Chapter 4, an extremely slight perturbation will perturb the parameter b from being rational to being irrational, and as a result there are no periodic orbits at all. Our analysis and extensive simulations strongly support that dissipativity is invariant (hence continuous) as a function of λ. Putting dissipativity into the context of phase transition gives rise to the following problem:

Problem 6.3 *It is obvious that the system composed of Eqs. (6.4)-(6.5) is dissipative at* λ *around but less than 1. How will it change as* λ *moves from 1 to 0? Is it invariant?*

If the system is dissipative, following Sec. 5.2, the system Σ_u with $a = 9/10$ and $b = -3/10$ has a Cantor set as an invariant set on which the system is topologically transitive, hence it is truly chaotic.

At $\lambda = 1$, we have a stable linear system. when λ is slightly less than 1, the system is nonlinear, but is still globally asymptotically stable. As λ moves further toward 0, nonlinearity becomes more and more prevalent and ends up with chaos at $\lambda = 0$. Our speculation is that it seems unlikely for periodicity to come into play in this process; if this were true, what bifurcation would be expected? This process might be fraught with bifurcations, how to discern the underlying patterns?

Up to this point, some comments of Feigenbaum [21] come to our mind, "..., while a vague impression of what one wants to know is sensibly clear, a precise delineation of many of these quests is not so readily available. In a state of ignorance, the most poignantly insightful questions are not yet ripe for formulation. Of course, this comment remains true despite the fact that, for technical exigencies, there are definite questions that one desperately wants the answers to."

6.4 Eigen-structure near $\lambda = 0$

In fact, one can go further by relaxing the restriction of λ on $[0, 1]$ to $(-\infty, \infty)$. The following result guarantees the existence of a bounded global attracting region of the system.

Theorem 6.3 *For each given $\lambda \in (-\infty, \infty)$, system (6.4) has a bounded global attracting region.*

Proof. By Eq. (6.4), one has

$$x_1(k+1) = (a+b)\, x_1(k) + s_k(\lambda - 1)\, b\,(x_1(k) - x_2(k)),$$

where

$$s_k = \begin{cases} 0 & \text{if } |x_1(k) - x_2(k)| > \delta, \\ 1 & \text{otherwise.} \end{cases}$$

With this observation, one obtains

$$\begin{aligned} |x_1(k+1)| &\leq |a+b|\,|x_1(k)| + |\lambda - 1|\,|b|\,\delta \\ &\leq |a+b|^{k+1}\,|x_1(0)| + \frac{1 - |a+b|^{k+1}}{1 - |a+b|}\,|\lambda - 1|\,|b|\,\delta, \end{aligned}$$

hence

$$|x_1(k+1)| \leq \frac{|\lambda - 1|\,|b|\,\delta}{1 - |a+b|}$$

for sufficiently large k. As a result, for each given $\lambda \in (-\infty, \infty)$, there exists a bounded globally attracting region. ■

Now we will show that for λ less than but sufficiently close to 0, there always exists an eigenvalue which is strictly greater than 1.

The two eigenvalues of system (6.4) are

$$\frac{1+a-\lambda+b\lambda \mp \sqrt{-4(a-a\lambda)+(-1-a+\lambda-b\lambda)^2}}{2}.$$

It turns out that one of these two eigenvalues is enough for the following development.

Define

$$f(\lambda) := \frac{1}{2}\left(1+a-\lambda+b\lambda+\sqrt{-4(a-a\lambda)+(-1-a+\lambda-b\lambda)^2}\right).$$

6.4.1 Case I: $|a| < 1$

In this case,

$$f(0) = \frac{1}{2}(1+a+|1-a|) = 1,$$

$$\begin{aligned} f'(0) &= \frac{1}{2}\left(b-1+\frac{4a+2(1+a)(b-1)}{|1-a|}\right) \\ &= \frac{1}{1-a}(b+a-1) < 0 \end{aligned}$$

Hence there exists $\lambda^* < 0$ such that $f(\lambda) > 1$ for $\lambda \in (\lambda^*, 0)$.

6.4.2 Case II: $a > 1$

In this case,

$$\begin{aligned} f(0) &= \frac{1}{2}(1+a+|1-a|) \\ &= \frac{1}{2}(1+a-1+a) \\ &= a > 1. \end{aligned}$$

Due to the continuous dependence of eigenvalues on system parameters, there exists $\delta > 0$ such that $f(\lambda) > 1$ for $\lambda \in (-\delta, \delta)$.

6.4.3 Case III: $a = 1$

In this case,

$$f(\lambda) = \frac{1}{2}\left(2 - \lambda + b\lambda - \sqrt{4(\lambda - 1) + (2 - \lambda + b\lambda)^2}\right).$$

Hence

$$f(0) = 1,$$

and for all $\lambda \neq 0$,

$$f'(\lambda) = \frac{1}{2}\left((b-1) + \frac{2 + (2 - \lambda + b\lambda)(b-1)}{\sqrt{4(\lambda - 1) + (2 - \lambda + b\lambda)^2}}\right). \tag{6.6}$$

Noting that $b < 0$, one has

$$2 + (2 - \lambda + b\lambda)(b - 1) < 0$$

for λ sufficiently close to 0, i.e.,

$$f'(\lambda) < 0$$

for λ sufficiently close to 0. As a consequence, there exists $\bar{\lambda} < 0$ such that $f(\lambda) > 1$ for $\lambda \in (\bar{\lambda}, 0)$.

6.5 Conclusions

In this chapter, we have proved that system (5.1) is not structurally stable by introducing a parameter λ to get a line of systems. Problems 6.1, 6.2 and 6.3 are the threads of our future research. We believe these problems are common in nonsmooth dynamical systems induced by state-dependent switchings. Therefore we hope the family of systems discussed here can serve as a model in this field of research.

Chapter 7

Chaos: two-dimensional case

The aim of this chapter is to study higher dimensional systems under the switching law specified in Chapter 3. Sec. 7.1 contains two motivational examples, one of which reveals the contracting and stretching nature of this class of systems; the other shows the evolution of attractors as some system parameter varies. System analysis constitutes Sec. 7.2, together with an example illustrating the rich dynamics in these systems.

7.1 Examples

In this section, two examples are used to illustrate the qualitative behavior of a higher dimensional system, the former reveals the contracting and stretching feature of this type of systems and the latter show the variation of attractors as some system parameter varies.

Example 7.1 Suppose the system G shown in Figure 3.2 is given by

$$\begin{aligned} x(k+1) &= 2x(k) + 3v(k), \\ y_c(k) &= x(k), \end{aligned}$$

and the controller C is given by

$$\begin{aligned} x_d(k+1) &= -2x_d(k) + 1.5e_c(k), \\ u_c(k) &= x_d(k), \\ e_c(k) &= r(k) - z(k), \end{aligned}$$

where $v(k)$ and $z(k)$ are outputs of Eqs. (3.4)-(3.5) respectively. Set $r \equiv 0$, fix $\delta = 1/100$ and denote the resulting system by Σ_o. It is easy to see that the closed-loop system without the constraints H_1 and H_2 is asymptotically stable. Under H_1 and H_2, starting from an initial condition, the asymptotic behavior of a trajectory is drawn in Figures 7.1–7.3. The first is for $(v(k-1), x(k))$, the second for $(z(k-1), x_d(k))$ and the last for $(x(k), x_d(k))$. Clearly the trajectory is formless.

Next nonlinear data analysis techniques will be employed to analyze the chaotic behavior of system Σ_o. The first to be demonstrated is of course sensitive dependence on initial conditions. Choose an initial condition

$$[v(-1),\ x(0),\ z(-1),\ x_d(0)] = [-1/1000,\ 1/1000,\ 2/1000,\ -1/1000],$$

set the iteration number to be $6 * 10^5$, then one gets a trajectory of x. Perturb the initial condition above slightly to $[-1/1000, 1/1000 + 1/10^{13},\ 2/1000, -1/1000]$, under the same iteration, another trajectory of x is obtained. Figure 7.4 is the difference between these two $x's$ of the last 1200 iterations. According to this figure, one can easily see sensitive dependence on initial conditions. In general, the

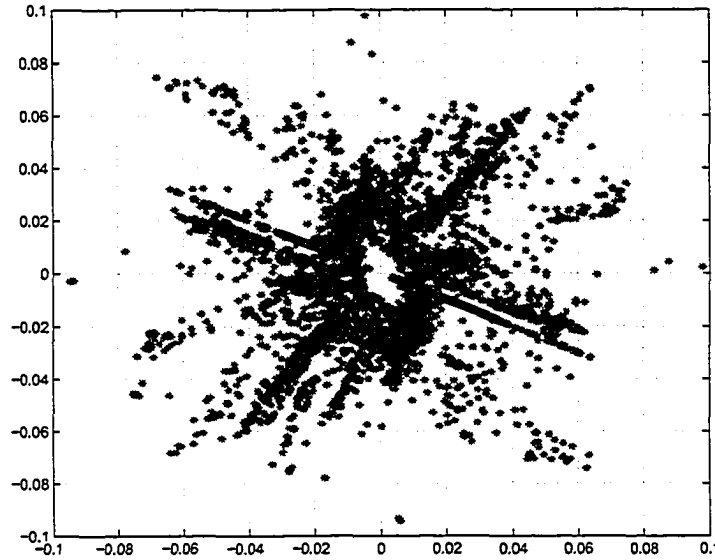

Figure 7.1: Plot of the asymptotic behavior of $(v(k-1), x(k))$

spectra of a chaotic orbit will be continuous. Figure 7.5 contains the spectrum of x starting from $[-1/1000, 1/1000, 2/1000, -1/1000]$, which confirms our conjecture.

As is well-known, a chaotic system normally has the geometric feature of contracting and stretching, hence the following development concentrates on the dynamics of the system in Example 7.1 geometrically. To simplify the discussion, suppose there is no constraint H_2 in Figure 3.2, i.e., $v(k) \equiv u_c(k)$. The fixed points of the system Σ_o are given by

$$\left\{(x, x_d, z_-) : x = \frac{3}{2}z_-,\ x_d = -\frac{1}{2}z_-,\ |z_-| \le 2\delta\right\}. \tag{7.1}$$

Define

$$\mathbf{x} := \begin{bmatrix} x & x_d & z_- \end{bmatrix}',$$

$$T := \begin{bmatrix} 1 & 0 & -\frac{3}{2} \\ 0 & 1 & \frac{1}{2} \\ 0 & 0 & 1 \end{bmatrix},$$

$$\tilde{\mathbf{x}} := \begin{bmatrix} \tilde{x} & \tilde{x}_d & \tilde{z}_- \end{bmatrix}' = T\mathbf{x}.$$

Then the system under the new coordinates is

$$\Sigma_{n1} : \tilde{\mathbf{x}}(k+1) = \begin{bmatrix} \frac{1}{2} & 3 & -\frac{3}{4} \\ -1 & -2 & -\frac{1}{2} \\ 1 & 0 & \frac{3}{2} \end{bmatrix} \tilde{\mathbf{x}}(k),$$

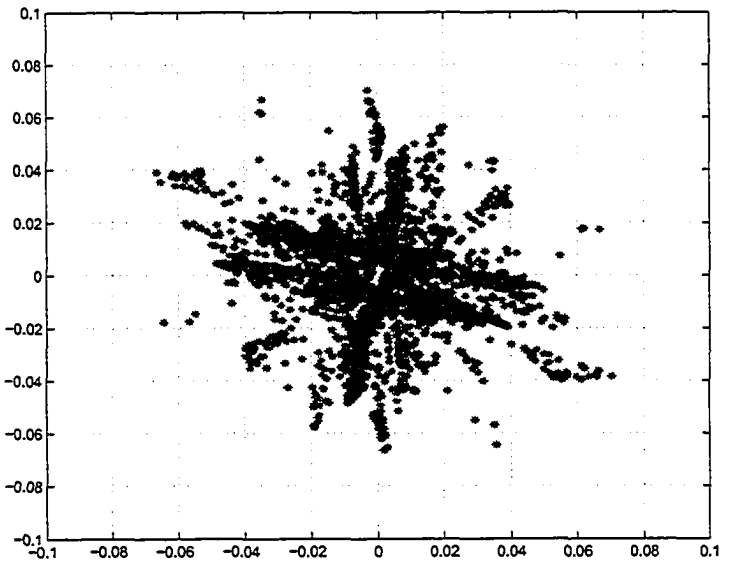

Figure 7.2: Plot of the asymptotic behavior $(z(k-1), x_d(k))$

under

$$|\tilde{x} - \tilde{z}_-| > \delta; \tag{7.2}$$

and

$$\Sigma_{n2} : \tilde{\mathbf{x}}(k+1) = \begin{bmatrix} 2 & 3 & 0 \\ 0 & -2 & 0 \\ 0 & 0 & 1 \end{bmatrix} \tilde{\mathbf{x}}(k),$$

under

$$|\tilde{x} - \tilde{z}_-| \leq \delta. \tag{7.3}$$

For convenience, denote this system by Σ_n. It is easy to see that the fixed points of Σ_n are

$$\{(0, 0, \tilde{z}_-) : |\tilde{z}_-| \leq 2\delta\}. \tag{7.4}$$

Some comments are appropriate here:

- The subsystem Σ_{n1} is a stable system.
- If Eq. (7.3) is satisfied, a trajectory (governed by Σ_{n2}) will move on a surface

$$\tilde{z}_- = \gamma$$

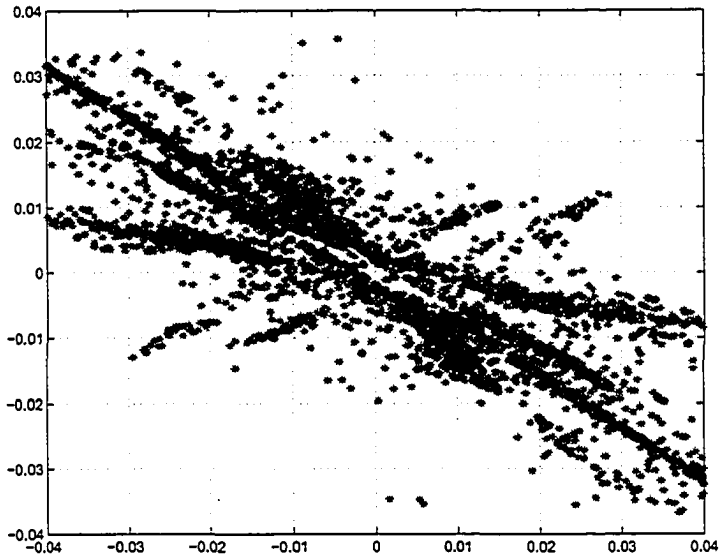

Figure 7.3: Plot of the asymptotic behavior $(x(k), x_d(k))$

for some $\gamma \in [-2\delta, 2\delta]$. Such a surface is denoted Ω_γ. The point $(0, 0, \gamma)$ is the origin of Σ_{n2} on Ω_γ. Furthermore, the line

$$\Gamma_{s,\gamma} : \tilde{x} = 0, \quad \tilde{z}_- = \gamma \tag{7.5}$$

is the stable manifold of Σ_{n2} on Ω_γ and similarly, the line

$$\Gamma_{u,\gamma} : \tilde{x}_d = 0, \quad \tilde{z}_- = \gamma \tag{7.6}$$

is the unstable manifold of Σ_{n2} on Ω_γ.

Suppose a trajectory Γ of the system Σ_n starts from a point p and is governed by Σ_{n2}. If $p \in \Gamma_{u,\gamma}$ (or in general $p \notin \Gamma_{s,\gamma}$) on some surface Ω_γ, then the trajectory will contract along the $\tilde{x}_d$−axis and stretch along the $\tilde{x}$−axis. Due to Eq. (7.3), after some iterations, Γ will move according to the stable subsystem Σ_{n1}. At this moment, Γ will leave the surface Ω_γ, and move toward the origin $(0, 0, 0)$. By Eq. (7.2), after some iterations, it will move again onto some surface $\Omega_{\gamma'}$ for some $\gamma' \in [-2\delta, 2\delta]$. If it is not exactly on the line $\Gamma_{s,\gamma'}$, it will once more contract along the $\tilde{x}_d$−axis and stretch along the $\tilde{x}$−axis and repeat the above behavior. So normally a trajectory never settles down. This contracting and stretching nature indicates the intriguing behavior system Σ_n.

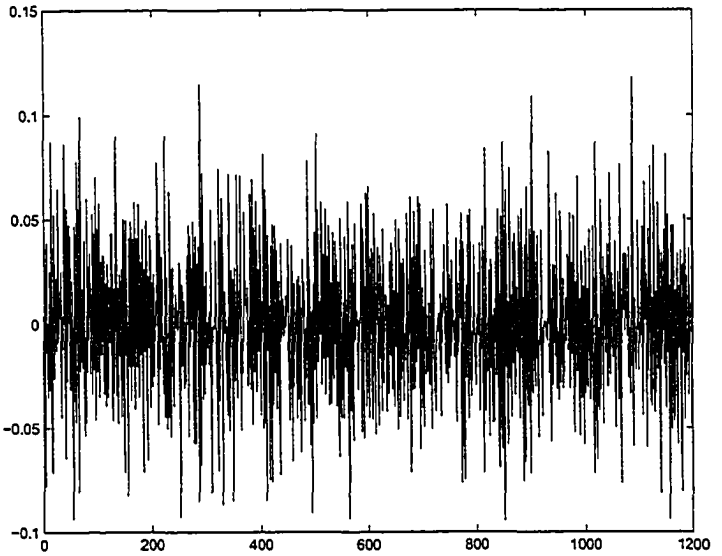

Figure 7.4: Sensitive dependence on initial conditions

Example 7.2 Consider the following system:

$$x(k+1) = \begin{cases} A_1 x(k), & \text{if } |x_1(k) - x_3(k)| > 1, \\ A_2 x(k), & \text{otherwise,} \end{cases} \tag{7.7}$$

where

$$A_1 = \begin{bmatrix} 1-\epsilon & 1 & 0 \\ -\epsilon/2 & 1 & 0 \\ 1 & 0 & 0 \end{bmatrix}, \; A_2 = \begin{bmatrix} 1-\epsilon & 1 & 0 \\ 0 & 1 & -\epsilon/2 \\ 0 & 0 & 1 \end{bmatrix}.$$

The variations of the trajectory, starting from $(1,\ 1/10^5,\ -1)$ as ϵ varies, are plotted in Figures 7.6-7.7. One can see the phase transition process vividly from these figures.

Figures 7.6-7.7 reveal the rich dynamics of a 3-d system governed by the switching law, which will be our future research topic.

7.2 System analysis

This section analyzes a two dimensional system with emphasis on its fixed points and periodic orbits. Consider the following system:

$$\begin{aligned} x_1(k+1) &= a_1 x_1(k) + b_1 x_2(k), \\ x_2(k+1) &= a_2 x_2(k) + b_2 v(k), \end{aligned}$$

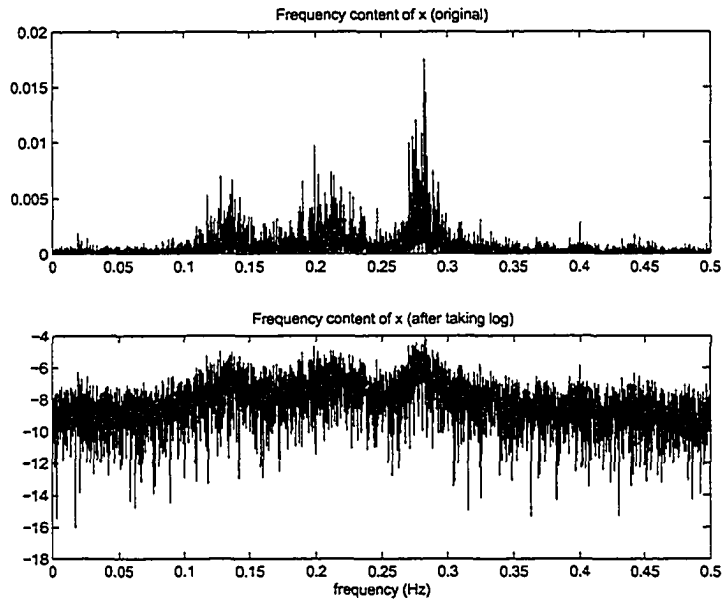

Figure 7.5: Sensitive dependence on initial conditions

where

$$v(k) = \begin{cases} x_1(k), & \text{if } |x_1(k) - v(k-1)| > \delta, \\ v(k-1), & \text{otherwise.} \end{cases}$$

Introduce a new variable

$$x_3(k) = v(k-1),$$

and define

$$x = \begin{bmatrix} x_1 \\ x_2 \\ x_3 \end{bmatrix}, \; A_1 = \begin{bmatrix} a_1 & b_1 & 0 \\ b_2 & a_2 & 0 \\ 1 & 0 & 0 \end{bmatrix}, \; A_2 = \begin{bmatrix} a_1 & b_1 & 0 \\ 0 & a_2 & b_2 \\ 0 & 0 & 1 \end{bmatrix},$$

then

$$x(k+1) = \begin{cases} A_1 x(k), & \text{if } |x_1(k) - x_3(k)| > \delta, \\ A_2 x(k), & \text{otherwise.} \end{cases} \tag{7.8}$$

7.2.1 Fixed points and switching surfaces

Suppose that $(\bar{x}_1, \bar{x}_2, \bar{x}_3)$ is a fixed point of system (7.8). Then

$$\begin{aligned} \bar{x}_1 &= a_1\bar{x}_1 + b_1\bar{x}_2, \\ \bar{x}_2 &= a_2\bar{x}_2 + b_2\bar{x}_3, \\ \bar{x}_3 &= \bar{x}_3. \end{aligned}$$

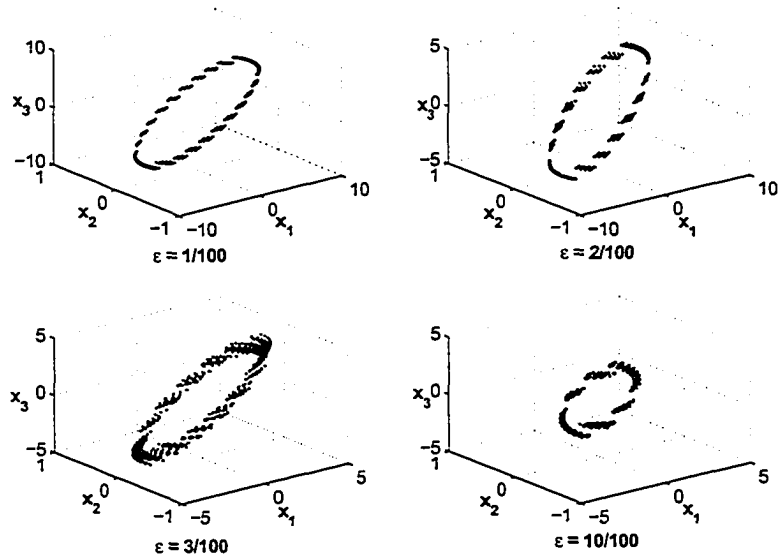

Figure 7.6: Attractors in 3-d:I

If $a_1 \neq 1$ and $a_2 \neq 1$,

$$\bar{x}_2 = \frac{b_2}{1-a_2}\bar{x}_3,\ \bar{x}_1 = \frac{b_1}{1-a_1}\frac{b_2}{1-a_2}\bar{x}_3, \tag{7.9}$$

where

$$|\bar{x}_3| \leq \frac{\delta}{\left|\frac{b_1 b_2}{(1-a_1)(1-a_2)} - 1\right|}. \tag{7.10}$$

For this case, the switching surfaces of this system are

$$x_1 - x_3 = \pm\delta,$$

hence the two intersecting points of the line segment of fixed points and the switching surfaces are

$$\pm\left(\frac{k_1}{k_1-1}\delta,\ \frac{b_2}{1-a_2}\frac{k_1}{k_1-1}\delta,\ \frac{1}{k_1-1}\delta\right),$$

where $k_1 = \frac{b_1}{1-a_1}\frac{b_2}{1-a_2}$. They are symmetric with respect to the origin.

If $a_1 \neq 1$ and $a_2 = 1$,

$$\bar{x}_3 = 0,\ \bar{x}_1 = \frac{b_1}{1-a_1}\bar{x}_2 \tag{7.11}$$

and

$$|\bar{x}_2| \leq \left|\frac{(1-a_1)\,\delta}{b_1}\right|. \tag{7.12}$$

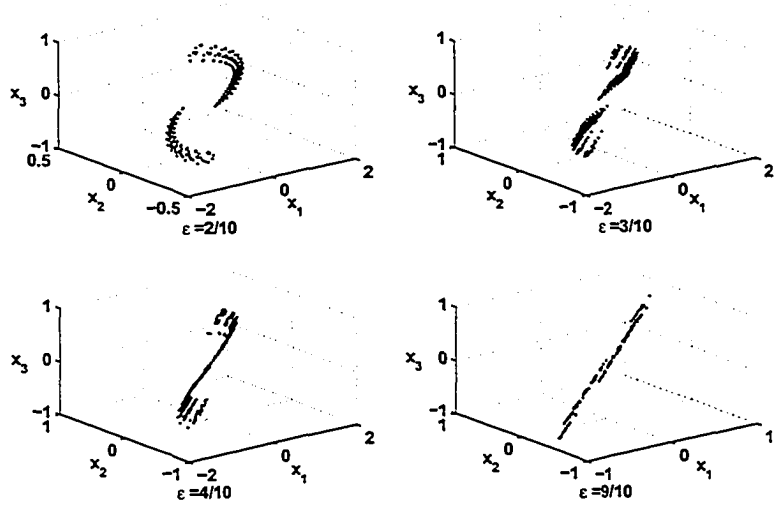

Figure 7.7: Attractors in 3-d:II

If $a_1 = 1$ and $a_2 \neq 1$,

$$\bar{x}_2 = 0,\ \bar{x}_3 = 0, \tag{7.13}$$

and

$$|\bar{x}_1| \leq \delta. \tag{7.14}$$

In all the three cases, fixed points constitute a line segment in $\mathbb{R}^3$. Note that the case of $a_1 = 1$ and $a_2 = 1$ is contained in the case composed of Eqs. (7.13)-(7.14).

7.2.2 Another example

In chapter 6, a line of two dimensional dynamical systems is studied with emphasis on their phase transition, now we discuss a three dimensional case. Here, the discussion is purely descriptive, for which we just present an example.

Example 7.1 Consider the following system:

$$x(k+1) = \begin{cases} A_1 x(k), & \text{if } |x_1(k) - x_3(k)| > 1, \\ A_2 x(k), & \text{otherwise,} \end{cases} \tag{7.15}$$

where

$$A_1 = \begin{bmatrix} a_1 & b_1 & 0 \\ b_2 & a_2 & 0 \\ 1 & 0 & 0 \end{bmatrix}, A_2 = \begin{bmatrix} a_1 & b_1 & 0 \\ \lambda b_2 & a_2 & (1-\lambda)b_2 \\ \lambda & 0 & 1-\lambda \end{bmatrix}$$

When $\lambda = 1$, $A_2 = A_1$. When $\lambda = 0$,

$$A_2 = \begin{bmatrix} a_1 & b_1 & 0 \\ 0 & a_2 & b_2 \\ 0 & 0 & 1 \end{bmatrix}.$$

Fix

$$a_1 = \frac{8}{10},\ b_1 = 1,\ a_2 = 1,\ b_2 = -\frac{1}{10},$$

we plot the variation of the trajectory starting from

$$(1,\ 1/10^5,\ -1)$$

as λ varies (see Figures 7.8-7.9); one can view the phase transition process vividly from these figures.)

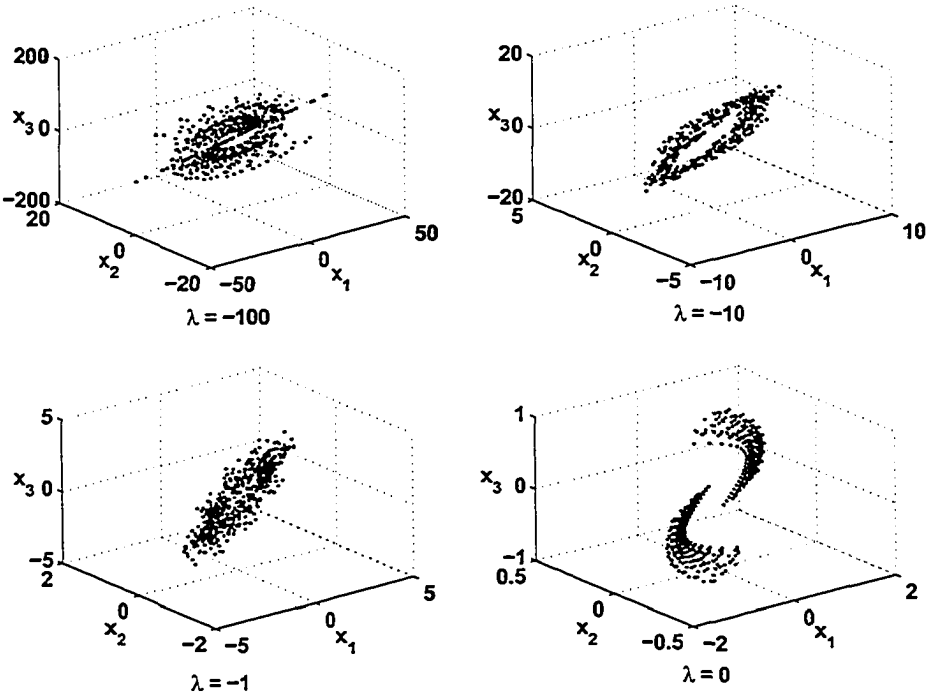

Figure 7.8: Attractors in 3-d:I

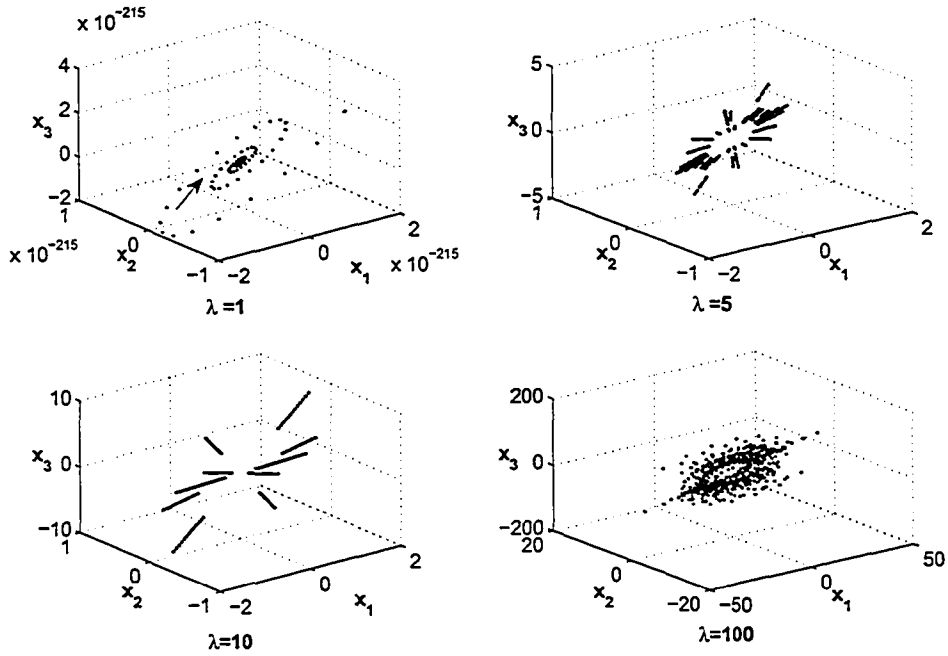

Figure 7.9: Attractors in 3-d:II

7.3 Conclusions

This chapter has discussed higher dimensional cases of the systems governed by the same switching law as those studied in the preceding chapters. The chaotic behavior manifests itself more clearly in these higher cases. Finally we have to mention that first return maps for higher dimensional systems are hard to construct, indicating that their analysis will be more involved than those in Chapters 4–6.

Chapter 8

Continuous case

This chapter studies a continuous-time system composed of two first-order ordinary differential equations with a piecewise constant input. This system is the counterpart of those studied in Chapter 7. As is expected, it also possesses very intricate dynamics: sensitive dependence on initial conditions, coexisting attractors, among others.

The chaotic behavior of this type of systems has at least two sources: The first one is that the piecewise constant input destroys the geometric structure required by the well-known Poincaré-Bendixson Theorem, hence this two-dimensional system may have dynamics which do not exist in a planar system consisting of two autonomous first-order ordinary differential equations. The second is that the solution of the system, namely, two exponential equations, involves an unstable mode. On the one hand, this unstable mode brings in complicated dynamical behavior; on the other hand, it gives rise to nontrivial numerical problems.

8.1 System setting

Consider the following system:

$$\begin{aligned} \dot{x}_1(t) &= a_1 x_1(t) + b_1 x_2(t), \\ \dot{x}_2(t) &= a_2 x_2(t) + b_2 v(t), \end{aligned} \tag{8.1}$$

where the matrix $A = \begin{pmatrix} a_1 & b_1 \\ b_2 & a_2 \end{pmatrix}$ is stable, and the switching law is given by

$$v(t) = \begin{cases} x_1(t), & \text{if } |x_1(t) - v(t_-)| > \delta, \\ v(t_-), & \text{otherwise,} \end{cases} \tag{8.2}$$

in which δ is a positive scalar.

As can be observed, the system governed by Eqs. (8.1)-(8.2) is the continuous-time counterpart of system (7.8). Note that the system consists of two first-order ordinary differential equations. Furthermore, if we fix $v(0_-)$ to be 0, then the above system is autonomous. Moreover, due to the switching nature of the system, the vector field of this system may not be continuous for some set of parameters, not to mention differentiability. This suggests that the well-known Poincaré-Bendixson theorem might not be applicable [30], i.e., besides equilibria and periodic orbits, the ω-limit set of this system may contain other attractors. This turns out to be true as shown by the following simulations. However, before doing that, let us first state a general result regarding the system composed of Eqs. (8.1)-(8.2).

Theorem 8.1 *The trajectories of the system given by Eqs. (8.1)-(8.2) are bounded. Moreover, they converge to the origin as δ tends to zero.*

Proof. For the ease of presentation, we focus on the following system parameters:

$$a_1 = -1, \quad b_1 = 2, \quad a_2 = -2, \quad b_2 = -2. \tag{8.3}$$

Since

$$\begin{aligned} \dot{x}_1(t) &= a_1 x_1(t) + b_1 x_2(t), \\ \dot{x}_2(t) &= a_2 x_2(t) + b_2 v(t) \\ &= a_2 x_2(t) + b_2 x_1(t) + b_2 (v(t) - x_1(t)), \end{aligned}$$

where

$$|v(t) - x_1(t)| \leq \delta. \tag{8.4}$$

Let

$$x(t) = \begin{bmatrix} x_1(t) \\ x_2(t) \end{bmatrix},$$

then

$$\dot{x}(t) = \begin{bmatrix} a_1 & b_1 \\ b_2 & a_2 \end{bmatrix} x(t) + \begin{bmatrix} 0 \\ b_2 \end{bmatrix} (v(t) - x_1(t)). \tag{8.5}$$

For convenience, let

$$A = \begin{bmatrix} a_1 & b_1 \\ b_2 & a_2 \end{bmatrix}, \quad B = \begin{bmatrix} 0 \\ b_2 \end{bmatrix}.$$

Substitute them into Eq. (8.5), we have

$$\dot{x}(t) = Ax(t) + B(v(t) - x_1(t)). \tag{8.6}$$

Solving this equation we get

$$x(t) = e^{At}x(0) + \int_0^t e^{A(t-\tau)}B(v(\tau) - x_1(\tau))\, d\tau.$$

Note that the matrix A is a stable matrix. To show the boundedness of the trajectory, it suffices to show that

$$y(t) := \int_0^t e^{A(t-\tau)}B(v(\tau) - x_1(\tau))\, d\tau \tag{8.7}$$

is bounded. Partition the matrix $e^{A(t-\tau)}$ and substitute (8.3) into it, we obtain

$$\begin{aligned} e^{A(t-\tau)} &= \begin{bmatrix} * & \frac{4e^{-3(t-\tau)/2}\sin\frac{\sqrt{15}}{2}(t-\tau)}{\sqrt{15}} \\ * & \frac{1}{15}e^{-3(t-\tau)/2}\left(15\cos\left(\frac{\sqrt{15}}{2}(t-\tau)\right) - 15\sin\left(\frac{\sqrt{15}}{2}(t-\tau)\right)\right) \end{bmatrix} \\ &= \begin{bmatrix} A_1 & A_2 \\ A_3 & A_4 \end{bmatrix}. \end{aligned}$$

Substituting the above into Eq. (8.7), one gets

$$\begin{aligned} y(t) &= \begin{bmatrix} y_1(t) \\ y_2(t) \end{bmatrix} = \begin{bmatrix} \int_0^t A_2 b_2 (v(\tau) - x_1(\tau))\, d\tau \\ \int_0^t A_4 b_2 (v(\tau) - x_1(\tau))\, d\tau \end{bmatrix} \\ &= \begin{bmatrix} -2\int_0^t \frac{4e^{-3(t-\tau)/2}\sin\frac{\sqrt{15}}{2}(t-\tau)}{\sqrt{15}} (v(\tau) - x_1(\tau))\, d\tau \\ -2\int_0^t e^{-3(t-\tau)/2}\left(\cos(2(t-\tau)) - \sin\left(\frac{\sqrt{15}}{2}(t-\tau)\right)\right)(v(\tau) - x_1(\tau))\, d\tau \end{bmatrix}. \end{aligned} \tag{8.8}$$

Obviously both $y_1(t)$ and $y_2(t)$ are bounded, so is $x(t)$. Meanwhile, according to Eqs. (8.4) and (8.8), $x(t)$ converges to the origin as δ goes to zero. ■

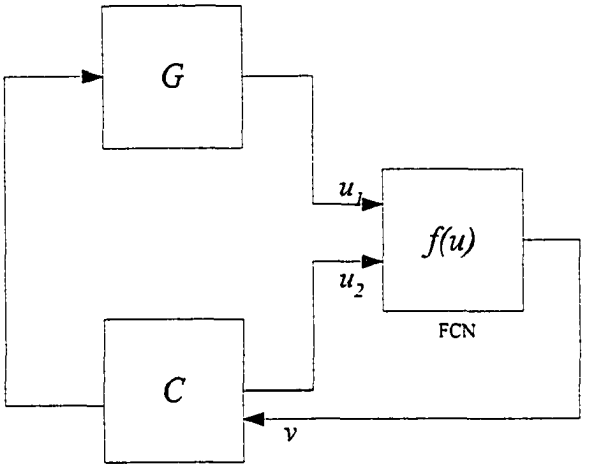

Figure 8.1: A continuous-time switching system

8.2 Simulations

Consider the Simulink model shown in Figure 8.1. The system G and the controller C are modeled by the first and the second equations in Eq. (8.1), respectively. The function FCN, modelling the switching function (8.2), is defined by

$$f(u) := u_1 + u_2 - u_2 * (|u_1 - u_2| > \delta) - u_1 * (|u_1 - u_2| \leq \delta) \ . \tag{8.9}$$

Thus, by letting

$$u = \begin{bmatrix} u_1 \\ u_2 \end{bmatrix},$$

one has

$$v := f(u) = \begin{cases} u_1, & \text{if } |u_1 - u_2| > \delta, \\ u_2, & \text{otherwise.} \end{cases} \tag{8.10}$$

Is the block FCN, the function f, well-defined? It suffices to verify the case at time 0. Firstly, choose $|x_1(0)| < \delta$. Then $u_1 = x_1(0)$. By simulation, it is found that $v = 0$. Secondly, choose $|x_1(0)| > \delta$. Then $u_1 = x_1(0)$. Simulation shows that $v = x_1(0)$. To simplify the notation, denote u_2 at time 0 by $v(0\_)$. Summarizing the above, one has

$$\begin{aligned} v(0\_) &= 0, \\ v(0) &= \begin{cases} x_1(0), & \text{if } |x_1(0) - v(0\_)| > \delta, \\ v(0\_), & \text{otherwise.} \end{cases} \end{aligned}$$

Similarly,

$$v(t) = \begin{cases} x_1(t), & \text{if } |x_1(0) - v(0_-)| > \delta, \\ v(t_-), & \text{otherwise,} \end{cases} \quad \text{for } t > 0,$$

where $v(t_-)$ is either some previous value of the state x_1, say $x_1(t - t_0)$ for some t_0 satisfying $0 < t_0 \leq t$, or $v(0_-) = 0$. Hence, the block FCN is well-defined.

Next, we find the equilibria of the system. As expected, the equilibria of the system constitute a line segment, just as in the discrete-time case. The equilibria are given by

$$\Lambda = \left\{ \left(x_1 = \frac{b_1 b_2}{a_1 a_2} v,\ x_2 = -\frac{b_2}{a_2} v,\ v \right) : |v| \leq \frac{\delta}{\left| 1 - \frac{b_1 b_2}{a_1 a_2} \right|} \right\}. \tag{8.11}$$

For the system composed of Eqs. (8.1)-(8.2), an interesting question is: Given an initial condition $x(0)$, will $x(t)$ settle to a certain equilibrium or converge to a periodic orbit or have more complex behavior? There are two ways of tracking a trajectory $x(t)$: one is to solve Eqs. (8.1)-(8.2) directly, and the other is by means of numerical methods. To get an analytic solution, one has to detect the discontinuous points of the right-hand side of Eq. (8.1). We first show that the number of the discontinuous points within any given time interval is finite.

Start at some time $t_0 \geq 0$ and assume that $(x_1(t_0), x_2(t_0))$ and $v(t_{0-}) = x_1(t_0)$ are given, without loss of generality. Suppose that the first jump of v is at instant $t_0 + T$. To be specific in the following calculation, let $t_0 = 0$. Then

$$\begin{aligned} x_1(T) &= e^{a_1 T} x_1(0) + \int_0^T e^{a_1(T-\tau)} b_1 x_2(\tau)\, d\tau, \\ x_2(T) &= e^{a_2 T} x_2(0) + \int_0^T e^{a_2(T-\tau)} b_2 x_1(0)\, d\tau \\ &= e^{a_2 T} x_2(0) + \int_0^T e^{a_2 u} du b_2 x_1(0). \end{aligned}$$

Consequently,

$$x_1(T) - x_1(0) = \left(e^{a_1 T} - 1\right) x_1(0) \left(1 - \frac{b_1 b_2}{a_1 a_2}\right) + \left(e^{a_2 T} - e^{a_1 T}\right) b_1 \frac{x_2(0) + \frac{b_2}{a_2} x_1(0)}{a_2 - a_1}. \tag{8.12}$$

As $T \to 0$, $e^{a_1 T} - 1 \to 0$, and $e^{a_2 T} - e^{a_1 T} \to 0$. Moreover, we have already shown the boundedness of solutions, so there exists a $T^* > 0$ such that

$$|x_1(T) - v(0)| = |x_1(T) - x_1(0)| < \delta \tag{8.13}$$

for all $T < T^*$. Thus, the finiteness of the number of the discontinuous points within any given time interval is established.

Based on this result, theoretically one can find the analytic solution of the system. However, it is difficult since the condition in Eq. (8.13) has to be checked all the time to determine the switching time T. Moreover, this process depends on the initial point, $(x_1(t_0), x_2(t_0))$, which is hard due to the impossibility of finding the exact T satisfying $|x_1(T) - v(0)| = \delta$. This problem will be addressed in more details in Sec. 8.3.

Another route to study this type of systems is by means of numerical analysis. In the following, some simulations will be shown to analyze the complexity of the system depicted in Figure 8.1. In all the following trajectory figures, the horizontal axes stands for x_1 and the vertical one is x_2.

8.2.1 Converging to some fixed point

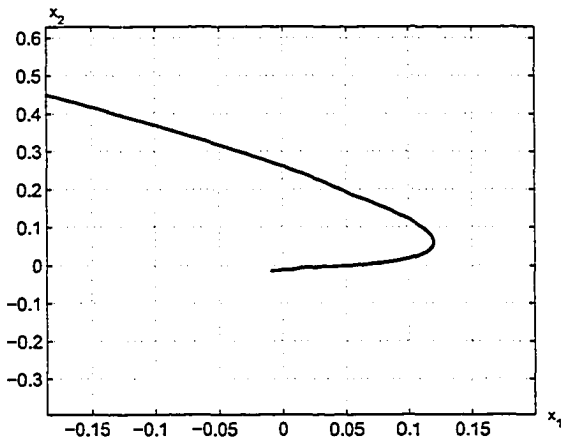

Figure 8.2: Converging to an equilibrium other than the origin

Fix those parameters shown in Figure 8.1 to be:

$$a_1 = -1, \quad b_1 = 2, \quad a_2 = -2, \quad b_2 = -2,$$

and choose an initial condition $(10, -10)$. Then, we get simulation results shown in Figure 8.2. One can see that this trajectory converges to a point specified by Eq. (8.11), which is close, but not equal, to the origin.

8.2.2 Sensitive dependence on initial conditions

First, fix system parameters as

$$a_1 = 1,\ b_1 = 2,\ a_2 = -2,\ b_2 = -2,\ \delta = 1, \tag{8.14}$$

and note that there is an *unstable* pole in the system G, namely, suppose

$$x_1(0) = 2, \quad x_2(0) = 1,$$

and

$$x_1(0) = 2 - 10^{-10}, \quad x_2(0) = 1.$$

Then, we get the simulation result shown in Figure 8.3, where the first two are

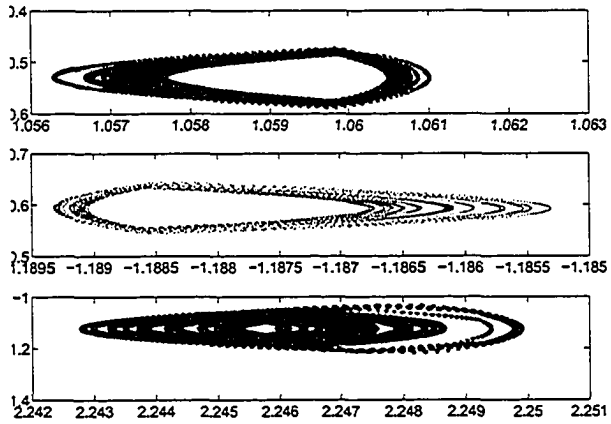

Figure 8.3: Sensitive dependence on initial conditions

trajectories from those two sets of initial conditions given above and the third one is their difference. Clearly, one can see the sensitive dependence on initial conditions.

8.2.3 Coexisting attractors

Adopt the system parameters as in Eq. (8.14). then, we have simulation results shown in Figure 8.4, where the largest initial differences of any two such trajectories is 10^{-3}. These attractors are all alike; however, they are located in different positions; that is, they are coexisting attractors.

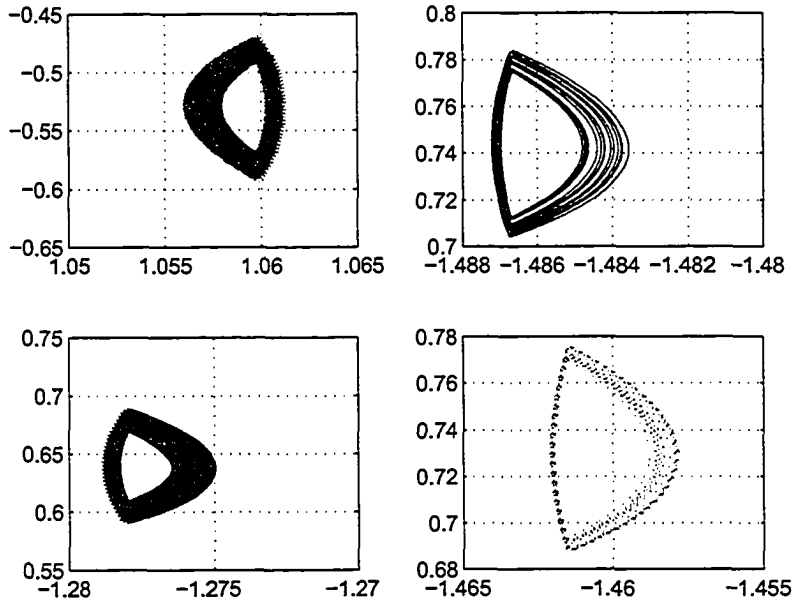

Figure 8.4: Several coexisting attractors (the horizontal axes is x_1 and the vertical stands for x_2)

8.2.4 A periodic orbit

Now, choose

$$a_1 = -11,\ b_1 = 1/4,\ a_2 = 10,\ b_2 = 1/4 - (a_1 - a_2)^2,\ \delta = 1. \tag{8.15}$$

Simulations show that most trajectories behave like the that shown in Figure 8.5, which is periodic.

Having observed various complex dynamics possessed by the system shown in Figure 8.1, one may ask the following question:

Is the complexity exhibited by the system due to numerical errors or is the system truly chaotic?

We received the following warning during our simulations using Simulink: *Block diagram "A continuous-time switching system" contains 1 algebraic loop(s).* This warning is due to the fact that one of the output of the function block FCN is its

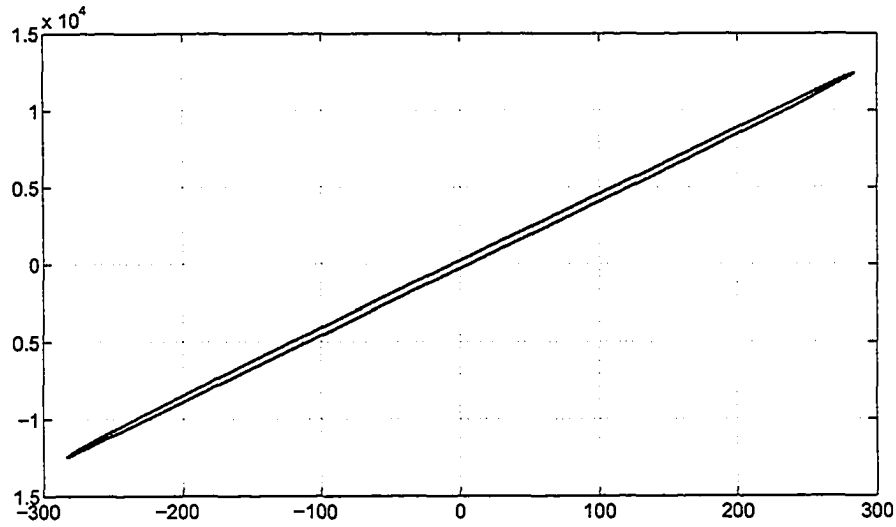

Figure 8.5: A periodic orbit

own input. Certainly, this may lead to numerical errors. So, a transport delay is added to rule out this possibility. This consideration leads to the following scheme (Figure 8.6):

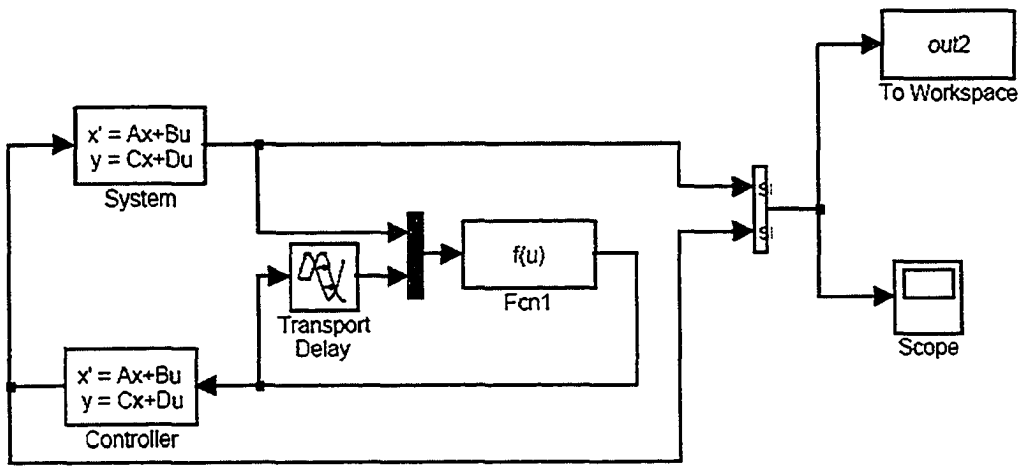

Figure 8.6: A modified continuous-time switching system

To correctly implement Eq. (8.2), the transport delay T must be small enough.

Here, it is fixed to be $T = 5 * 10^{-2}$. Suppose that system parameters are given by Eq. (8.14) and choose two sets of initial conditions, $(2, 1)$ and $(2 - 10^{-6}, 1)$. Then, we get Figure 8.7. According to the upper part of this plot, two trajectories

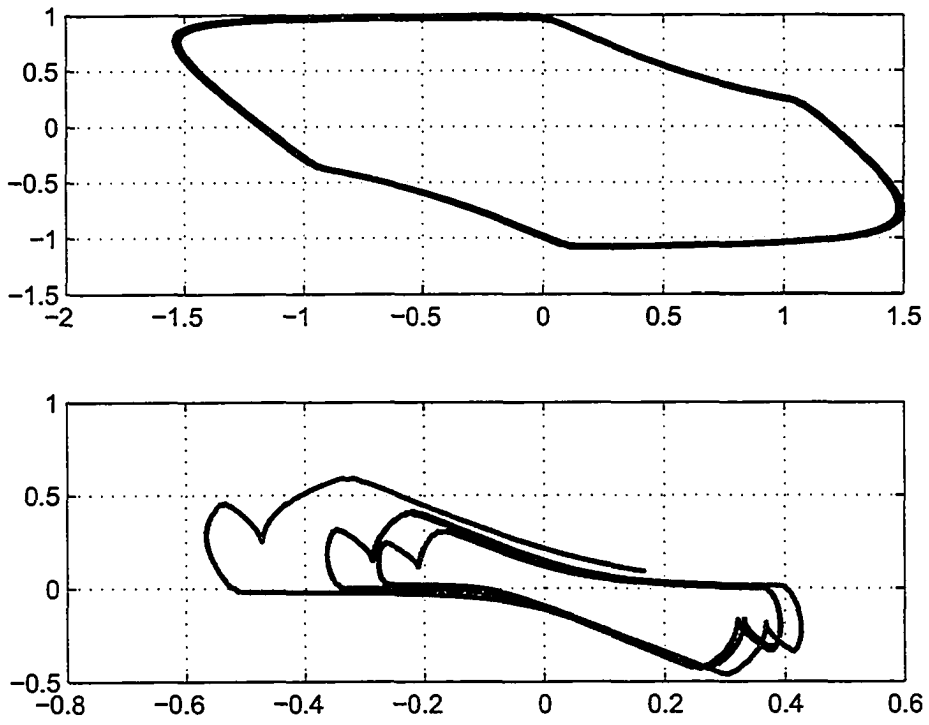

Figure 8.7: Sensitive dependence on initial conditions

almost coincide; however, the lower plot clearly reveals sensitive dependence on initial conditions.

For a sufficiently small transport delay T, many simulations show that the complicated attractor is unique, but sensitive dependence on initial conditions still persists. Apparently, this phenomenon needs further investigations.

8.3 Computational complexity

We have visualized some complex behaviors of system (8.1)-(8.2), but we have not answered the question posed above. In this section, we study this problem in some

details.

Consider the following system:

$$\begin{aligned} \dot{x}_1(t) &= a_1 x_1(t) + b_1 x_2(t), \\ \dot{x}_2(t) &= a_2 x_2(t) + b_2 p, \end{aligned} \tag{8.16}$$

where

$$a_1 = 1,\ b_1 = 2,\ a_2 = -2;\ b_2 = -2,\ \delta = 1,$$

and p is a scalar. At $t = 0$, let

$$x_1(0) = p,\ x_2(0) = q.$$

Then, a direct calculation gives

$$\begin{aligned} x_1(t) &= 2p - \frac{1}{3}e^{t}(p - 2q) - \frac{2}{3}e^{-2t}(p + q), \\ x_2(t) &= -p + e^{-2t}(p + q). \end{aligned} \tag{8.17}$$

Suppose $p \neq 2q$. Then, there exists an instant $t_0 > 0$ such that

$$|p - x_1(t_0)| = 1. \tag{8.18}$$

Set

$$p = x_1(t_0).$$

And then solve equations (8.16) starting from $(x_1(t_0),\ x_2(t_0))$ at time t_0. Repeat this procedure (update p whenever Eq. (8.18) is satisfied) to get an analytic solution of the system starting from $(x_1(0), x_2(0)) = (p, q)$.

Now, it is easy to realize that the complexity may probably be due to the following reasons:

- There is an unstable mode in $x_1(t)$ in Eq. (8.17).
- It is hard to find the exact switching time, e.g., t_0 in Eq. (8.18), even numerically. Because of this, numerical errors will accumulate and be exaggerated from time to time by the unstable mode. Further research is required to study the effect of the accumulated errors on the dynamics of the system.
- Sec. 8.2.4 tells us the first item alone can not guarantee complex behavior.

8.4 Conclusions

This chapter investigates the qualitative behavior of a type of continuous-time switching systems which is the counterpart of those discrete-time ones studied in Chapter 7. Simulations in Sec. 8.2 reveal the bewildering behavior of numerical solutions of this category of systems. Sec. 8.3 tells us the exact analysis of this type of systems is very difficult.

According to the well-known Poincaré-Bendixson theorem, the attracting sets of a planar system can only be equilibria or limit cycles. However the systems studied in this chapter do not satisfy the condition of continuous differentiability of the vector fields, therefore indicating that the complexity may be possible, instead of just a computer artifact. This consideration gives rise to the following problem.

Problem 8.1 *Is the behavior of the class of two-dimensional systems studied in this chapter indeed chaotic? To put it in another way, Are those strange attractors genuine properties of these systems or just computer artifacts?*

Chapter 9

Control

This chapter will take a closer look at the control problem under the network data transmission strategy proposed in Chapter 3. Sec. 9.1 addresses the chaotic control problem. In Sec. 9.2 a simple example is used to illustrate that some modification of the underlying control law can improve the performance of both the network and the control system. Sec. 9.3 discusses how to convert the control problem to an optimization problem. Sec. 9.4 contains some discussions on limited information control.

9.1 Chaotic control?

The complex dynamic behavior of the system shown in Figure 3.2 has been studied in detail in the foregoing chapters. Compared to the standard control scheme such as that shown in Figure 3.1, whose dynamics can only be either converging to the origin, or being periodic or unbounded trajectories, the scheme adopted in Figure 3.2 provides much more dynamical properties. This provides a control engineer with more flexibilities at his/her disposal, which is particularly attractive from the viewpoint of multi-purpose control. This may be one of the main merits that the control scheme proposed here can provide. In this section, the following problem will be addressed: Given a control performance specification, can we achieve it by possibly adjusting the system parameters? The following discussions concentrate on two control specifications:

(1) The system has only one operating point and it is desirable that the system operates around this point.

(2) A periodic orbit is desirable.

For item (1), without loss of generality, assume that the desirable unique operating point is the origin. If the parameter a in system (4.1) satisfies $|a| < 1$, then asymptotic stability with respect to the origin can be achieved by adjusting the nonlinear block H_1. According to Figure 4.7, it suffices to let the value $v(k-1)$ stored in H_1 be 0 when $|x(k)| < \delta$ (This feature is illustrated in Figures 4.8-4.9). Then the trajectory will move along the $x-$axis toward the origin, i.e., the asymptotic stability of the origin is achieved. If the parameter a in system (4.1) satisfies $|a| \geq 1$, one can not expect asymptotic stability of the origin because it itself is unstable. However, the trajectory can be kept arbitrarily close to the origin after some iterations, by adopting the following scheme. Suppose it is desirable to keep the trajectory within the distance ϵ around the origin. Then choose δ small enough so that $x(k^*)$ satisfies $|x(k^*)| < \epsilon/|a|^2$ at some time instant k^*(this can be realized, see Figure 4.12). Set $v(k^*-1) = 0$. If $|a| = 1$, then the trajectory will stay at $(0, x(k^*))$ forever. The goal is achieved. On the other hand, assume $a > 1$. If $x(k^*) > 0$, first let the trajectory move along the $x-$axis, then one gets $x(k^*+1) < \epsilon/|a|$ at time k^*+1. Now choose

$v(k^*)$ satisfying $\epsilon/|b| < v(k^*) < \epsilon/(a^2|b|)$. In this way $(x(k^*+1), v(k^*))$ is below the line segment of fixed points ($(x(k^*+1), v(k^*))$ will hence move downward at the next step) such that

$$x(k^*+2) > 0,$$

and

$$x(k^*+2) = ax(k^*+1) + bv(k^*) < \epsilon/a^2.$$

(Note this is guaranteed by the property of the vector field of the system.) Then let $v(k^*+1) = 0$, and repeat the above procedure. Similarly if $x(k^*) < 0$, all we need to do is choose a suitable $v(k^*) < 0$ such that $(x(k^*+1), v(k^*))$ is above the line segment of fixed points, then follow the above procedure. In this way we can keep the trajectory within the distance ϵ of the origin. Based on the above analysis, we observe that the instability of the parameter a poses a difficulty for implementing our scheme. The foregoing discussion is reminiscent of Proposition 2.2 in [16], however our scheme is better since the K_1 in that paper can be ∞ here. Moreover, our algorithm is simpler too.

For the item (2), suppose it is desired that the system operates on a periodic orbit Γ of periodic T. If $a = 1$, according to Theorem 4.4, by suitably choosing b, a periodic orbit of period T can be built. If $a \neq 1$, then following the discussion after Theorem 4.4, it is also possible to construct a periodic orbit of period T. Then the real question is: Can one really find an initial condition which produces or converges to the desirable periodic orbit Γ? If Γ is within a strange attractor, then from almost all initial points, trajectories will be within an arbitrarily small neighborhood of Γ at some time k; this is the property of a stranger attractor. So one can simply pick up such an initial condition, let the system run automatically first, and apply control similarly to the case in item (1) when the trajectory is sufficiently close to Γ, and keep it remain within a small neighborhood of Γ. Therefore the problem boils down to constructing a strange attractor containing Γ. This is still an open problem. Note that the chaotic systems studied seem different than many known chaotic systems, which have strange attractors within which there are periodic orbits of any periods. However in light of Corollary 4.2, there may be no periodic orbits at all when a is rational and b is irrational. This annoying fact may probably be due to that the scheme we are proposing involves discontinuities. It has already been

illustrated that there may be a great variety of dynamics this scheme can produce, which brings more freedom to a control engineer, and especially suitable for multi-purpose controller design. However in order to make the proposed scheme more useful, a more thorough study of this scheme has to be conducted.

9.2 A simple example

In this section a simple tracking problem is investigated. Suppose the controller C has been designed for the system G shown in Figure 3.1 so that the output y tracks the reference signal r; how does the nonlinear constraint H_1 and H_2 affect this tracking problem? We will investigate this problem via a simple example.

Example 9.1 Consider the following discrete-time system G:

$$\frac{0.005z^{-1} + 0.005z^{-2}}{1 - 2z^{-1} + z^{-2}}.$$

Note that this system is *unstable*. Suppose we have already designed a controller K of the form

$$\frac{37.33 - 33.78z^{-1}}{1 - 0.1111z^{-1}},$$

which achieves step tracking. First, we check the data transmission strategy by simulating the system shown in Figure 3.2, with $r \equiv 1$ but without H_2 involved therein. Choose $\delta_1 = 1$. Then, the tracking error is plotted (the $*$ line in Figure 9.1). After that, we modify the control law as follows:

$$v(k) = H_1\left(u_c(k), v(k-1)\right) = \begin{cases} u_c(k), & \text{if } |u_c(k) - v(k-1)| > 1, \\ \varepsilon_1 v(k-1) + \varepsilon_2 x(k), & \text{otherwise,} \end{cases}$$

where $\varepsilon_1 \in \mathbb{R}$, $\varepsilon_2 \in \mathbb{R}^{1\times 2}$ are to be determined. Here, we assume that the state x of the system G is available. When there is no transmission from C to G, instead of simply using the previously stored control value $v(k-1)$, $\varepsilon_1 v(k-1) + \varepsilon_2 x(k)$ is used. The reason is that by adjusting ε_1 and ε_2 sensibly we may achieve better control performance. By selecting

$$\varepsilon_1 = 0.86,\ \varepsilon_2 = [-0.21\ 0.21],$$

the tracking error is plotted (the dotted line in Figure 9.1). In this simulation, iteration time is 350, so the dropping rate can also be obtained: the former is

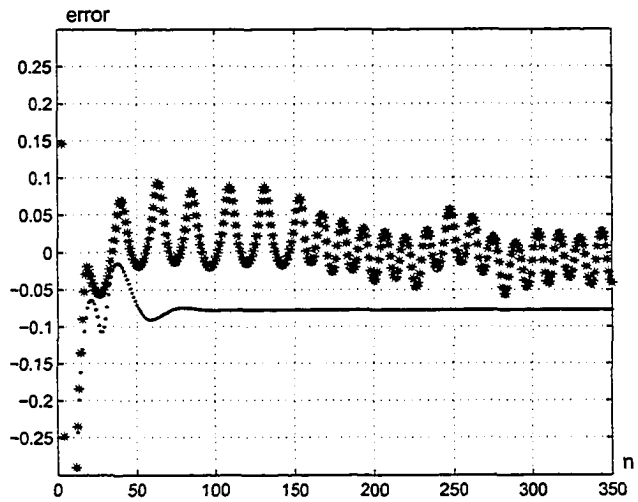

Figure 9.1: Tracking error with $\delta_1 = 1$

85.14% and the latter is 96.57%. Hence, the modified control law is more efficient in reducing data traffics. The steady-state error shown in Figure 9.1 under the modified control law is around 0.0774. Next, we choose $\delta_1 = 1/2$, and get the result shown in Figure 9.2 following the same procedure. The dropping rates are 83.14% for the original and 96.29% for the modified. In this case the steady-state tracking error for the modified system is around 0.0079. So, by modifying the control law, we increased the dropping rate therefore reduced the data traffics, and at the same time improved the performance of the control system.

9.3 An optimization problem

In the above example, it is shown that for simple control systems it is possible to improve the performance of both the network and the control system by modifying the underlying control law. Clearly, it is more mathematically involved when one confronts a more complex system. We next transform this problem into an optimization problem.

Define $\varsigma = \eta - \xi$, and $e_r := e_c - e$. By subtracting the system in (3.3) from that

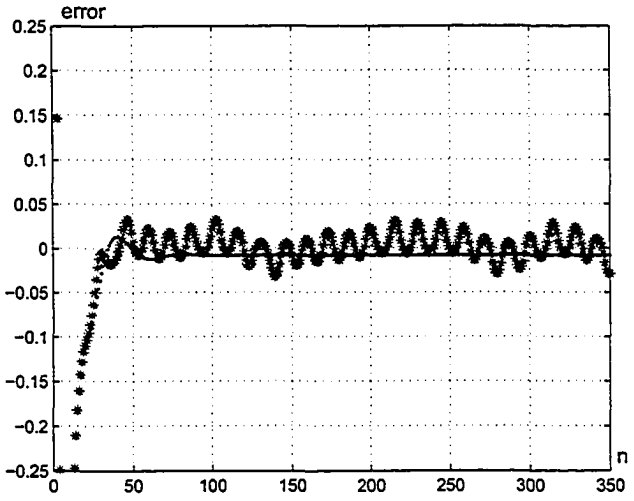

Figure 9.2: Tracking error with $\delta_1 = 1/2$

in (3.6), we get

$$\begin{aligned} \varsigma(k+1) &= \check{A}\varsigma(k) + \begin{bmatrix} B & BD_d \\ 0 & B_d \end{bmatrix} \left(\begin{bmatrix} H_1(u_c(k), v(k-1)) \\ H_2(y_c(k), z(k-1)) \end{bmatrix} - \begin{bmatrix} u_c(k) \\ y_c(k) \end{bmatrix} \right), \\ e_r(k) &= \begin{bmatrix} -C & 0 \end{bmatrix} \varsigma(k) + z(k) - y_c(k). \end{aligned} \tag{9.1}$$

Then, the tracking error e_c of system (3.6) can be obtained via tracking error e of system (3.3), which is a standard feedback system.

To study the tracking error e_r, we employ the l_∞-norm of signals [3]. According to (9.1), we have

$$\|\varsigma\|_\infty \leq \left\| \left(z^{-1}I - \begin{bmatrix} A - BD_dC & BC_d \\ -B_dC & A_d \end{bmatrix} \right)^{-1} \begin{bmatrix} B & BD_d \\ 0 & B_d \end{bmatrix} \right\|_1 \bar{\delta}, \tag{9.2}$$

and

$$\begin{aligned} \|e_r\|_\infty &\leq \left\| \begin{bmatrix} -C & 0 \end{bmatrix} \left(z^{-1}I - \begin{bmatrix} A - BD_dC & BC_d \\ -B_dC & A_d \end{bmatrix} \right)^{-1} \begin{bmatrix} B & BD_d \\ 0 & B_d \end{bmatrix} \right\|_1 \\ &\quad \times \left\| \begin{bmatrix} H_1(u_c(k), v(k-1)) \\ H_2(y_c(k), z(k-1)) \end{bmatrix} - \begin{bmatrix} u_c(k) \\ y_c(k) \end{bmatrix} \right\|_\infty + \delta_2 \\ &\leq \bar{\delta} \left\| \begin{bmatrix} -C & 0 \end{bmatrix} \left(z^{-1}I - \begin{bmatrix} A - BD_dC & BC_d \\ -B_dC & A_d \end{bmatrix} \right)^{-1} \begin{bmatrix} B & BD_d \\ 0 & B_d \end{bmatrix} \right\|_1 + \delta_2. \end{aligned} \tag{9.3}$$

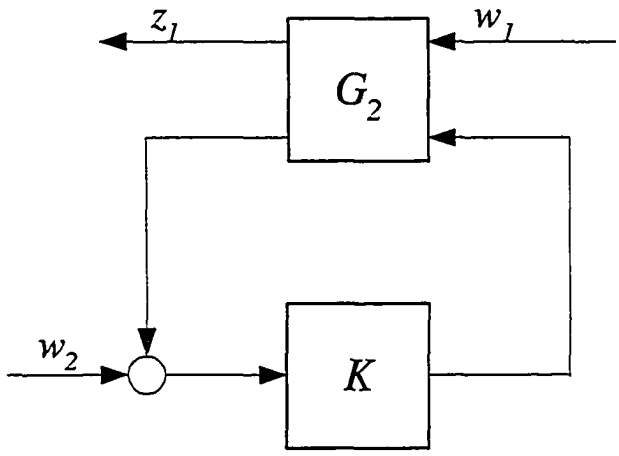

Figure 9.3: An ℓ_1 minimization problem

Remark 9.1 Eq. (9.3) gives an upper bound of the difference of the tracking error for the systems shown in Figs. 3.1 and 3.2. In light of (9.2) and (9.3), with δ_1 and δ_2 fixed, minimizing the size of an attractor and the tracking error can be converted to the problem of designing a controller K that achieves step tracking in Figure 3.1 and minimizes $\|z_1\|_\infty$ in Figure 9.3 simultaneously, with

$$G_2 = \left[\begin{array}{c|cc} A & B & B \\ \hline -C & 0 & 0 \\ -C & 0 & 0 \end{array}\right], \quad K = \left[\begin{array}{c|c} A_d & B_d \\ \hline C_d & D_d \end{array}\right], \quad \|w_1\|_\infty \leq 1, \ \|w_2\|_\infty \leq 1.$$

For this multiple-objective control problem, LMI techniques can be applied. More specifically, by parameterizing all stabilizing controllers, the step tracking problem has an equality constraint for the l^1control problem shown in Figure 9.3, which can be modified as an LMI minimization problem (see [13] and [11] for more details).

9.4 Further discussions

Interestingly, one application of this network data transmission strategy is the so-called limited communication control in control and coordination of multiple subsystems. One example is: A single decision maker controls many subsystems over a communication channel of a finite capacity, where the decision maker can control only one subsystem at a time. Let us consider the following situation: Suppose there are several systems sharing a common communication channel, where at each trans-

mission time only one system can send a signal. Is it possible that each subsystem adopts the transmission strategy proposed here so that the whole system can achieve some desired control performance? Note that under the proposed transmission strategy, each system just send "necessary" signals, leaving communication resources to the others to use. Thus, if we design the *transmission sequence* carefully, the whole system might perform well. A similar but essentially different problem was discussed in [31], which is an extension of the work of [7]. The problem studied therein is: Given a set of control systems controlled by a single decision maker, which can communicate with only one system at a time, design a communication sequence so that the whole network is asymptotically stable. Using augmentation, this problem can be converted to a mathematical programming problem for which some algorithms are currently available. Here, under the proposed transmission strategy, the communication strategy depends severely on the control systems. Hence the communication sequence depends explicitly on all subsystems, adding more constraints to the design of the communication sequence. This important yet challenging problem will be our future research topic.

Problem 9.1 *Under the network data transmission strategy proposed, how to design controllers to guarantee satisfactory control performance? Is this transmission strategy practically realizable?*

To put the proposed network data transmission strategy into practical applications in the limited information control, this problem must be investigated thoroughly.

Chapter 10

Future research directions

In this thesis, a type of nonsmooth dynamical systems is studied from the perspective of its dynamics as well as its possible applications. The intriguing complexity inherent in this class of systems has been addressed in some depth. It is hoped that this study can shed some light on the common nature of nonsmooth dynamics, which are apparently more common than smooth dynamics in the real world.

This study evolves originally from the consideration of networked control systems; simulations show the effectiveness of the proposed data transmission strategy. We hope it is of some use in practical applications.

We have posed several problems in various chapters, which will constitute our future research directions. For clarity, we re-list them here and append one more. However we have to admit that probably the most essential problems still lurk somewhere. Mother Nature knows better.

1. **Problem** 4.1. Given a, b and δ, how to find the exact ω-limit set of system Eq. (4.1)?

2. **Problem** 4.2. Why are the asymptotic behaviors of the systems with $|b| < a$ and $|b| > a$ dramatically different?

3. **Problem** 5.1. How to determine if the system in Eq. (5.1) is dissipative? If this can be resolved, then the dissipativity of the family of systems in Eq. (6.4) may be determined in the same way.

4. **Problem** 6.1. Assume parameters a, b, δ are given in the system composed of Eqs. (6.4)-(6.5). As far as a particular orbit is concerned, for instance, the one starting from $(-10, 10)$ in the example studied above, is there a $\lambda_0 \in (0, 1)$ such that the orbit converges to the origin for all $1 \geq \lambda > \lambda_0$, whereas it oscillates for all $0 \leq \lambda < \lambda_0$? If there is, what behavior will the orbit starting from $(-10, 10)$ run into: converge to the origin or a periodic orbit, oscillate or be periodic?

5. **Problem** 6.2. Is there a $\lambda_1 \in (0, 1)$ such that all orbits will converge for all $1 \geq \lambda > \lambda_1$, whereas there is at least one oscillating orbit for each $0 \leq \lambda < \lambda_1$? Again, for this λ_1, what will trajectories end up with?

6. **Problem** 6.3 It is obvious that the system composed of Eqs. (6.4)-(6.5) is dissipative at λ around but less than 1. How will it change as λ moves from 1 to 0? Is it invariant? This problem echoes Problem 5.1 listed above.

7. **Problem** 8.1. Is the behavior of the class of two-dimensional continuous systems studied in Chapter 8 indeed chaotic? To put it in another way, Are those strange attractors genuine properties of these systems or just computer artifacts?

8. **Problem** 9.1. Under the network transmission strategy proposed here, how to design controllers to guarantee satisfactory control performance? Is this transmission strategy practically realizable?

9. Based on the discussions in previous chapters, one finds that the qualitative behavior of this type of nonsmooth dynamical systems is rather hard to analyze

analytically. As is well-known that time series analysis is a very common and effective tool in the analysis of chaotic systems. For instance, it is now customary to define a strange attractor to be one that is fractal. Hence this perspective may provide us some insight. However the difficulties given by non-smoothness may still persist in this context. For example, many chaotic data analysis algorithms are based on the space reconstruction technique, which is obvious inappropriate for a nonsmooth dynamical system. This tells us that there are much more to be done more rigorously.

Bibliography

Bibliography

[1] P. Antsaklis and J. Baillieul, *Guest editorial: special issue on networked control* systems, IEEE Trans. Auto. Contr., vol. 49, pp. 1421-1423, 2004.

[2] K. Åström, J. Hagander, and J. Sternby, Zeros of sampled systems, Automatica, vol. 20, pp. 31-38, 1984.

[3] B. Bamieh, Intersample and finite wordlength effects in sampled-data problems, IEEE Trans. Auto. Contr., vol. 48, pp. 639-643, 2003.

[4] L. Blum, F. Cucher, M. Shub, and S. Smale, Complexity and real computation: a manifesto, Int. J. Bifurcation and Chaos, vol. 6, pp. 3-26, 1996.

[5] A. Boyarsky and P. Góra, Laws Of Chaos: Invariant Measures And Dynamical Systems In One Dimension, Birkhäuser, Boston, 1997.

[6] R. Brockett and D. Liberzon, Quantized feedback stabilization of linear systems, IEEE Trans. Auto. Contr., vol. 45, pp. 1279-1289, 2000.

[7] R. Brockett, Stabilization of motor networks, IEEE, conf. Decision and Control, pp. 1484-1488, 1995.

[8] L. Bushnell, Networks and control, IEEE Control Systems Magazine, vol. 21, pp. 22-23, 2001.

[9] E. Bai and Y. Wu, Limiting zero distribution of sampled systems, Automatica, vol. 38, pp. 843-851, 2002.

[10] T. Chen and B. Francis, Input-output stability of sampled-data control, IEEE Trans. Auto. Contr., vol. 36, pp. 387-397, 1991.

[11] T. Chen and B. Francis, Optimal Sampled-Data Control Systems, Springer, London, 1995.

[12] A. Cervin, D. Henriksson, B. Lincoln, J. Eker, and K. Arzén, How does control timing affect performance? IEEE Control Systems Magazine, vol. 23, pp. 16-30, 2003.

[13] X. Chen and J. Wen, A linear matrix inequality approach to the discrete-time mixed $l_1/\mathcal{H}_\infty$ control problem, IEEE, conf. Decision and Control, pp. 3670-3675, 1995.

[14] D. Delchamps, The stabilization of linear systems with quantized feedback, IEEE, conf. Decision and Control, pp. 405-410, 1988.

[15] D. Delchamps, Controlling the flow of information in feedback systems with measurement quantization, IEEE, conf. Decision and Control, pp. 2355-2360, 1989.

[16] D. Delchamps, Stabilizing a linear system with quantized state feedback, IEEE Trans. Auto. Contr., vol. 35, pp. 916-924, 1990.

[17] R. Devancy, An Introduction To Chaotic Dynamical Systems, WestView, 2003.

[18] J. Doyle, Complexity, Presented at Georgia Institute of Technology, Nov 22, 2004.

[19] N. Elia, When Bode meets Shannon: control-oriented feedback communication schemes, IEEE Trans. Auto. Contr., vol. 49, pp. 1477-1488, 2004.

[20] N. Elia and S. Mitter, Stabilization of linear systems with limited information, IEEE Trans. Auto. Contr., vol. 46, pp. 1384-1400, 2001.

[21] M. Feigenbaum, The transition to chaos, in Chaos: The New Science, the 26th Nobel Conference, pp. 45-53, 1990.

[22] G. Franklin and J. Powell, Digital Control Of Dynamic Systems, Reading, MA: Addison-Wesley, 1980.

[23] F. Fagnani and S. Zampieri, Stability analysis and synthesis for scalar linear systems with a quantized feedback, IEEE Trans. Auto. Contr., vol. 48, 1569-1583, 2003.

[24] F. Fagnani and S. Zampieri, Quantized stabilization of linear systems: complexity versus performance, IEEE Trans. Auto. Contr., vol. 49, pp. 1534-1548, 2004.

[25] S. Galatolo, Global and local complexity in weakly chaotic dynamical systems, Discrete and Continuous Dynamical Systems, vol. 9, pp. 1607-1624, 2003.

[26] J. Guckenheimer and P. Holmes, Nonlinear Oscillations, Dynamical Systems, And Bifurcations Of Vector Fields, Springer-Verlag, 1983.

[27] G. Goodwin, H. Haimovich, D. Quevedo, and J. Welsh, A moving horizon approach to networked control system design, IEEE Trans. Auto. Contr., vol. 49, pp. 1427-1445, 2004.

[28] K. Glover, All optimal Hankel-norm approximations of linear multivariable systems and their L_∞-error bounds, Int. J. Control, vol. 39, pp. 1115-1193, 1984.

[29] L. Huang, Linear Algebra In Systems And Control, Science Press (in Chinese), 1984.

[30] L. Hale and H. Kocak, Dynamics And Bifurcations, Springer-Verlag, 1991.

[31] D. Hristu and K. Morgansen, Limited communication control, Systems & control letters, vol. 37, pp. 193-205, 1999.

[32] Y. Halevi and A. Ray, Integrated communication and control systems: part I – analysis, ASME Journal of Dynamic Systems, Measurement and Control, vol. 110, pp. 367-373, 1988.

[33] Y. Halevi and A. Ray, Analysis of integrated communication and control system networks, ASME Journal of Dynamic Systems, Measurement and Control, vol. 113, pp. 365-371, 1990.

[34] C. N. Hadjicostis and R. Touri, Feedback Control utilizing Packet Dropping Network Links, IEEE, conf. Decision and Control, pp. 1205-1210, 2002.

[35] T. Hagiwara, T. Yuasa, and M. Araki, Stability of the limiting zeros of sampled-data systems with zero and first-order holds, Int. J. of Control, vol. 58, pp. 1325-1346, 1993.

[36] S. Hu and W. Zhu, Stochastic optimal control and analysis of stability of networked control systems with long delay, Automatica, vol. 39, pp. 1877-1884, 2003.

[37] H. Ishii and B. Francis, Stabilization with control networks, Automatica, vol. 38, pp. 1745-1751, 2002.

[38] H. Ishii and B. Francis, Quadratic stabilization of sampled-data systems with quantization, Automatica, vol. 39, pp. 1793-1800, 2003.

[39] H. Khalil, Nonlinear Systems, Prentice Hall (Second Edition), 1996.

[40] C. Kopf, Symbol sequences and entropy for piecewise monotone transformations with discontinuities, Discrete and Continuous Dynamical Systems, vol. 6, pp. 299-304, 2000.

[41] Z. Kowalczuk, Discrete approximation of continuous-time systems: a survey, IEE Proceedings-G, no. 144, pp. 264-278, 1993.

[42] R. Krtolica, Ü. Özgüner, D. Chan, G. Göktas, J. Winkelman, and M. Liubakka, Stability of linear feedback systems with random communication delays, Int. J. Control, vol. 59, pp. 925-953, 1994.

[43] P. Kumar, New technological vistas for systems and control: the example of wireless networks, IEEE Control Systems Magazine, vol. 24-37, pp. 24-37, 2001.

[44] L. Li and J. Baillieul, Robust quantization for digital finite communication bandwidth (DFCB) control, IEEE Trans. Auto. Contr., vol. 49, pp. 1573-1584, 2004.

[45] D. Liberzon, Switching In Systems And Control, Birkhäuser, Boston, 2003.

[46] Q. Ling and M.D. Lemmon, Robust performance of soft real-time networked control systems with data dropouts, IEEE, conf. Decision and Control, pp. 1225- 1230, 2002.

[47] A. Lasota and M. Mackey, Chaos, Fractals, And Noise: Stochastic Aspects Of Dynamics, (2nd edition), Springer-Verlag, 1994.

[48] F. Lian, J. Moyne, and D. Tilbury, Performance evaluation of control networks, IEEE Control Systems Magazine, vol. 21, pp. 66-83, 2001.

[49] F. Lian, J. Moyne, and D. Tilbury, Networked design consideration for distributed control systems, IEEE Trans. Contr. Syst. Techno., vol. 10, pp. 297-307, 2002.

[50] L-W. Liou and A. Ray, On modeling of integrated communication and control systems, ASME Journal of Dynamic Systems, Measurement and Control, vol. 112, pp. 790-794, 1990

[51] L-W. Liou and A. Ray, Integrated communication and control systems: part III – non-identical sensor and controller sampling, ASME Journal of Dynamic Systems, Measurement and Control, vol. 112, pp. 357-364, 1990.

[52] R. Luck and A. Ray, An observer-based compensator for distributed delays, Automatica, Vol. 26, pp. 903-908, 1990.

[53] L-W. Liou and A. Ray, A stochastic regulator for integrated communication and control systems: part I – formulation of control law, ASME Journal of Dynamic Systems, Measurement and Control, vol. 113, pp. 604-611, 1991.

[54] L-W. Liou and A. Ray, A stochastic regulator for integrated communication and control systems: part II – numerical analysis and simulation, ASME Journal of Dynamic Systems, Measurement and Control, vol. 113, pp. 612-619, 1991.

[55] A. Lasota and J. Yorke, On the existence of invariant measures for piecewise monotonic transformations, Trans. Amer. Math. Soc., no. 186, pp. 481-488, 1973.

[56] T. Li and J. Yorke, Ergodic transformations from an interval to itself, Trans. Amer. Math. Soc., no. 235, pp. 183-192, 1978.

[57] L. Montestruque and P. Antsaklis, Stability of model-based networked control systems with time-varying transmission times, IEEE Trans. Auto. Contr., vol. 49, pp. 1562-1572, 2004.

[58] R. Murray, K. Åström, S. Boyd, R. Brockett, and G. Stein, Future directions in control in an information-rich world, IEEE Control Systems Magazine, vol. 23, pp. 20-33, 2003.

[59] A. Malinowshi, T. Booth, S. Grady, and B. Huggins, Real time control of a robotic manipulator via unreliable internet connection, IEEE, conf. Indus. Elect. Society, IECON'01, pp. 170-175, 2001.

[60] J. Nilsson and B. Bernhardsson, Analysis of real-time control systems with time delays, IEEE, conf. Decision and Control, pp. 3173-3178, 1996.

[61] J. Nilsson, B. Bernhardssont and B. Witenmark, Stochastic analysis and control of real-time systems with random time delays, Automatica, vol. 34, pp. 57-64, 1998.

[62] J. Nilsson, B. Bernhardsson, and B. Wittenmark, Some topics in real-time control, Proc. American Control Conference, pp. 2386-2390, 1998.

[63] G. Nair and R. Evans, Exponential stabizability of finite-dimensional linear system with limited data rates, Automatica, vol. 39, pp. 585-593, 2003.

[64] G. Nair, R. Evans, I. Mareels, and W. Moran, Topological feedback entropy and nonlinear stabilization, IEEE Trans. Auto. Contr., vol. 49, pp. 1585-1597, 2004.

[65] D. Nesic and A. R. Teel, Sampled-data control of nonlinear systems: an vverview of recent results, Perspectives on Robust Control, R. S. O. Moheimani (Ed.), Springer-Verlag: New York, pp. 221-239, 2001.

[66] D. Nesic and A. R. Teel, "Input output stability properties of networked control systems,", IEEE Trans. Automat. Contr., vol. 49, pp. 1650-1667, 2004.

[67] S. Osburn and D. Bernstein, An exact treatment of the achievable closed-loop H^∞ performance of sampled-data controllers: from continuous- time to open-loop, Automatica, vol. 31, pp. 617-620, 1995.

[68] U. Özgüner, H. Goktag, and H. Chan, Automative suspension control through a computer communication network, IEEE, conf. Control Applications, pp. 895-900, 1992.

[69] Y. Oishi, Asymptotic properties of the best sampled-data control performance, IEEE Trans. Auto. Control, vol. 46, pp. 1132-1137, 2001.

[70] Y. Oishi, The best achievable performance of sampled-data control systems with a small sampling period, IEEE, conf. Decision and Control, pp. 3603-3608, 1997.

[71] P. Octanez, J. Monyne, and D. Tilbury, Using deadbands to reduce communication in networked control systems, Proc. American Control Conference, pp. 3015-2020, 2002.

[72] L. Peterson and B. Davie, Computer Networks: A Systems Approach, Morgan Kaufmann Publishers (Second Edition), 2000.

[73] H. Park, Y. Kim, D. Kim and W. Kwon, A scheduling method for network-based control systems, IEEE Trans. Contr. Syst. Techno., vol. 10, pp. 318-330, 2002.

[74] L. Qiu and E. Davison, Pointwise gap metrics on transfer matrices, IEEE Trans. Auto. Contr., vol. 37, pp. 741-758, 1992.

[75] A. Ray, Performance evaluation of medium access control protocols for distributed digital avionics, ASME Journal of Dynamic Systems, Measurement and Control, no. 109, pp. 370-377, 1987.

[76] A. Ray, Network access protocols for real-time distributed control systems, IEEE Trans. Indus. Appli., vol. 24, pp. 897-904, 1988.

[77] A. Ray, Distributed data communication networks for real-time process control, Chemical Engineering Communications, vol. 65, pp. 139-154, 1988.

[78] A. Ray, Introduction to networking for integrated controls Systems, IEEE Control Systems Magazine, vol. 9, pp. 76-79, 1989.

[79] R. Raji, Smart networks for control, IEEE Spectrum, pp. 49-53, 1994.

[80] N. Rafee, T. Chen, and O. Malik, A technique for optimal digital redesign of analog controllers, IEEE Trans. Contr. Syst. Techno., vol. 5, pp. 89-99, 1997.

[81] A. Ray and Y. Halevi, Integrated communication and control systems: part II – design considerations, ASME Journal of Dynamic Systems, Measurement and Control, Vol. 110, pp. 374-381, 1988.

[82] J. Richard, Time-delay systems: an overview of some recent advances and open problems, Automatica, vol. 39, pp. 1667-1694, 2003.

[83] A. Ray, L-W. Liou and J.H. Shen, State estimation using randomly delayed measurements, ASME Journal of Dynamic Systems, Measurement and Control, vol. 115, pp. 19-26, 1993.

[84] J. W. Robbin, "Topological conjugacy and structural stability for discrete dynamical systems," Bell. Amer.Math. Soc. vol. 78, pp:923-952.

[85] C. Robinson, Dynamical Systems: Stability, Symbolic Dynamics And Chaos, CRC Press, 1995.

[86] C. Robinson, An Introduction To Dynamical Systems: Continuous And Discrete, Pearson Prentice Hall, 2004.

[87] A. Ray and Y. Halevi, Integrated communication and control systems: part II – design considerations, ASME Journal of Dynamic Systems, Measurement and Control, vol. 110, pp. 374-381, 1988.

[88] T. Sogo and N. Adachi, A limiting property of the inverse of sampled-data systems on a finite-time interval, IEEE Trans. Auto. Contr., vol. 46, pp. 761-765, 2001.

[89] H. Schuster, Handbook Of Chaos Control, Wiley-VCH, 1999.

[90] L. Shieh, B. Decrocq, and J. Zhang, Optimal digital redesign of cascaded analogue controllers, Optimal Control: Application and Methods, vol. 12, pp. 205-219, 1991.

[91] R. Safaric, K. Jezernik, D. Calkin, and R. Parkin, Telerobot control via internet, Proc. IEEE sympo. Indus. Elect., vol. 1, pp. 298-303, 1999.

[92] T. Simsek, R. Jain, and P. Varaiya, Scalar estimation and control with noisy binary observations, IEEE Trans. Auto. Contr., vol. 49, pp. 1598-1603, 2004.

[93] S. Smale, Differentiable dynamical systems, Bull. Amer. Math. Soc., no. 73, pp. 747-817, 1967.

[94] J. Sparks, Low-cost technologies for aerospace applications, Microprocessors and Microsystems, no. 20, pp. 449-454, 1997.

[95] W. A. Sethares, and T. W. Staley, Periodicity transforms IEEE Trans. Sign. Proc., vol. 47, pp. 2953-2964, 1999.

[96] B. Sinopoli, L. Schenato, M. Franceschetti, K. Poolla, M. Jordan, and S. Sastry, Kalman filtering with intermittent observations, IEEE Trans. Auto. Contr., vol. 49, pp. 1453-1464, 2004.

[97] S. Tatikonda and S. Mitter, Control under communication constraints, IEEE Trans. Auto. Contr., vol. 49, pp. 1056-1068, 2004.

[98] S. Tatikonda and S. Mitter, Control over noisy channels, IEEE Trans. Auto. Contr., vol. 49, pp. 1196-1201, 2004.

[99] H. Trentelman and A. Stoorvogel, Sampled-data and discrete-time H_∞ optimal control, SIAM J. Contr. Optim., vol. 33, pp. 834-862, 1995.

[100] S. Tatikonda, A. Sahai, and S. Mitter, Stochastic linear control over a communication channel, IEEE Trans. Auto. Contr., vol. 49, pp. 1549-1561, 2004.

[101] M. Vidyasagar, The graph metric for unstable plants and robustness estimates for feedback stability, IEEE Trans. Auto. Contr., vol. 29, pp. 403-418, 1984.

[102] J. Walrand and P. Varaiya, High Performance Communication Networks, Morgan Kaufmann Publishers, 1996.

[103] G. Walsh, O. Beldiman, and L. Bushnell, Error encoding algorithms for networked control systems, IEEE, conf. Decision and Control, pp. 4933-4938, 1999.

[104] G. Walsh, O. Beldiman, and L. Bushnell, Asymptotic behavior of nonlinear networked control systems, IEEE, Trans. Auto. Contr., vol. 46, pp. 1093 -1097, 2001.

[105] G. Walsh, Y. Hong, and L. Bushnell, Stability analysis of networked control systems, IEEE Trans. Contr. Syst. Techno., vol. 10, pp. 438-446, 2002.

[106] G. Walsh, Y. Hong, and L. Bushnell, Error encoding algorithms for networked control systems, Automatica, vol. 38, pp. 261-267, 2002.

[107] W. Wong and R. Brockett, Systems with finite communication bandwidth constraints, part II: stabilization with limited information feedback, IEEE Trans. Auto. Contr., vol. 44, pp. 1049-1053, 1999.

[108] S. Weller, W. Moran, B. Ninness, and A. Pollington, Sampling zeros and the Euler-Frobenius polynomials, IEEE Trans. Auto. Contr. vol. 46, pp. 340-343, 2001.

[109] B. Wittenmark, J. Nilsson, and M. Töngren, Timing problems in real-time control systems, Proc. American Control Conference, pp. 2000-2004, 1995.

[110] G. Walsh and H. Ye, Scheduling of networked control systems, IEEE Control Systems Magazine, vol. 21, pp. 57-65, 2001.

[111] D. Yue, Q. Han, and J. Lam, Network-based robust H_∞ control of systems with uncertainty, Automatica, vol. 41, pp. 999-1007, 2005.

[112] G. Zhang and T. Chen, Comparing digital implementation via the bilinear and step-invariant transformations, Automatica, vol. 40, pp.327-330, 2004.

[113] G. Zhang and T. Chen, Networked control systems: a perspective from chaos, to appear on the Int. J. of Bifurcation and Chaos, 2005.

[114] W. Zhang, M. Branicky, and S. Phillips, Stability of networked control systems, IEEE Control Systems Magazine, vol. 21, pp. 84-99, 2001.

[115] K. Zhou and J. Doyle, Essentials Of Robust Control, Prentice Hall, NJ, 1998.

[116] Q. Zhong, Robust stability analysis of simple systems controlled over communication networks. Automatica, vol. 39, pp.1309-1312, 2003.

[117] P. Zhivoglyadov and R. Middleton, Networked control design for linear systems, Automatica, vol. 39, pp. 743-750, 2003.

[118] L. Zhang, Y. Shi, T. Chen and B. Huang, A new method for stabilization of networked control systems with random delays, IEEE Trans. Auto. Contr., accepted, 2005.